The identification of novel antivirals and enhancers of influenza virus replication via high-throughput screening of small molecular weight compounds

Dissertation zur Erlangung des akademischen Grades des

Doktors der Naturwissenschaften (Dr. rer.nat.)

eingereicht im Fachbereich Biologie, Chemie, Pharmazie

der Freien Universitaet Berlin

vorgelegt von

Hans-Heinrich Hoffmann

aus Berlin

April, 2010

The dissertation was conducted at the Mount Sinai School of Medicine in New York (NY) under the supervision of Dr. Peter Palese and Dr. Megan Shaw.

1. Gutachter: Dr. Peter Palese

2. Gutachter: Dr. Petra Knaus

Disputation am 28. Mai 2010

ACKNOWLEDGEMENT

I would like to thank my supervisor Professor Peter Palese for giving me the opportunity to complete my thesis work in his laboratory in New York. I am grateful for his patience and for giving me the freedom to explore many scientific fields; this was a great experience, I am deeply thankful for.

Many special thanks to Professor Megan Shaw. The tremendous level of support, her ideas, her advice and constructive critiques throughout the whole period of my thesis work were outstanding.

I would like to thank Professor Petra Knaus, who took over the supervision of my thesis work in Berlin. She made it possible for me to spend my PhD time abroad.

I would also like to thank all the people working in Dr. Palese's laboratory. I have seen a lot of people coming and leaving during my time as a graduate student. Each of them was helpful in teaching science and practical techniques but especially Dmitriy Zamarin, Laurel Glaser and Silke Stertz.

I also received substantial support from Professor Matthew Evans, Estanislao Nistal-Villan and Su Chiang from the ICCB at Harvard Medical School.

My special thanks go to my very dear friends in New York and back home in Europe.

A very special note of thanks goes to my parents and siblings for their encouragement.

SUMMARY

Every year, influenza viruses cause up to 5 million cases of severe illness and up to 500,000 deaths worldwide. The spread of highly pathogenic avian influenza across several continents and the emergence of a highly transmissible pandemic H1N1 strain in 2009 underline the urgent need for novel antivirals and innovations in vaccine production. Currently, there are only four FDA-approved drugs available for the treatment and prevention of influenza: the M2 ion channel inhibitors (adamantanes), amantadine and rimantadine, and the neuraminidase inhibitors, oseltamivir and zanamivir. Unfortunately, the emergence of resistant influenza virus strains has precluded the use of adamantanes for the past influenza seasons. Vaccines have been efficient in preventing illness, but they are not accessible for a greater part due to the increasing demand which is often beyond manufactures capacities. We have developed a cell-based high throughput screen assay for the identification of compounds that modulate influenza virus replication either negatively or positively. For this purpose, we designed a luciferase reporter gene that is expressed in human lung epithelial (A549) cells and mimics a viral RNA segment (vRNA) after being transcribed. Infection of these cells with the influenza A/WSN/33 (H1N1) virus provides the viral polymerase to initiate the production of luciferase which is measured as an indication of viral replication. Potential inhibitors can therefore be identified as they suppress luciferase signals. In contrast, an increase in luminescence indicates enhanced viral polymerase activity and therefore leads to the identification of compounds that boost viral replication. Such compounds could be beneficial for use in the production of tissue culture-grown vaccines. The antiviral high throughput screen assay was optimized in a 96-well format and its validity confirmed by exhibiting z' factors of ~ 0.79. Adaptation to a 384-well format allowes screening of standardized compound libraries. We screened approximately 73,000 compounds at the Institute of Chemistry and Cell Biology (ICCB) at Harvard Medical School. Screening known bioactive compounds, we identified distinct groups of inhibitors and enhancers which act directly on cellular sodium channels and regulate intracellular sodium concentrations or affect protein kinase C (PKC). Inhibition of epithelial sodium channels or

activation of PKC leads to enhanced virus production. In direct contrast, a sodium channel opener, a sodium ionophore and Na^+/K^+-ATPase inhibitors, as well as PKC inhibitors significantly reduce viral replication. Future work will reveal the role of intracellular sodium concentration and molecular mechanism behind these effects. Among compounds with unknown biological properties, we identified 18 that exhibit anti-influenza virus activity at non-cytotoxic concentrations. Through the use of influenza virus-like particle (VLP) and pseudotyped particle (PP) entry assays we could show that one compound, namely C2, targets the entry step of influenza virus infection. As a recently described vATPase inhibitor, C2 has broad antiviral activity against various viruses that enter via receptor mediated endocytosis and require a low pH during entry. Currently, *in vivo* studies in mice are performed to determine whether C2 can be utilized for the treatment of viral infections. Employing influenza virus mini-genome assays and primer extension assays, we identified two compounds (A3 and A35) that target the influenza virus polymerase function. Interestingly, compound A3 shows *in vitro* increased potency over ribavirin, a broadband antiviral. Furthermore, A3 inhibits the replication of both influenza A and B viruses as well as of RNA viruses of different families such as vesicular stomatitis virus (VSV) and Sindbis virus (SINV). Future studies will reveal A3's mode of action and its *in vivo* capacity as a broadband antiviral. Compound A35 potently inhibits viral replication *in vitro* prior and post infection. It is specific for the influenza A/WSN/33 virus and inhibits the interaction of the viral polymerase complex with the nucleoprotein (NP) as demonstrated by Co-immunoprecipitation. Further studies are needed to determine whether A35 blocks replication and/or transcription of the viral genome. An identified putative compound binding site in NP needs to be confirmed in binding assays or by co-crystallization.

In summary, we found that the intracellular sodium concentration and PKC activity can affect viral replication in a positive or negative manner. In addition, three novel lead compounds were identified that target either viral entry or the influenza virus replication complex. Two compounds exhibit broadband antiviral activity and one targets the viral NP protein – a novel influenza antiviral target.

ZUSAMMENFASSUNG

Die Zahl schwerer Atemwegserkrankungen hervorgerufen durch das Influenza Virus liegt jaehrlich bei 3-5 Millionen and verursacht bis zu 500,000 Todesfaelle weltweit. Der Ausbruch und die Verbreitung hoch pathogenen Vogelgrippe-Viren in Verbindung mit dem Auftauchen eines neuen hoch ansteckenden Pandemievirus' im Jahre 2009, unterstreichen die dringende Notwendigkeit fuer neue antivirale Medikamente, sowie Innovationen in der Impfstoffproduktion. Derzeit gibt es in den USA lediglich vier staatlich zugelassene Medikamente zur Behandlung und Vorbeugung von Influenza. Adamantan-derivate wie Amantadine (Symmetrel®) und Rimantadine (Flumadine®) blocken den viralen M2 Ionenkanal and Oseltamivir (Tamiflu®) and Zanamivir (Relenza®) inhibieren die virale Neuraminidase. Das Auftauchen resistenter Viren gegen beide Wirkstoffklassen und die weite Verbreitung solcher hat den Gebrauch von Adamantanen in den letzten Jahren eingeschraenkt. Grippeschutzimpfungen beugen effizient der Verbreitung von Influenza Viren vor, sind aber nicht immer zugaenglich fuer die breite Bevoelkerung aufgrund stetig steigender Nachfrage oder Produktionsengpaessen. Wir entwickelten einen zellkultur-basierten High-Throughput Screen Assay, der Wirkstoffe identifizieren kann, die die virale Replikation negativ oder auch positiv beinflussen koennen. Fuer diese Assay wurde ein Luziferase-Reportergen konstruiert, welches einem viralen RNA (vRNA) Segment gleicht, wenn in humanen lungepithelialen (A549) Zellen exprimiert. Waehrend einer Infektion dieser Zellen, wenn die virale Polymerase zahlreich vorhanden ist, wird Luziferase produziert, deren Aktivitaet einen quantitativen Indikator fuer virale Replikation darstellt. Wirkstoffe werden als potentielle Inhibitoren klassifiziert, wenn sie das Luziferasesignal vermindern, wohingegen ein erhoehtes Signal auf verstaerkte virale Replikation hindeutet und somit ein "Enhancer-Molekuel" identifizieren kann. Molekuele solcher Art koennten sich als hilfreich heraustellen, fuer die Produktion von Impfstoffen in Zellkultur. Nach der Optimierung des High-Throughput Screen Assays in 96-well Zellkultur-Platten wurde dessen Qualitaet verifiziert mit einem z' factor von ~0.79. Im Institut fuer Chemie und Zellbiologie der Harvard Medical School wurde der Assay auf das 384-well Plattenformat

adaptiert und Bibliotheken mit ungefaehr 73,000 Molekulen systematisch getestet. Unter den Molekuelen mit bekannten bioaktiven Eigenschaften, identifizierten wir zwei Klassen von Inhibitoren und Enhancern, die einen direkten Einfluss auf zellulaere Natriumkanaele und die innerzellulaere Natriumkonzentration ausueben oder auf die Protein Kinase C (PKC). Die Inhibition von epithelialen Natriumkanaelen (ENaCs) und die Aktivierung von PKC fuehren zu einer erhoehten Virusproduktion *in vitro*. Dementsprechend verringern die Oeffnung von ENaCs, Natriumionophore, Inhibierung von Na^+/K^+-ATPasen, sowie die Inhibition von PKC, die virale Replikation deutlich. Zukuenftige Arbeit wird zeigen, welche Rolle die intrazellulaere Natriumkonzentration im viralen Replikationszyklus spielt. Der Grossteil der getesteten Molekuele besitzt *ad dato* keine bekannten bioaktive Eigenschaften. Unter diesen wurden 18 identifiziert, die antivirale Wirkung, spezifisch gegen das Influenza Virus aufweisen, ohne dabei Zelltoxizitaet hervorzurufen. Unter der Zuhilfenahme von Influenza Virus-like particle (VLP) und pseudotyped particle (PP) Entry Assays konnten wir fuer das Molekuel C2 zeigen, dass es das Eindringen von Influenza Viren in die Zelle blockt. Kuerzlich wurde C2 als ein Inhibitor von zellulaeren vATPases beschrieben; wir konnten zeigen, dass diverse Viren, die mittels rezeptor-vermittelter Endozytose und niedrigem pH Wert in die Zelle gelangen, von C2 inhibiert werden. Inwieweit C2 genutzt werden kann fuer die Behandlung von Infektionen dieser Art Viren, wird derzeit in *in vivo* Studien getestet. In Influenza Virus Mini-Genome Assays and Primer Extension Assays wurden 2 Molekuele (A3 und A35) entdeckt, die die Funktion der viralen Polymerase inhibieren. A3 weist erhoehte *in vitro* Wirksamkeit auf verglichen zu Ribavirin, einem Breitband antiviralem Medikament. Interessanterweise inhibiert A3 nicht nur alle bislang getesteten Influenza A Viren, sondern auch das Influenza B Virus und andere RNA Viren unterschiedlicher Familien, wie zum Beispiel, das Vesicular-Stomatitis-Virus und das Sindbis Virus. Weiterfuehrende Arbeit wird zeigen, welchem Mechanismus die Inhibition durch A3 zugrunde liegt und ob sich die Breitband antivirale Wirkung *in vivo* bestaetigen laesst. Das Molekuel A35 ist ein starker viraler Inhibitor, selbst spaet im Replikationszyklus. Es ist spezifisch fuer das Influenza A/WSN/33 (H1N1) Virus und inhibiert die Interaktion zwischen dem viralen Polymerasekomplex und dem Nucleoprotein (NP), gezeigt mittles Co-immunoprezipitation. Zukuenftige Arbeit mit A35 sollte zeigen, ob durch die Inhibition der viralen Polymerase die

Replikation und/oder die Transkription blockiert wird. Die in dieser Studie identifizierte Bindungsstelle von A35 in NP wird in Zukunft in speziellen Bindungsassays oder mittels Co-Kristallisation bestaetigt werden.

Zusammenfassend wird in dieser Arbeit gezeigt, dass die intrazellulaere Natriumkonzentration und die Aktivitaet der PKC die virale Replikation positiv und negativ beeinflussen kann. Es wurden drei Molekule identifiziert, die den viralen Eintritt in die Zelle oder den viralen Replikationskomplex inhibieren. Zwei dieser Molekuele weisen Breitband antivirale Wirkung auf, und eines, inhibiert das virale Nukleoprotein, welches bislang noch nicht als Target antiviraler Wirkstoffe beschrieben wurde.

LIST OF PUBLICATIONS

1. **Hoffmann, H.H.**, Palese, P. and Shaw, M.L., 2008. Modulation of influenza virus replication by alteration of sodium ion transport and protein kinase C activity. Antiviral Res 80(2), 124-34.

2. Konig, R., Stertz, S., Zhou, Y., Inoue, A., **Hoffmann, H.H.**, Bhattacharyya, S., Alamares, J.G., Tscherne, D.M., Ortigoza, M.B., Liang, Y., Gao, Q., Andrews, S.E., Bandyopadhyay, S., De Jesus, P., Tu, B.P., Pache, L., Shih, C., Orth, A., Bonamy, G., Miraglia, L., Ideker, T., Garcia-Sastre, A., Young, J.A., Palese, P., Shaw, M.L. and Chanda, S.K. (2010) Human host factors required for influenza virus replication. Nature 463(7282), 813-7.

TABLE OF CONTENTS

Tables "Introduction"

Figures "Chapter I"

Tables "Chapter I"

Figures "Chapter II"

Tables "Chapter II"

Figures "Chapter III"

Tables "Chapter III"

INTRODUCTION

Influenza viruses can cause highly contagious respiratory illness. Every year, 5-20% of the US population gets infected which results in an estimated 200,000 hospitalizations and 36,000 deaths (CDC, 2010b). Influenza is not only a major health burden but also has a tremendous economic impact worldwide at a cost of up to approximately 71-167 billion dollars annually (WHO, 2003). There have been three major pandemics in the last 100 years (1918, 1957 and 1968), which claimed millions of lives. The emergence of a highly pathogenic avian virus (H5N1) in 1997 (Claas et al., 1998) was alarming and was feared to cause a pandemic in humans. To date, 15 countries reported human infections with H5N1 viruses that killed 289 people (WHO, 2010a). In 2009, a new H1N1 virus appeared that caused relatively mild infections in humans but was highly transmissible and the World Health Organization (WHO) declared a new influenza pandemic for the first time since 1968.

Influenza viruses were first isolated as the causative agent of influenza in 1933 by Wilson Smith. They belong to the *Orthomyxoviridae* family and are divided into three genera, namely influenza A, B and C viruses. The genera can be distinguished by their internal protein antigens (Palese and Young, 1982). Influenza A and B viruses can cause major outbreaks and severe disease, whereas influenza C viruses are mostly responsible for sporadic upper respiratory tract illness in children. It is believed that most mammalian influenza A viruses are derived from an avian influenza virus pool, which circulates in wild aquatic birds (Webster et al., 1992). The influenza B and C viruses diverged from the influenza A virus lineage several centuries ago and adapted to infect humans only. In contrast, influenza A viruses can infect a wide range of species (Fig. I-1).

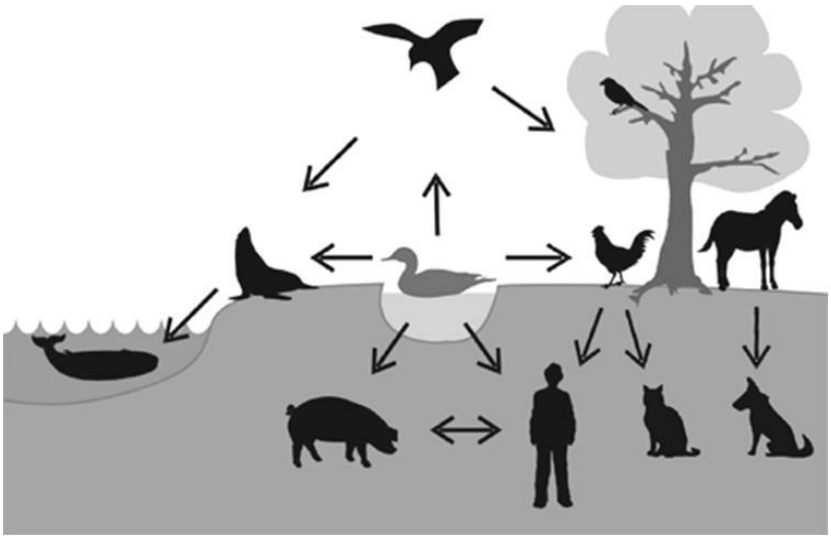

Fig. I-1. Influenza A virus reservoir. Wild aquatic birds are the main reservoir of influenza A viruses. Virus transmission has been reported from wild water fowl to poultry, sea mammals, pigs, horses, and humans. Viruses are also transmitted between pigs and humans, and from poultry to humans. Equine influenza viruses have recently been transmitted to dogs (adapted from Fields Virology, 5th Edition, Chapter of *Orthomyxoviridae*; Wright, Neumann and Kawaoka).

Influenza viruses can occasionally be transmitted from wild aquatic birds to poultry, sea mammals, pigs, horses and humans. Virus transmission may also occur from pigs and poultry to humans. Influenza epidemics are caused every year by seasonal viruses that circulate within the human population. These viruses accumulate mutations in the surface glycoproteins from one year to the next in a process referred to as antigenic drift which allows viruses to re-infect individuals. In contrast, the emergence of viruses with antigenically novel surface antigens which is referred to as antigenic shift may cause pandemics. Pandemic strains may appear from an intermediate host such as pigs (Scholtissek, 1994) and can spread rapidly in a naïve population. Such pandemics differ in their severity e.g. compare the Spanish influenza pandemic of 1918 which resulted in more than 50 million deaths worldwide (Ahmed et al., 2007) and the recent 2009 H1N1 pandemic which has caused less than 20,000 deaths so far (WHO, 2010b).

The influenza virus has a segmented genome; therefore, co-infections of viruses of different origin, e.g. avian and human, can give rise to new reassortant which contain a mix of the genetic material of both parental viruses (Fig.I-2).

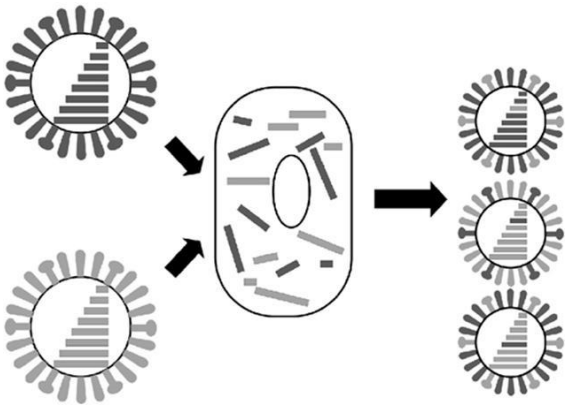

Fig. I-2. Reassortment. Co-infections of cells with two different influenza A viruses can theoretically result in 256 different genotypes. Reassortment is a major mechanism for the generation of pandemic influenza viruses as demonstrated in 1957 (Asian Flu) and 1968 (Hong Kong Flu), (adapted from Fields Virology, 5th Edition, Chapter of *Orthomyxoviridae*; Wright, Neumann and Kawaoka).

Reassortants appeared and caused pandemics in 1918, 1957, 1968 and recently in 2009. The pandemic viruses in 1957, 1968 and most likely in 1918 are reassortants of human and avian viruses whereas the current pandemic is a triple reassortant containing the genetic material of human, avian and swine viruses. H1N1 viruses have circulated since 1918 (after the emergence of the Spanish influenza pandemic virus) and were displaced by an H2N2 virus in 1957 that caused the Asian influenza pandemic. H2N2 viruses continued to circulate until 1968 before they in turn were replaced by an H3N2 virus that caused the Hong Kong influenza pandemic (Kawaoka et al., 1989; Scholtissek et al., 1978). H3N2 viruses have circulated since then causing seasonal epidemics. In 1977 H1N1 viruses have re-appeared and they have been found co-circulating with H3N2 viruses since that time. Interestingly, for the current influenza season 2009/10 the vast majority of reported cases in the US are infections with the pandemic 2009 H1N1 strain. Infections with seasonal H1N1 and H3N2 viruses are rather sporadic and account for only 0.1% (CDC, 2010a). It is too early to draw conclusions and surveillance data from other countries are needed but the pandemic 2009 H1N1 virus may have replaced the former circulating viruses as has been seen in the past.

THE VIRION

Influenza A virus particles are enveloped and highly pleomorphic. They are mostly spherical with a diameter of about 100 nm (Fig. I-3A), although clinical isolates can be often filamentous (Choppin et al., 1960). The viral genome is segmented and consists of negative-sense, single-stranded RNA (Lamb and Choppin, 1983; Palese and Shaw, 2007). Each viral segment has non-coding regions at the 3'- and 5'-ends that are partly complementary to each other and form the viral promoter (Desselberger et al., 1980). The eight segments encode up to 11 viral proteins, namely PB1, PB2, PA, NP, HA, NA, M1, M2, NS1, NEP/NS2 and PB1-F2 (Palese and Shaw, 2007). There is recent evidence for a 12^{th} viral protein, N-40 which is a truncation product of PB1 (Wise et al., 2009) but whose function is not yet understood. The glycoproteins HA, NA and the ion channel protein M2 (Lamb et al., 1985) are embedded in the lipid envelope that contains an M1 protein layer beneath it. The viral polymerase complex composed of PB1, PB2 and PA binds to each viral segment that is coated by NP proteins to form a characteristic secondary structure (Baudin et al., 1994; Compans et al., 1972; Martin-Benito et al., 2001). The NEP/NS2 protein is also found in viral particles (Richardson and Akkina, 1991; Yasuda et al., 1993), whereas the NS1 and PB1-F2 proteins are not packaged into nascent virions (Fig. I-3B).

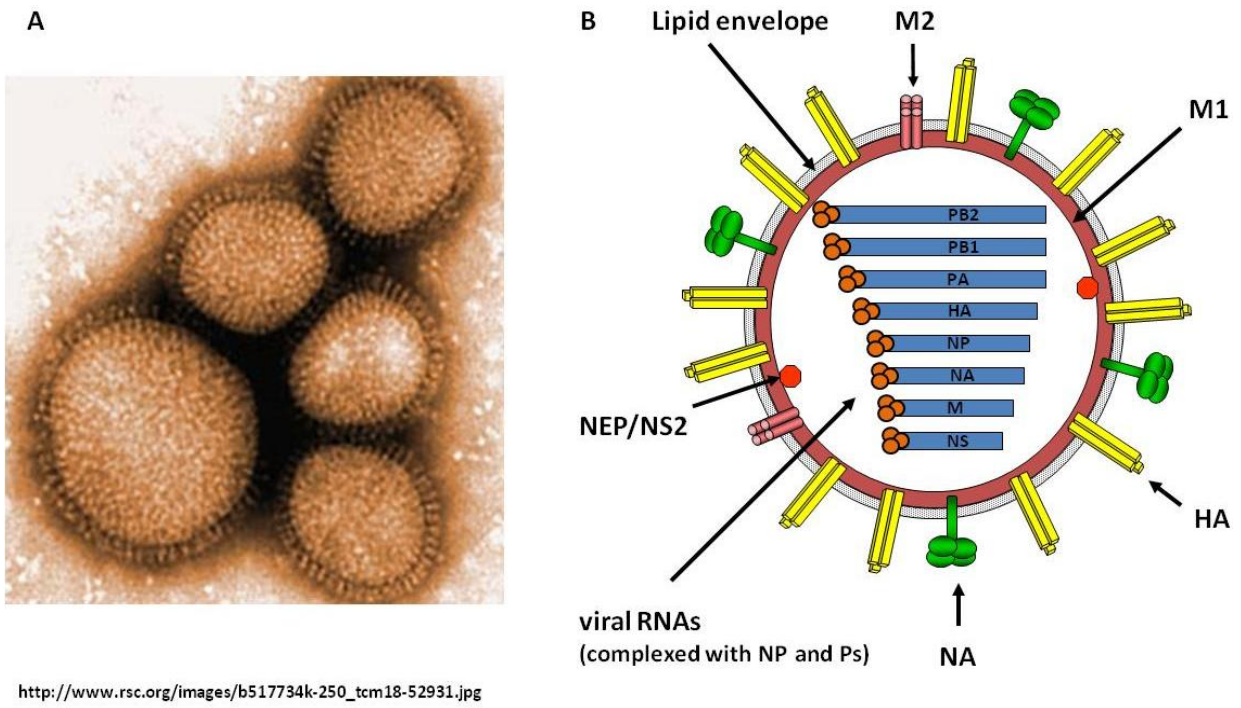

Fig. I-3. Electron micrograph and schematic diagram of an influenza virus particle. (A) Electron micrograph of a negatively stained influenza virus particle with the HA and NA spikes visible on the surface (diameter ~100nm). (B) The hemagglutinin (HA), neuraminidase (NA) and M2 proteins are embedded into the host-derived lipid envelope. HA is found as a trimer, and NA and M2 both as tetramers. The matrix (M1) protein underlies the lipid envelope. A nuclear export protein (NEP/NS2) is also associated with the virus. The viral RNA segments are coated with nucleoprotein and are bound by the polymerase complex (adapted from Fields Virology, 5th Edition, Chapter of *Orthomyxoviridae*, Palese and Shaw).

VIRAL PROTEINS

The Hemagglutinin (HA) protein

The protein was named after its ability to agglutinate erythrocytes. As of now, there are 16 different hemagglutinin subtypes described (H1-H16) in wild water fowl (Fouchier et al., 2005). Among these, only viruses with H1, H2 and H3 HA have established themselves in humans causing seasonal influenza epidemics and are responsible for all known human influenza pandemics. The HA protein forms a rod-shaped trimeric complex. In an infected host cell, the precursor protein HA_0 is cleaved by a trypsin-like (furin) protease into HA_1 and HA_2 subunits.

However, both subunits remain connected through a disulfide bond. The HA_1 forms a globular domain and binds to sialic acid of glycosylated cell surface proteins or lipids. Subsequently, the virus is internalized via pH-dependent endocytosis. The acidification of endosomes provokes a dramatic conformational change in the HA_1/HA_2 structure which exposes the fusion peptide in the HA_2 subunit and promotes fusion of the viral membrane with the endosomal membrane (Fig. I-4). Besides its role in receptor-binding and fusion, the HA protein is a major antigen which can be recognized by the adaptive immune system of the host. The selection pressure created by neutralizing antibodies can lead to escape mutants mostly found in the HA_1 domain. The accumulation of gradual changes in the antigenic structure of HA_1 in viruses that circulate between pandemic years is referred to as antigenic drift. It allows closely-related viruses of the same subtype to re-infect individuals and that requires us to annually produce new vaccines that match the circulating strains.

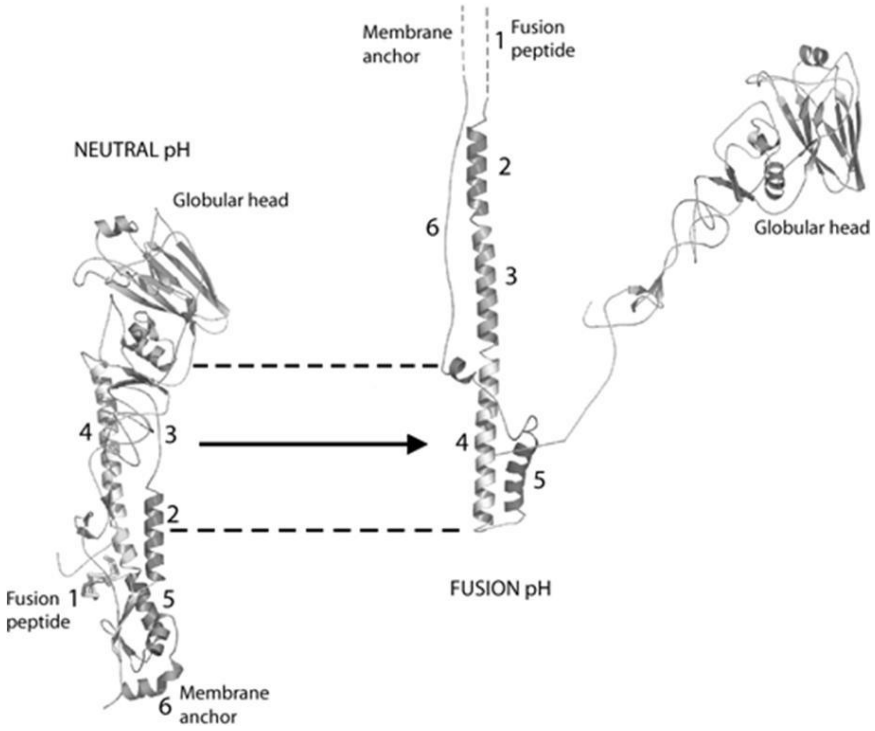

Fig. I-4. Ribbon presentation of structural changes that occur in HA at low pH. The numbered segments are utilized to follow the structural changes and relocations of domains that occur during membrane fusion (adapted from Fields Virology, 5th Edition, Chapter of *Orthomyxoviridae*, Palese and Shaw).

The Neuraminidase (NA) protein

The NA protein was named after its ability to catalyze the cleavage of neuraminic acid that is also known as sialic acid. There are currently 9 NA subtypes (N1-N9) identified in wild water fowls. It forms a homo-tetrameric complex that has a globular domain on top of a short stem region. The removal of sialic acid from cell surface proteins and viral particles by the NA protein allows efficient release of mature, newly synthesized particles from the host cell membrane as well as enhanced spread of the virus. This is crucial for the virus to propagate and the NA is thus a suitable drug target. Besides the HA protein, the NA protein can also generate an immune response that results in non-neutralizing antibodies. Although receptor-binding of the virus is not affected, viral spread can be restricted to a certain degree that may allow the host to control the viral infection.

The M proteins M1 and M2

The M segment encodes for 2 viral proteins, the M1 and the M2 proteins. The first eight amino acids of the N-terminus of the M1 and M2 proteins are identical. The M1 protein is translated from unprocessed mRNA whereas the M2 protein is translated from a spliced mRNA variant.

M1 – the matrix protein

The M1 protein is the most abundant viral protein in an infected cell along with the NP protein. In a virus particle, the M1 is associated with the lipid membrane. Although the M1 lacks a transmembrane domain, it is believed that this association is mediated by the interaction with the cytosolic domains of the surface transmembrane proteins HA, NA and M2. In addition, an interaction of M1 with the NP protein of packaged RNPs has been described (Martin and Helenius, 1991). In the infected cell, the M1 is necessary for the export of RNPs out of the nucleus. During nuclear export, the M1 protein interacts with both the NP protein and vRNAs. This M1/RNP-complex binds via M1 to the NEP/NS2 protein and eventually via NEP/NS2 to Crm1. Crm1 is a cellular export receptor and therefore part of the export machinery that directs the export of the M1/RNP/NEP-

complex into the cytosol (Elton et al., 2001; Ma et al., 2001; Watanabe et al., 2001) (Fig. I-5).

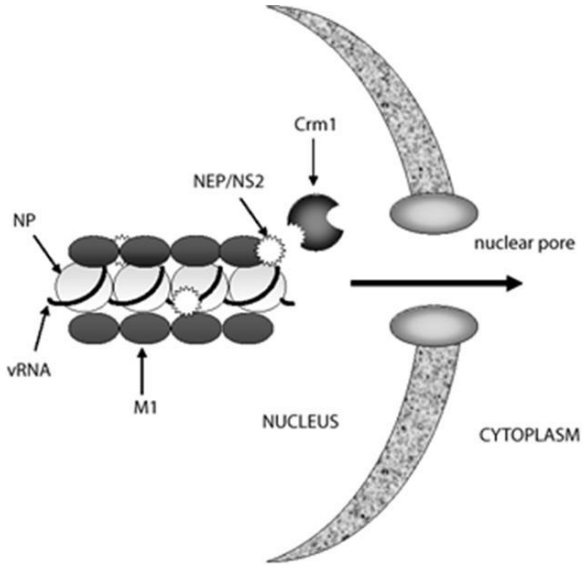

Fig. I-5. Illustration of influenza viral RNP nuclear export. The nuclear export of newly synthesized viral RNP complexes is mediated by the viral NEP/NS2. It interacts with the cellular export factor Crm1 and with the viral RNPs via the M1 protein. The interaction with the cellular export machinery facilitates the transport of the viral genome through the nuclear pore into the cytoplasm (adapted from Fields Virology, 5th Edition, Chapter of *Orthomyxoviridae*, Palese and Shaw).

M2 – an ion channel protein

The M2 forms a tetrameric complex that is embedded in the lipid bilayer of the virion (Sugrue and Hay, 1991). It functions as an ion channel which is activated at a low pH (Pinto et al., 1992) and has an early and late role in the viral life cycle (Hay et al., 1985; Helenius, 1992). Early on during the infection it pumps protons from the acidified endosome into the virion. The low pH within the virion weakens binding of the M1 to the RNPs and allows their release into the cytosol after fusion of viral and endosomal membranes (Martin and Helenius, 1991). Its late role in the infection is associated with the regulation of the pH in the trans-Golgi network. By pumping protons out of the Golgi network, it lowers the intra vesicular pH and thus prevents the premature conformational change of the HA_1/HA_2 protein which is transported to the budding site. Residue 37 (HIS) serves as a pH sensor in M2 (Wang et al., 1995) and residue 41 (TRP) is

the gate which occludes the C-terminal end of the closed channel (Tang et al., 2002). The side chains of both residues form the narrowest point in the channel, to small to allow anything to pass. The protonation of His37 at a low pH is a critical event in channel opening. The positively charged imidazole rings of His37 and their electrostatic repulsion is responsible for destabilizing the helix-helix packing and widening of the pore. It is believed that once the channel is open, the pH gradient drives the protons from the low pH side to the high pH side by diffusion. The M2 protein is another target of antivirals besides the NA protein. Derivatives of adamantane were found in the 1960s to inhibit influenza virus replication (Davies et al., 1964). It is controversial whether these antivirals bind on the outside or inside of the M2 tetramer in order to block the ion channel activity (Schnell and Chou, 2008; Stouffer et al., 2008; Stouffer et al., 2005). However, drug binding stabilizes the tightly packed closed channel conformation which makes it harder to initiate conductance (Schnell and Chou, 2008). It is controversial, whether the extensive use of adamantanes led to the emergence of escape mutations preferentially S31N but also L26F and L38F. Those drug-resistance mutations destabilize the closed conformation of the channel, allowing activation to proceed as normal upon activation of His37. The widespread resistance to adamantanes led to their preclusion for the treatment of influenza in recent seasons (Bright et al., 2005; Bright et al., 2006). It is important to note that the M2 is highly conserved throughout different strains and there are approaches to develop M2-based universal vaccines, based on evidence that M2 antibodies are protective (Liu et al., 2004; Slepushkin et al., 1995).

The NS proteins NS1 and NEP/NS2

The NS segment encodes for two proteins, the NS1 and the NEP/NS2 proteins. The NS1 is translated from a full-length NS mRNA, whereas the NEP/NS2 is derived from a spliced NS mRNA and the two proteins share the first nine amino acids of their N-terminus. The efficiency of nuclear export of the unspliced NS1 mRNA is very high (Alonso-Caplen et al., 1992) therefore minimizing its chances of being spliced. Thus, the level of spliced viral transcripts is only 10% of

the level of unspliced transcripts (Lamb et al., 1980). This ensures that the NS1 protein is present at early stages of the virus replication cycle in order to counteract the host's antiviral response. This mechanism also avoids the early expression of the NEP/NS2 protein, and thus prevents the premature export of vRNPs.

NS1 – an interferon antagonist

The NS1 protein forms a dimeric complex that has dsRNA-binding activity in order to prevent recognition of viral RNA by the RNA helicase retinoic acid-inducible gene I (RIG-I) and protein kinase R (PKR). RIG-I senses the 5'-triphosphates (Pichlmair et al., 2006) of viral segments and triggers a signaling cascade that activates the interferon regulatory factor 3 (IRF3) and the nuclear factor-kappa B (NF-kB), which eventually leads to the transcription of type I interferon (IFN). NS1 forms a complex with RIG-I which leads to the inhibition of IRF-3 activation and prevents transcription and secretion of IFN-β. Secretion of IFN-β will stimulate the IFN α/β receptor in an autocrine and paracrine manner and subsequently activates the expression of interferon stimulated genes (ISGs) such as PKR. PKR in turn phosphorylates the α-subunit of eukaryotic translation initiation factor 2 (eIF-2α) to shut down protein translation and thus inhibits viral replication. The viral NS1 protein counteracts PKR activity by directly binding to it as well as by preventing its activation due to dsRNA sequestration. Genetically engineered viruses lacking the NS1 protein or expressing truncated versions of NS1 are highly attenuated (Fig. I-6). This has lead to the development of novel live attenuated vaccine candidates (Ferko et al., 2005; Kochs et al., 2007; Quinlivan et al., 2005; Solorzano et al., 2005).

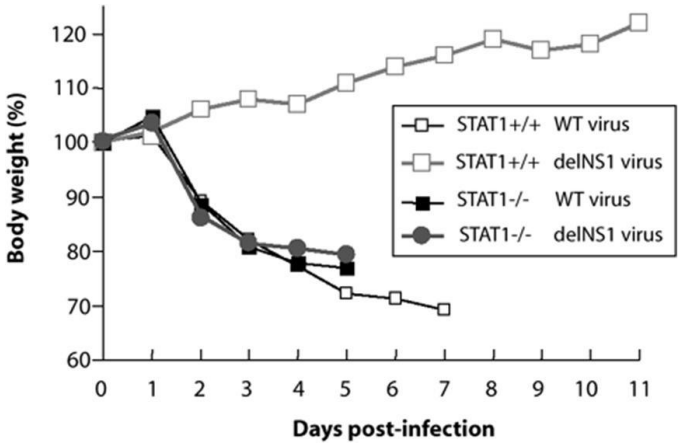

Fig. I-6. Pathogenicity of influenza A virus lacking NS1 expression in STAT1 -/- mice. Wild type (STAT1 +/+) or STAT1 -/- mice were infected with either WT or delNS1 viruses as indicated. DelNS1 virus is apathogenic in STAT1 +/+ mice but equally lethal in STAT1 -/- mice compared to the WT virus (adapted from Fields Virology, 5th Edition, Chapter of *Orthomyxoviridae*, Palese and Shaw).

NEP/NS2 – the nuclear export protein

The NEP/NS2 protein functions as an adaptor protein for the nuclear receptor Crm1 and the viral M1 protein. It directs the nuclear export of newly synthesized RNPs that are complexed to M1 (Fig. I-4). The M1-binding site of NEP/NS2 masks a nuclear localization signal (NLS) in M1 and that may prevent the re-entry of RNPs into the nucleus.

The PB1-F2 protein

The accessory protein PB1-F2 is expressed from an alternative +1 open reading frame in the PB1 segment of some influenza virus strains (Chen et al., 2001). It has been shown to be a pathogenicity factor in the pandemic influenza strain of 1918 and in a highly virulent H5N1 isolate A/Hong Kong/97 (Conenello et al., 2007; McAuley et al., 2007; Zamarin et al., 2006). PB1-F2 may exert its function as a virulence factor by modulating the immune response (Conenello et al., 2007) and enhance secondary bacterial infections which are shown to increase morbidity in influenza patients (McAuley et al., 2007). *In vitro* studies have shown that PB1-F2 localizes to the mitochondria and induces apoptosis by disruption of the mitochondrial membrane potential (Chen et al., 2001; Gibbs et al., 2003; Zamarin et al., 2005). It oligomerizes

and forms pores in mitochondrial membranes to promote the release of cytochrome C (Zamarin et al., 2005).

The Polymerase complex PB1, PB2 and PA

The viral RNA-dependent RNA polymerase complex is composed of three subunits, the PB1, PB2 and PA proteins. Transcription and replication takes place in the nucleus and all three subunits have nuclear localization signals (Mukaigawa and Nayak, 1991; Nath and Nayak, 1990; Nieto et al., 1992). However, PB1 and PA enter the nucleus as a dimer (Fodor and Smith, 2004) and then form a complex with PB2 which is imported independently. Once the viral RNAs are transported into the nucleus, they are transcribed into mRNAs which are capped and polyadenylated. The cap is derived from host cell pre-mRNAs by a process called “cap-snatching” and the poly-A-tail is generated by the viral polymerase via a stuttering maechanism. The replication of the viral genome is a two-step process. The negative-sense vRNA is copied into positive-sense complementary cRNA (1^{st} step of replication) which itself serves as a template to generate more vRNA (2^{nd} step of replication). The influenza virus polymerase complex is capable of catalyzing three different reactions; vRNA-directed mRNA synthesis, vRNA-directed cRNA synthesis and cRNA-directed vRNA synthesis (Fig. I-7).

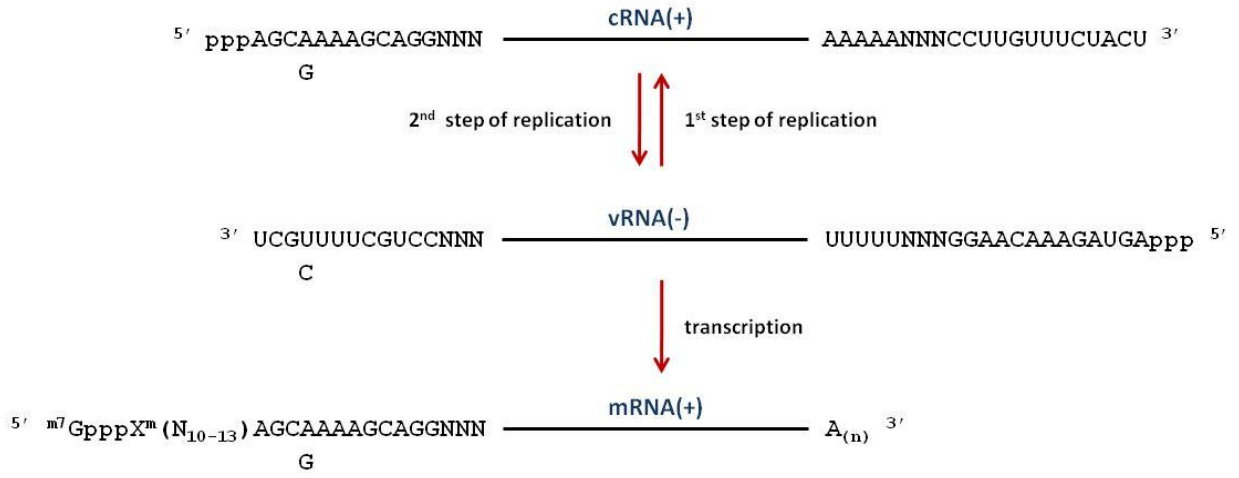

Fig. I-7. Influenza virus RNA synthesis. The incoming negative sense vRNA has conserved non-coding sequences on either end. The poly-(A)-signal consists of a poly-(U)-stretch at the 5′ end of the vRNA. The mRNA derives its cap and 10-13 5′ nucleotides from host mRNAs and has a poly-(A)-tail. The cRNA is an exact complementary copy of the incoming vRNA. Variation at position 4 in the 3′ vRNA non-coding region is indicated (adapted from Fields Virology, 5th Edition, Chapter of *Orthomyxoviridae*, Palese and Shaw).

It is important to note that the viral polymerase does not contain the capability of proof-reading. It is error-prone and generates a mismatch in every 10,000th nucleotide which means that every newly synthesized viral genome contains at least one mutation. This relatively high mutation rate leads to a high number of abortive particles but enables the virus to easily escape the host's immune response.

PB1 – polymerase basic protein 1

The PB1 protein harbors the conserved motifs characteristic for an RNA-dependent RNA polymerase (Biswas and Nayak, 1994). Within the replication complex it catalyzes the sequential addition of nucleotides to RNA transcripts. PB1 initiates replication and transcription by binding to both ends of vRNA or cRNA (Biswas and Nayak, 1994).

PB2 – polymerase basic protein 2

The PB2 protein has the ability to bind caps of host pre-mRNAs (Fechter et al., 2003). It delivers these RNAs to the PA subunit which in turn cleaves them 9-17 nucleotides downstream of the cap. This process is called "cap-snatching" due to the fact that the

caps are derived from host cell pre-mRNAs. The PB2 protein is an important determinant of mammalian adaptation and virulence (Subbarao et al., 1993). The residue 627 is usually a glutamine in avian viruses and a lysine in human isolates. H5N1 viruses that contain a glutamine at position 627 are of low pathogenicity and in contrast, isolates that contain a lysine are highly pathogenic. An E627K change in PB2 was found in fatal human isolates and shown to be more virulent in a mouse model (Hatta et al., 2001). In addition to the E627K mutation, the PB2 mutation T271A enhances polymerase activity in human cells (Bussey et al.). Position 701 in PB2 has also been shown to be important for pathogenesis and transmission of seasonal as well as highly pathogenic influenza A viruses (Gao et al., 2009; Steel et al., 2009).

PA – polymerase acidic protein

PA is required for replication and transcription and has been shown to contain endonuclease activity (Fechter et al., 2003; Fodor and Smith, 2004; Huarte et al., 2003; Jung and Brownlee, 2006). The N-terminal domain of PA was shown to have cap-dependent endonuclease with a highly conserverd active site (Dias et al., 2009; Yuan et al., 2009). The viral polymerase complex was also shown to associate with the host cell RNA polymerase II (RNAP II) (Rodriguez et al., 2007). It specifically degrades the hypo-phosphorylated form of the largest subunit of RNAP II by using the proteolytic activity of the PA subunit (Rodriguez et al., 2007). This degradation correlates with the shutdown of host cell transcription and the onset of viral transcription and replication.

The Nucleoprotein (NP)

The NP protein is a major component of ribonucleoprotein (RNP) complexes. It binds genomic RNA segments and forms helical, rod-like RNP structures (Klumpp et al., 1997; Noda et al., 2006). It is one of the most abundant viral proteins and involved in a variety of viral processes, including intracellular trafficking of the viral genome, viral RNA replication, viral genome packaging, and virus assembly.

Recently the crystal structures of influenza A virus NP from strains A/WSN/33 (Ye et al., 2006) and A/HK/483/97 (Ng et al., 2008) have been determined. The overall structure of NP can be divided into two domains, a head (residues 150-272 and 438-452) and a body (residues 21-149, 273-396 and 453-489) that are joined together by a polypeptide chain at three regions (Fig. 1-8).

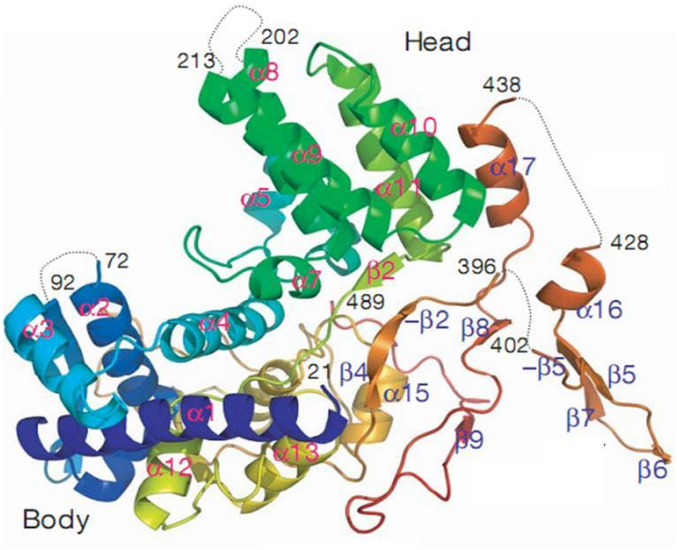

Fig. I-8. Ribbon structure of the influenza A/WSN/33 virus nucleoprotein. The head and body domain are connected by a polypeptide chain. Helical structures are indicated by "α" and sheets by "β". The protein structure can be read α1, α2, β1, - β1, α3, α4, α5, α6, α7, α8, α9, α10, α11, β2, α12 , α13, β3, α14, α15, -β3, β4, -β2, β5, β6, β7, -β6, -β5, α16, α17, β8, β9 (adapted from Ye et al., 2006).

NP RNA binding

The influenza virus NP has an RNA binding activity with little or no sequence specificity (Baudin et al., 1994; Yamanaka et al., 1990). It has been estimated that one NP protein binds to every 24 nucleotides of RNA (Compans et al., 1972; Ortega et al., 2000). The NP crystal structure displays a deep groove between the head and body domain which is most likely the RNA binding site (Ye et al., 2006). The surface of the groove is made up of a large number of basic residues (15x arginine and 1x lysine) that may interact with the RNA's phosphodiester backbone. Interestingly, eleven out of these 16 residues are

conserved among influenza A, B and C viruses which further underlines their importance. Binding RNA to NP gave K_ds in the low- to mid-nanomolar range (Baudin et al., 1994; Elton et al., 1999b). The RNA binding affinity is likely to be affected by NP self-oligomerization. NP self-oligomerization in turn is enhanced by RNA binding which may be beneficial during the vRNA encapsidation process. In contrast to viruses like rabies virus (Albertini et al., 2006), vesicular stomatitis virus (Green et al., 2006) or borna virus (Rudolph et al., 2003) that have their RNA binding grooves facing the interior, the influenza virus vRNA is likely to be largely exposed on the external surface of RNPs, thus allowing easy access to genetic sequence information while functioning as template for RNA synthesis. The external RNA binding mode may also facilitate the recognition of specific virus packaging signals in vRNAs during virus assembly.

NP self-oligomerization

Oligomeric NP can be observed both in virus-infected cells and *in vitro*. NP-NP interactions have been estimated to have a K_d in the mid-nanomolar range (Elton et al., 1999a) and found to be important and sufficient for maintaining RNP structures once they are assembled. NP forms the core scaffold of the RNP, although the vRNA and viral polymerase complex may play an important role in orchestrating the RNP assembly. The NP tail loop mediates NP polymerization in a linear fashion. Residues in the NP-NP interaction area (e.g. R416) have not only been found to be crucial for oligomer formation but also for influenza virus gene expression suggesting proper NP-NP interaction is necessary for viral functions (Elton et al., 1999b; Mena et al., 1999).

NP phosphorylation

Analysis of NP from different influenza A virus strains revealed that they are all phosphorylated *in vivo* and that NP shows a dynamic phosphorylation pattern during the viral replication cycle (Kistner et al., 1989). It was shown that infected cells treated with a protein kinase C (PKC) inhibitor had increased levels of nuclear NP whereas increased levels of cytoplasmic NP were seen when the infected cells were treated with a PKC stimulator. Hence, phosphorylation may play a role in nucleo-cytoplasmic

trafficking of NP (Bui et al., 2002), (Neumann et al., 1997). NP has non-specific RNA binding activity and was found to bind host nucleic acid. It has been reported that rhabdovirus NP phosphorylation reduces non-specific binding (Toriumi et al., 2004). The opposite was shown for influenza virus NP which was treated with alkaline phosphatase and led to enhanced RNA binding activity (Yamanaka et al., 1990). Thus it is possible that phosphorylation of NP by a not yet identified kinase may play a role in virus specific RNA synthesis.

NP and viral replication

Besides its structural role in RNPs, the NP is also required for RNA replication (Palese and Shaw, 2007). Viral RNA templates for transcription and replication are coated by NP. One of the roles of NP during viral replication is to promote anti-termination at the U-tract. Binding of NP to the nascent RNA prevents the template from slipping backwards at this site and from copying a poly(U)-tail (Beaton and Krug, 1986; Shapiro and Krug, 1988). The block of early termination thereby enables the polymerase to synthesize a full-length cRNA of the vRNA template. For the polymerase to switch from transcription mode into replication mode means also to switch from capped RNA-primed initiation to unprimed initiation and there are three models proposed for the NP to facilitate this switch. In the “stabilization model”, NP binds and stabilizes the nascent v- and c-RNA transcripts in order to prevent their degradation (NP binds to v- and c-RNA but not to mRNA) (Vreede et al., 2004). In the “template notification model”, NP binds to template RNA and alters its structure to favor unprimed RNA synthesis (Portela and Digard, 2002). In the third model, the “polymerase notification model”, is a direct protein-protein interaction proposed between the NP and one or more of the polymerase subunits, which in turn results in a polymerase modification that favors the unprimed initiation (Portela and Digard, 2002). NP co-immunoprecipitates with all three proteins of the trimeric polymerase complex (Labadie et al., 2007) but it is not known which of the subunits in complex formation interacts with NP. In *in vitro* studies, NP was found to co-immunoprecipitate with PB1 and PB2 when transfected individually (Biswas et al.,

1998). The implicated binding regions of PB1 and PB2 in NP (aa 1-160, 256-340 and 340-498) are for the most part localized in the body domain (Biswas et al., 1998).

NP nucleo-cytoplasmic trafficking

In the early stage of an infection RNPs are imported into the nucleus and exported only at a late stage of infection (Boulo et al., 2007). NP can mediate nuclear trafficking of itself and also of RNPs. Two NLS signals have been identified in NP, a nonconventional NLS near the N-terminus and a bipartite NLS near the middle of the polypeptide (Neumann et al., 1997; Wang et al., 1997). RNPs get imported into the nucleus by interaction of NP with host cell karyopherin-α (importin-α) (Fig. I-9).

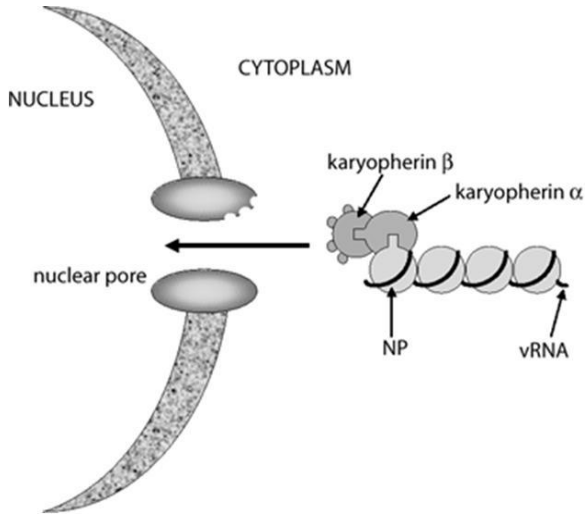

Fig. I-9. Illustration of influenza viral RNP nuclear import. Viral RNPs are imported into the nucleus by an energy-dependent process, requiring interactions with host factors. NP interacts with karyopherin-α via its NLS. Karyopherin-α binds to karyopherin-β (importin-β) which mediates interaction with the nuclear pore complex (adapted from Fields Virology, 5th Edition, Chapter of *Orthomyxoviridae*, Palese and Shaw).

Late in the infection, RNPs interact via NP with M1. M1 most likely masks the NLS signals of NP and in turn interacts with NEP/N2 and then the host cell exportin CRM1, which leads to the nuclear export of RNPs (Fig. I-5).

ANTI-INFLUENZA DRUGS and RESISTANCE

Vaccination is by far the best means we have for preventing infection, minimizing the severity of disease and spreading of the virus. During a pandemic there is often little or no time to produce and deliver enough vaccines and therefore effective drugs are needed to treat or even prevent infections and to shorten the time of illness and shedding. Usually viral proteins are targeted and inhibited by antivirals. The specificity for viral proteins is desirable, but drives selection pressure, such that these viruses mutate, which they do rapidly as due to the error-prone viral polymerase. Viruses preferentially emerge that are resistant to these antivirals.

Another possible approach which is currently under investigation is the development of drugs that target cellular proteins that are essential for the viral life cycle (Konig et al.). Such an approach makes it more difficult for the virus to escape, although targeting a host cell protein may also affect the host itself. However, since influenza is an acute infection, treatment needs to be only temporary and thus may be acceptable if the adverse reactions are low.

U.S. Food and Drug Administration (FDA)-approved drugs

Currently, there are four FDA-approved drugs available for the treatment of influenza virus infections. These drugs fall into two groups, M2 ion channel inhibitors and neuraminidase inhibitors.

M2 Ion channel Inhibitors

Amantadine (Symmetrel®) and rimantadine (Flumadine®) are derivatives of adamantanes. Amantadine was approved by the FDA in 1966 for the treatment of influenza A infections. Rimantadine which exhibits increased potency over amantadine was approved by the FDA in 1994 (Fig. I-10). Both drugs are given orally and can shorten the duration and moderate the

severity of influenza A virus infections. They are not effective against influenza B viruses due to their different M2 protein. As mentioned earlier, M2 forms a tetrameric complex and functions as an ion channel that pumps protons across membranes. The drugs inhibit the ion channel activity of the M2 and thus prevent the acidification of the virion during the entry step and eventually the release of the viral genome into the cytosol. Viruses easily gain resistance to both drugs by mutating residues in the transmembrane domain, preferentially at position 31 from a serine to an asparagine. In the influenza seasons 2008/09 and 2009/10, all circulating H3N2 viruses as well as the currently circulating 2009 pandemic H1N1 virus were resistant to adamantanes, which restricted the clinical use of amantadine and rimantadine. There are efforts to develop novel adamantane derivatives that are less likely to result in resistance by the virus.

Fig. I-10. Chemical structures of M2 ion channel inhibitors amantadine and rimantadine.

Neuraminidase Inhibitors

Oseltamivir (Tamiflu®) and zanamivir (Relenza®) were approved by the FDA in 1999 for the treatment of infections with both influenza viruses A and B (Fig. I-11). Tamiflu is taken orally whereas Relenza has to be inhaled. The common feature of these drugs is the inhibition of NA of both influenza A and B viruses by competing with sialic acid as a binding substrate. This way, newly synthesized budding viruses are trapped on the host cell membrane due to their inability to cleave off sialic acid from host glycoproteins (glycolipids). Unfortunately, seasonal H1N1 viruses acquired nearly complete resistance (99.6%) within the last four years mostly due to a mutation in the NA at position 274 from a histidine to a tyrosine. However, the 2009 pandemic H1N1 strain is still sensitive to oseltamivir. There are only a few reports for zanamivir-resistant

isolates of influenza viruses (Tab. I-1). However one of the drawbacks of zanamivir is the difficulty of its administration. Also, it has been reported that the inhalation of zanamivir can cause bronchospasms in patients with underlying asthma or chronic obstructive pulmonary disease (FDA, 2000).

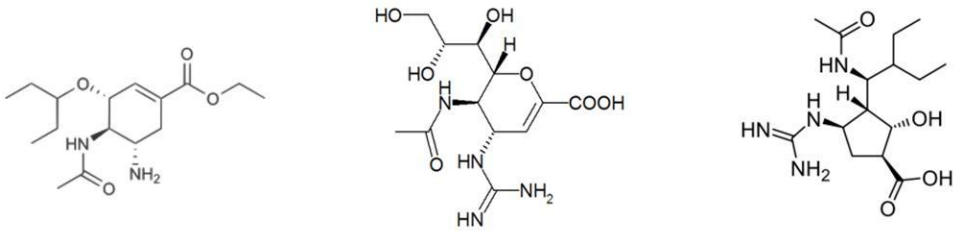

Fig. I-11. Chemical structures of neuraminidase inhibitors and their route of delivery.

Tab. I-1. Resistance of circulating influenza viruses to FDA-approved drugs for the 2008/09 and 2009/10 season. * data for seasonal influenza A and B viruses from season 2008/2009; † data for 2009 H1N1 SOIV from season 2009/10; n/a not applicable (CDC, 2010a).

	Adamantanes	Oseltamivir	Zanamivir
Influenza A Virus – Seasonal H1N1 *	0.6%	99.6%	0%
Influenza A Virus – H3N2 *	100%	0%	0%
Influenza B Virus *	n/a	0%	0%
2009 SOIV H1N1 †	100%	1.3%	0%

Drugs in development

Drugs that target the NA protein

Peramivir, a neuraminidase inhibitor (Fig. I-11) in clinical phase III studies, was authorized in 2009 for the emergency treatment of patients with known or suspected 2009 H1N1 influenza. The drug is administered intravenously in cases where other methods of treatment are ineffective or unavailable, e.g. a patient is unable to take oseltamivir via the oral route and zanamivir via the inhalation route.

CS-8958 (Laninamivir), the pro-drug of R-125489, is structurally related to zanamivir and targets the neuraminidase. It inhibits various type A and B influenza viruses including N1-N9 subtypes and oseltamivir-resistant viruses (Kubo et al.). Therapeutic and prophylactic *in vivo* efficacy was shown to be similar to zanamivir when administered intranasally (Kiso et al.).

Drugs that target the viral polymerase

Favipiravir (T-705) and its derivatives T-1105 and T-1106 (Fig. I-12) are antiviral compounds that are believed to be converted to the ribofuranosyl triphosphate form by host cell enzymes and inhibit the viral RNA-dependent RNA polymerase of influenza A, B and C viruses (Furuta et al., 2002). As of now, the antiviral mechanism of T-705 is yet not fully understood. The active form may inhibit the viral RNA-dependent RNA polymerase directly or it may be incorporated into viral RNA causing lethal hypermutations. However, its *in vivo* efficacy was not only demonstrated for influenza viruses (A, B and C) but also for several other RNA viruses such as flaviviruses (West Nile Virus, Yellow Fever Virus), bunyaviruses (Punta Toro Virus, Rift Valley Fever), arenaviruses (Pichinde Virus) and picornaviruses (Foot-and-mouth disease virus) (Furuta et al., 2009).

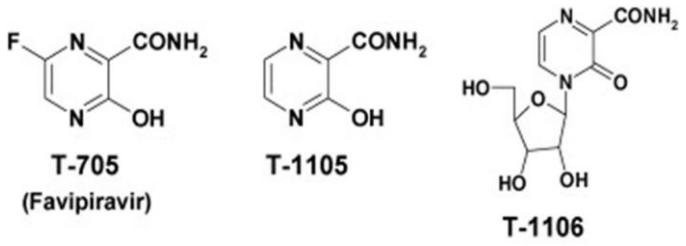

Fig. I-12. Chemical structure of favipiravir (T-705) and its derivatives T-1105 and T-1106.

Drugs that target receptor binding

Fludase (DAS-181) is a recombinant fusion protein that inactivates sialic receptors in the airway epithelium, therefore preventing viral entry into cells. The fusion protein consists of two parts: a sialidase plus a cell-surface anchoring domain, designed to attach to the respiratory epithelium, thereby increasing retention time and drug potency. Fludase prevents in addition to influenza virus also parainfluenza virus from both infecting the human body and amplifying in already-infected individuals. Fludase was shown to inhibit the 2009 pandemic H1N1 virus *in vitro* (Triana-Baltzer et al., 2009) and protects mice prophylactically and therapeutically from lethal H5N1 infections (Belser et al., 2007).

HIGH-THROUGHPUT SCREENS

High-throughput screening (HTS) is a method to identify novel chemical entities that target a biological system of interest. It is commonly used in drug discovery and relevant to the fields of biology and chemistry. The goal of HTS is to accelerate drug discovery for example by screening large libraries often composed of hundreds of thousands of compounds (drug candidates) at a rate that may exceed thousands of compounds a day. A step further is ultra high-throughput screening (uHTS) where the number of tested compounds exceeds 100,000 per day. The assay is typically performed in micro-plates that contain 96, 384 or even 1536 wells. Robotic equipment is crucial in conducting and handling a HTS. Robots transport the assay plates from station to station for sample and reagent addition, mixing, incubation, and finally readout or detection. The biggest obstacle in developing a screening assay is its miniaturization. An assay

may work perfectly in a 6-well or even 12-well plate but the consistent reproduction of the same assay in a 384-well plate can be difficult.

METHODS AND MATERIALS

Cell lines, viruses and plasmids

Human alveolar basal epithelial (A549) cells, African green monkey kidney (Vero) cells, human kidney (293T) cells, chicken embryo fibroblast (DF1) cells, mouse embryo fibroblast (MEF) cells, Madin-Darby canine kidney (MDCK) cells and human tracheal-bronchial epithelial (HTBE) cells were obtained from the American Type Culture Collection (ATCC, Manassas, VA). A549 cells, Vero cells, 293T cells, DF1 cells and MEF cells were cultured in Dulbecco's modified Eagle's medium (DMEM) (Invitrogen Corp., Carlsbad, CA) supplemented with 10% fetal bovine serum (FBS) (HyClone; South Logan, UT) and 100 U/mL penicillin G sodium and 100 µg/mL streptomycin sulfate (Invitrogen Corp., Carlsbad, CA). MDCK cells were cultured in Minimum Essential Medium (MEM) (Invitrogen Corp., Carlsbad, CA) supplemented with 10% FBS, 2 mM L-glutamine (Invitrogen Corp., Carlsbad, CA), 100 U/mL penicillin G sodium and 100 mg/L streptomycin sulfate and 0.15% $NaHCO_3$ (Invitrogen Corp., Carlsbad, CA). HTBE cells were cultured in Bronchial Epithelial Cell Growth Medium (BEGM) supplemented with the BEGM SingleQuot kit (Lonza).

Influenza viruses A/WSN/33 and B/Yamagata/88 were grown in MDCK cells in MEM-post-infection medium (MEM supplemented with 0.3% bovine serum albumin (BSA), 0.1% FBS, 2 mM L-glutamine, 100 U/mL penicillin G sodium and 100 µg/mL streptomycin sulfate and 0.15% $NaHCO_3$). Viruses were titered by standard plaque assay in MDCK cells. Sindbis virus (SINV) and vesicular stomatitis virus expressing the green fluorescence protein (VSV-GFP) were grown in Vero cells in DMEM-post-infection medium (DMEM supplemented with 0.3% bovine serum albumin (BSA), 0.1% FBS, 100 U/mL penicillin G sodium and 100 µg/mL streptomycin sulfate). Both viruses were titered by standard plaque assay in Vero cells. Newcastle disease virus strain B1 (rNDV/B1) was grown in 10-day-old embryonated hens' eggs and titered in DF1 cells. The human isolates influenza viruses A/HongKong/68, A/Victoria/3/75, A/Texas/91, A/Moscow/10/99, A/Wyoming/03/2003 and the labratory strains influenza viruses A/PR/8/34 and A/Udorn/72 were grown in 8-day-old embryonated hens' eggs and titered in MDCK cells.

The recombinant influenza viruses A/PR/8/34, A/PR/8/34 (NP P283S), A/WSN/33 and A/WSN/33 (NP D51G; NP S283P; NP V285I), the HA-modified A/VN/1203/04 and the 6:2 influenza A/PR/8/34 virus reassortant expressing a low virulence hemagglutinin (HA) and the neuraminidase (NA) of influenza A/VN/1203/04 virus (referred to as H5N1/PR8) (Park et al., 2006; Steel et al., 2008) were rescued using reverse genetics (Fodor et al., 1999). The HA of influenza A/VN/1203/04 virus was mutated by removing the multibasic cleavage site which is associated with high pathogenicity in chickens (Senne et al., 1996). The viruses were grown in 8-day-old embryonated hens' eggs and titered in MDCK cells.

For the construction of the influenza mini-genome reporter (pPolI-wtLuc and pPolI-358Luc) the firefly luciferase open reading frame from pGL3 (Promega Corp., Madison, WI) was amplified by PCR and the 5' and 3' ends of the cRNA promoter of the influenza A/WSN/33 virus NP segment were incorporated on either end (Neumann and Hobom, 1995). This product was then inserted into the pPolI vector (Pleschka et al., 1996) with the luciferase gene in the negative sense. For pPolI-358Luc, mutations at position 3, 5 and 8 at the 3'-end of the reporter (vRNA promoter) were introduced by site directed mutagenesis using the QuickChange XL site-directed mutangenesis Kit (Invitrogen) according to the specifications of the manufacturer.

High-throughput screening

The assay was performed in duplicate using solid white 384-well tissue culture treated plates (Corning Life Sciences; Lowell, MA). A549 cells were cultured to 90% confluency, trypsinized with 0.05% Trypsin-EDTA (Invitrogen Corp., Carlsbad, CA), and resuspended in phenol red-free DMEM growth medium supplemented with 10% FBS at $7.2x10^5$ cells/mL. Transfections were done in bulk and for each well, 12.5 ng of the reporter pPolI-358Luc was diluted in 6.25 µL OptiMEM (Invitrogen Corp., Carlsbad, CA) and mixed with 6.25 µL OptiMEM containing 0.025 µL Lipofectamine2000 (Invitrogen Corp., Carlsbad, CA). The transfection mix was incubated for 20 min before adding 12.5 µL of resuspended A549 cells (approximately $9x10^3$ cells). The medium

also included 0.25 µg/mL Scriptaid (BIOMOL, Plymouth Meeting, PA) and 1.0 µg/mL 5-aza-2-deoxycytidine (Sigma-Aldrich; St.Louis, MO), which were added to enhance reproducibility of the assay (Hellebrekers et al., 2007). The mix of cells and reporter DNA was transferred into 384-well plates using the Matrix Wellmate plate filler. Loaded plates were subsequently centrifuged at 1000 rpm for 5 min to ensure an equal distribution of cells within each well. The cells were incubated for 18 hours at 37°C, 5% CO_2, 95% humidity before the addition of 100 nL of compounds by the Epson compound transfer robot (Epson America, Inc.; Long Beach, CA). The cells were incubated for a further 6 hours before infection with influenza A/WSN/33 virus directly into the medium at an MOI of 2.5. The virus was added automatically to the plates using the Matrix Wellmate plate filler and the plates were subsequently centrifuged at 1000 rpm for 2 min. Each plate also contained mock-infected cells that were used as a positive control and cells that were infected but untreated, which were used as a negative control. The two approved classes of influenza antiviral drugs could not be used as positive controls in this screen because i) influenza A/WSN/33 virus is resistant to amantadine and ii) the assay does not detect multicycle replication which is necessary to see the effects of oseltamivir as it targets virus release. Infection was allowed to proceed for 18-20 hours at 37°C, 5% CO_2, 95% humidity. At that time 50% of the medium in each well was removed and the plates were equilibrated to room temperature for at least 20 min. The Matrix Wellmate plate filler was used to add 16 µL of BrightGloLuciferase reagent (Promega Corp., Madison, WI) to each well automatically and following a 2 min centrifugation at 2000 rpm, luminescence was measured for 0.1 s/well with the EnVision2 plate reader (Perkin Elmer Inc., Waltham, MA).

To eliminate cytotoxic compounds that appear as false positives, a counter screen was performed in parallel. This consisted of A549 cells transfected with pGL3 and seeded at a density of 2500 cells per well of a 384-well plate. The remainder of the assay was performed as described above except that the cells were not infected.

Data analysis

To evaluate the robustness of the HTS assay, 384-well plates containing no compounds were run separately on two different days. Statistical parameters were determined as follows: $Z' = 1 - ((3\sigma_i + 3\sigma_m)/|\mu_i - \mu_m|)$, where μ_i is the mean signal for the negative control (infected cells), σ_i the standard deviation for the negative control, μ_m the mean signal for the positive control (mock infected cells), and σ_m is the standard deviation for the positive control. The percent coefficient of variation (CV) = σ_i/μ_i x100, the signal-to-background ratio (S/B) = μ_i/μ_m and the signal-to-noise ratio (S/N) = $(\mu_i - \mu_m)/((\sigma_i)^2 + (\sigma_m)^2)^{1/2}$ (Zhang et al., 1999), (Ghosh et al., 2005).

The data from the influenza HTS assay and counter screen were analyzed with Microsoft Office Excel. The average of the negative control of each plate was set at 100% luminescence and the percent luminescence of each compound-containing well was determined in relation to this internal control. The average percent luminescence for the duplicate screenings was calculated and the compounds were classified into strong or medium inhibitors based on a 90-100% or 70-89% reduction in luminescence, respectively. Compounds leading to an increase in luminescence were considered as enhancers with at least a 2 fold induction above the negative control. The HTS data were compared to the corresponding data from the counter screen. A reduction in luminescence greater than 20-30% in the counter screen was considered to be caused by cytotoxicity and therefore the compound was defined as a false positive and eliminated from further analysis. This threshold was decreased down to 50% in cases where the compound caused a > 95% reduction of luminescent signal in the influenza HTS assay.

Small molecular weight compounds

Chapter II – Screening known bioactive compounds

The Prestwick Chemical Library (1120 compounds; Prestwick Chemical, Inc., Washington, DC), the NINDS custom collection 2 (1040 compounds; National Institute of Neurological Disorders and Stroke; Bethesda, MD) and BIOMOL Known Bioactives-2 library (480 compounds; BIOMOL, Plymouth Meeting, PA) were provided by The Institute of Chemistry and Cell Biology (ICCB), National Screening Laboratory for the Regional Centers of Excellence in Biodefense and Emerging Infectious Disease (NSRB) (Harvard University, Boston, MA). The compounds were dissolved in DMSO at 2 mg/mL for the Prestwick library, 5 mg/mL for the BIOMOL2 library and at 10 mM for the NINDS2 library.

For secondary analyses 2',4'-dichlorobenzamil and SDZ-201106 were purchased from BIOMOL (Plymouth Meeting, PA) while 3',4'-dichlorobenzamil, phenamil, phorbol 12-myristate 13-acetate (PMA), mezerein, rottlerin, lasalocid, staurosporin, ouabain, lanatoside C and digitoxigenin were purchased from Sigma-Aldrich (St.Louis, MO). All compounds were dissolved in either H_2O or dimethyl sulfoxide (DMSO) to a stock concentration of 10mM. The final concentration of DMSO in the culture medium did not exceed 0.004%.

Chapter III – Screening compounds of unknown biological properties

The Asinex 1 library (12,378 compounds screened; ASINEX Corp., Winston-Salem, NC), the Biomol TimTec 1 library (8,517 compounds screened; TimTec Inc., Newark, DE), the ChemBridge 3 library (10,560 compounds screened; ChemBridge Corp., San Diego, CA), the ChemDiv 3, 4 and 5 libraries (17,686 compounds screened; ChemDiv Inc., San Diego, CA), the Enamine 2 library (352 compounds screened; ENAMINE Ltd., Kiev, Ukraine), the LifeChemicals 1 library (3,893 compounds screened; Life Chemicals Inc., Burlington, Canada) and the MayBridge 4 and 5 libraries (7,788 compounds screened; Maybridge Ltd., Cornwall, UK) were provided by The Institute of Chemistry and Cell Biology (ICCB), National Screening Laboratory for the Regional Centers of Excellence in Biodefense and Emerging Infectious Disease (NSRB) (Harvard University, Boston, MA). The compounds were dissolved in DMSO at 5 mg/mL.

For secondary analyses compounds were purchased from ASINEX Corp. (Winston-Salem, NC) TimTec Inc. (Newark, DE), ChemBridge Corp. (San Diego, CA), ChemDiv Inc. (San Diego, CA), Life Chemicals Inc. (Burlington, Canada) and Maybridge Ltd. (Cornwall, UK). All compounds were dissolved in dimethyl sulfoxide (DMSO) to a stock concentration of 10, 20 or 50mM. The final concentration of DMSO in the culture medium did not exceed 0.1%. Ribavirin was purchased from Sigma-Aldrich (St.Louis, MO) and diluted in water to a stock concentration of 100mM.

Cell viability assay

Chapter II - Screening known bioactive compounds

The CellTiter 96 AQ_{ueous} One Solution Cell Proliferation Assay (referred to as the MTS assay in this study) (Promega Corp., Madison, WI) was used to detect cell viability according to the specifications of the manufacturer. Briefly, A549 cells were seeded into 96-well plates (Corning Life Sciences, Lowell, MA) at $1.25x10^3$ cells per well and allowed to incubate for 24 hours at 37°C, 5% CO_2. After incubation, the medium was aspirated and replaced with 100 µL of fresh DMEM containing the compounds at various concentrations. Following a further 24 hour incubation, the MTS solution was added to each well and left to incubate for 2 hours before measuring absorbance at 450 nm using a Beckman Coulter DTX 880 plate reader (Beckman Coulter, Inc., Fullerton, CA).

Chapter III – Screening compounds of unknown biological properties

The CellTiterGlo Cell Viability Assay (Promega Corp., Madison, WI) was used to detect cell viability according to the specifications of the manufacturer. Briefly, A549 cells were seeded into 96-well plates (Corning Life Sciences, Lowell, MA) at $1.25x10^3$ cells per well and allowed to incubate for 24 hours at 37°C, 5% CO_2. After incubation, the medium was aspirated and replaced with 100 µL of fresh DMEM containing the compounds at various concentrations. Following a further 24 hour incubation, the same volume of the CellTiterGlo solution was added to each well and left to incubate for 5 min before

measuring luminescence using a Beckman Coulter DTX 880 plate reader (Beckman Coulter, Inc., Fullerton, CA).

Viral growth assays in the presence of inhibitors or enhancers

Chapter II - Screening known bioactive compounds

A549 cells were seeded into 6-well plates at $5x10^5$ cells per well. After incubation for 24 hours at 37°C and 5% CO_2, the cells were washed with phosphate buffered saline (PBS) (Invitrogen Corp., Carlsbad, CA) and the medium was replaced with DMEM post infection medium containing the compound of interest. Compounds that enhance viral replication were used at their most potent concentration (400 nM for 2',4'-dichlorobenzamil and 3',4'-dichlorobenzamil, 10 µM for phenamil, 250 nM for mezerein and 250 nM for PMA). Compounds that inhibit viral replication were used at their most potent, but non-toxic, concentration (12.5 µM for SDZ-201106, 1.25 µM for lasalocid and for rottlerin). Cardioactive glycosides were tested at concentrations that maintained at least 80% cell viability (20 nM for ouabain, 78 nM for lanatoside C and 320 nM for digitoxigenin). The cells were incubated in the compound-containing media for 4-6 hours prior to infection. When testing the response of influenza A/WSN/33 virus and of H5N1/PR8 virus to enhancers in A549 cells, infections were done at a multiplicity of 0.001 in order to observe a potential increase in viral replication. In contrast, a high multiplicity of 1 was used when testing the response of influenza A/WSN/33 virus to inhibitors. Testing enhancers in Vero cells, infections of influenza A/WSN/33 virus were done at a multiplicity of 0.0001. For the human isolates, influenza viruses A/Texas/91, A/Moscow/10/99, A/Wyoming/03/2003 and A/Vietnam/1203/04 infections were done at an MOI of 0.01 when testing enhancers. For influenza B/Yamagata/88 virus, infections were done at a multiplicity of 5 when testing inhibitors and a multiplicity of 0.1 when testing enhancers. Compounds were absent during the 1 hour incubation with the virus but were present in the DMEM post-infection medium (DMEM supplemented with 0.3% BSA, 0.1% FBS and 100 U/mL penicillin G sodium and 100

µg/mL streptomycin sulfate). For infection with influenza B virus, the human influenza A virus isolates and the H5N1/PR8 virus this post-infection medium also contained 1 µg/ml TPCK-treated trypsin (Sigma-Aldrich; St.Louis, MO). The infected cells were incubated at 37°C with the exception for influenza B virus infected cells, which were incubated at 33°C. The viral titers for all viruses were determined at various times post infection by standard plaque assay in MDCK cells. When testing the effects of the cardioactive glycosides on the growth of NDV and VSV-GFP, infections were performed at an MOI of 1. Viral titers were determined at 24 hours post infection by standard plaque assay in Vero cells for VSV-GFP and in DF1 cells for NDV/B1. The NDV plaques were visualized by immuno-staining with an anti-NP antibody (Matrosovich et al., 2006).

Chapter III – Screening compounds of unknown biological properties

A549 cells were seeded into 12-well plates at $2x10^5$ cells per well. After incubation for 24 hours at 37°C and 5% CO_2, the cells were washed with PBS (Invitrogen Corp., Carlsbad, CA) and the medium was replaced with DMEM post-infection medium supplemented with the compounds of interest at their CC_{10} (concentration of 90% cell viability). The cells were incubated in the compound-containing media for 4-6 hours prior to infection. Infections were performed at an MOI of 0.01 and 1. Compounds were absent during the 1 hour incubation with the virus but were present in the post-infection medium. The infected cells were incubated at 37°C with the exception for influenza B virus infected cells, which were incubated at 33°C. The viral titers of tested influenza viruses were determined at various times post infection first by hemagglutination assays using chicken red blood cells followed by standard plaque assays in MDCK cells. When testing the effects of compounds on the growth of SINV and NDV, infections were performed at an MOI of 1 and for VSV-GFP at 0.01. Viral titers were determined at 24 hours post infection by standard plaque assay in Vero cells for SINV and VSV-GFP and in DF1 cells for NDV/B1. The NDV plaques were visualized by immuno-staining with an anti-NP antibody (Matrosovich et al., 2006).

Generation of escape mutants by passaging influenza virus in A549 cells

Chapter II - Screening known bioactive compounds

A549 cells were seeded into 6-well plates at $5x10^5$ cells per well and incubated overnight at 37°C and 5% CO_2. Next, they were infected with influenza A/WSN/33 virus at an MOI of 0.01, followed by an incubation period of 48 hours at 37°C and 5% CO_2. Cells were incubated for 4 hours prior to infection with DMEM post-infection medium supplemented with compounds at a non-toxic concentration (SDZ-201106 at 10µM and rottlerin at 1 µM) or DMSO. After removal of the virus inocula, supplemented DMEM was re-added. Viral titers were determined by standard plaque assay in MDCK cells and accordingly diluted for a next round of infection under the same conditions.

Chapter III – Screening compounds of unknown biological properties

A549 cells were seeded into 6-well plates at $5x10^5$ cells per well and incubated overnight at 37°C and 5% CO_2. Next, they were infected with influenza A/WSN/33 virus at an MOI of 0.01, followed by an incubation period of 48 hours at 37°C and 5% CO_2. Cells were incubated for 4 hours prior to infection with DMEM post-infection medium supplemented with compounds at a semi-inhibitory concentration (C2 at 2 µM, A3 at 500 nM and A35 at 8 µM) or DMSO. After removal of the virus inocula, supplemented DMEM was re-added. Viral titers were determined by performing HA assays and accordingly diluted for a next round of infection under similar conditions. The compound concentration was increased from passage to passage if necessary. A35-resistant viruses and DMSO-passaged viruses of the same passage were plaque purified on MDCK cells. Viral RNA of 10 individual clones was extracted and their NP and PB2 segments were sequenced at the Mount Sinai DNA Core Sequencing facility.

Entry assay using pseudotyped lentiviral particles (PPs)

All pseudotyped lentiviral particles (Flu-PP, VSV-PP and MuLV-PP) were kindly provided by Dr. Matthew Evans (MSSM, Evans Lab). A549 cells were seeded into 96-well plates at $5x10^3$ cells per well and incubated overnight at 37°C, 5% CO_2. VSV-PPs efficiently infected A549 cells and were used at a 1:1000 dilution. Different dilutions of Flu-PPs and MuLV-PPs were tested in order to determine equal infectivity compared to VSV-PPs. For the following assays, VSV-PPs were used at a 1:1000 dilution, Flu-PPs at a 1:100 dilution and MuLV-PPs at a 1:10 dilution of their stocks. PPs that lack glycoproteins which facilitate entry were used as a negative control at a 1:10 dilution. For the entry assay, A549 cells were seeded into 96-well plates at $5x10^3$ cells per well and incubated over night at 37°C, 5% CO_2. The medium was changed 4 hours prior to infection to DMEM supplemented with 10% fetal calf serum (FCS), 1% penicillin/streptomycin, 20mM HEPES, 4µg/mL polybrene and compound of interest at its CC_{10}. The PPs were added directly into the medium at mentioned dilutions and infections were allowed to proceed for 18 hours. Next, cells were washed 3-4 times with PBS and fresh DMEM supplemented with 10% fetal calf serum (FCS) and 1% penicillin/streptomycin was added. Following a further 24 hour incubation, the supernatant containing secreted gaussia luciferase was subjected to measuring luminescence using the *Renilla* Luciferase Assay Kit (Promega). Equal volumes of the supernatant and 2x *Renilla* luciferase lysis buffer were combined and mixed at a dilution of 1:6 with the *Renilla* luciferase substrate. The luminescence was measured using a Beckman Coulter DTX 880 plate reader (Beckman Coulter, Inc., Fullerton, CA).

Entry assay using influenza virus-like particles (VLPs)

VLPs were provided by Dr. Donna Tscherne (MSSM, Garcia-Sastre Lab) (Tscherne et al., 2009). Briefly, pCAGGS protein expression vectors encoding for influenza A/WSN/33 virus HA, NA and M1 that is fused to beta-lactamase were transfected into 293T cells. Supernatants containing released VLPs were harvested 48 hours post transfection and treated with 2µg/mL TPCK-trypsin for 20 min. This step was followed by a treatment with 10µg/mL soybean trypsin inhibitor for 10 min before VLP samples were frozen down at -80°C. For the entry assay, A549 cells were

seeded into 12-well plates at $2x10^5$ cells per well and incubated over night at 37°C and 5% CO_2. Cells were pre-treated with OptiMEM (Invitrogen) supplemented with compounds at their CC_{10} for 4 hours. Next, cells were washed with PBS and spinoculated with 250µL of VLP preparations for 90 min at 4°C (VLP inocula contained compounds at their CC_{10}). Subsequently, samples were incubated for 3-4 hours at 37°C and 5% CO_2 to allow VLP entry. Next, cells were trypsinized, harvested and subjected to the beta-lactamase assay using the LiveBLAzer™ FRET – B/G Loading Kit (Invitrogen) according to the specifications of the manufacturer.

Influenza virus induced hemolysis assay

Viruses subjected to the hemolysis assay were normalized to an HA titer of 8 wells. One volume of virus was mixed with one volume PBS containing 4% chicken red blood cells. This mix was incubated on ice for 15 min before adding 2 volumes of a citric buffer with a known pH value. The samples were subsequently incubated at 37°C for 90 min, followed by a centrifugation step to harvest the supernatant. The heme of lysed red blood cells that was released into the supernatant was quantified by measuring its absorbance at 405nm using a Beckman Coulter DTX 880 plate reader (Beckman Coulter, Inc., Fullerton, CA).

Influenza virus mini-genome assay

A549 cells were seeded into 12-well plates at $2x10^5$ cells per well and incubated overnight at 37°C and 5% CO_2. Next, they were transfected (in mono-layer) using Lipofectamin2000 (Invitrogen) with pCAGGS protein expression vectors encoding the PB1, PB2 and PA subunits of the viral polymerase (100ng of each) and the nucleocapsid protein (200ng) of influenza virus strains A/WSN/33 or A/PR/8/34. The transfection mix also contained the RNA polymerase II driven *Renilla* luciferase reporter pRLTK (Promega) (200ng) to normalize for transfection efficiency as well as the influenza virus specific, RNA polymerase I driven, firefly luciferase reporter (pPolI Luc) (150ng), described earlier. Cells were cultured in DMEM (described in chapter I) which was supplemented 4 hours prior to the transfection with compounds at their

CC_{10} or DMSO. The transfection was performed in OptiMEM (Invitrogen) which was also supplemented with compounds or DMSO. The OptiMEM was replaced 4 hours post transfection to DMEM containing compounds or DMSO. After a 24 hour incubation period at 37°C and 5% CO_2, cells were harvested and lysed using the passive lysis buffer of the Dual Luciferase Assay Kit (Promega). Luminescence of firefly luciferase and *Renilla* luciferase was subsequently measured using the Dual Luciferase Assay Kit according to the specifications of the manufacturer.

Primer Extension Assay

A549 cells were seeded into 12-well plates at $2x10^5$ cells per well. After incubation for 24 hours at 37°C and 5% CO_2, the cells were washed with PBS (Invitrogen Corp., Carlsbad, CA) and the medium was replaced with DMEM post-infection medium supplemented with DMSO or compounds A3 (2 and 10µM), A35 (5 and 10µM) and ribavirin (10 and 100µM). The cells were incubated in the compound-containing media for 4 hours prior to infection. Infections with influenza viruses A/PR/8/34 (NP wt) and A/PR/8/34 (NP P283S) were performed at an MOI of 7 (Chase et al., 2008). The infected cells were incubated at 37°C before the viral RNA was extracted at 3, 6 and 9 hours post infection using the QIAamp viral RNA kit (Qiagen), as per instruction. Primers for the RT reaction were radio-labeled with P^{32} using T4-kinase (Invitrogen) and γ-ATP according to the specifications of the manufacturer. Viral RNA (2µg per reaction) was reverse transcribed into cDNA using radio-labeled primers for v- and c/mRNA in the same reaction with the SuperScript First-Strand Synthesis System (Invitrogen) according to the specifications of the manufacturer. Samples consisting of different cDNA species were separated on a 6% SDS-PAGE that contained 5M urea. Autoradiographicfilms (World Wide Medical Products, Inc., WWMP) were exposed for 24 to 72 hours at -80°C to membranes that contained the transferred and crosslinked nucleic acid samples.

Generation of chimeric NP proteins

Protein expression vectors encoding for NP of influenza viruses A/WSN/33 and A/PR/8/34 were digested with AvrII, XcmI, SphI, BstBI restriction enzymes (New England Biolabs, NEB) individually or in combination (AvrII + XcmI, AvrII + SphI, AvrII + BstBI). NP pieces of both viruses were mixed and re-ligated using the Rapid DNA Ligation Kit (Roche) according to the specifications of the manufacturer. Re-ligated plasmids were transformed into DH5α cells, plated and incubated for 24 to 48 hours at 30°C. Next, individually clones were picked, grown up at 30°C and plasmid DNA was isolated and sequenced at the Mount Sinai DNA Core Sequencing facility. Mutations of single amino acids were introduced directly into the protein expression vectors using the QuickChange XL site-directed mutangenesis Kit (Invitrogen) according to the specifications of the manufacturer.

RNA extraction and segment specific cDNA amplification

RNA of viruses grown in MDCK cells or eggs was isolated using the QIAamp viral RNA kit (Qiagen), as per instruction. Viral RNA was reverse transcribed into cDNA using an influenza virus 3'end-specific primer and the SuperScript First-Strand Synthesis System (Invitrogen) according to the specifications of the manufacturer. The virus cDNA was used in a PCR reaction to amplify the viral segment of interest by using segment-specific primers. Briefly, samples were denatured at 95°C for an initial 3 min and amplified in 30 cycles of DNA denaturing (95°C/30 sec), primer annealing (54°C/30 sec) and DNA polymerisation (72°C/3 min). A final primer extension was performed at 72°C for 10 min. Amplified DNA samples were run together with a DNA marker on a 1% agarose gel in TAE supplemented with 2 µl ethidium bromide and photographed under ultraviolet light. Bands of interest were excised; the DNA was purified using the PCR Purification Kit (Qiagen) and send for sequencing using the Mount Sinai DNA Core Sequencing facility.

Reverse Genetics for recombinant viruses

The reverse genetics technique for the generation of recombinant influenza viruses has been described previously (Fodor et al., 1999). Briefly, 293T cells were transfected with eight pPolI vectors encoding the viral genomic RNA segments for the influenza A/WSN/33 virus (PB1, PB2, PA, NP, HA, NA, M, NS) and four pCAGGS protein expression vectors encoding its subunits of the viral polymerase (PB1, PB2, PA) and the nucleocapsid protein (NP). For the mutant viruses, the pPolI vector encoding the NP segment was mutated as follows: D51G, S283P or V285I. Mutations were introduced using the QuickChange XL site-directed mutangenesis Kit (Invitrogen) according to the specifications of the manufacturer. The supernatant was 24 hours later transferred onto MDCK cells that were seeded in 6-well plates to near confluence. The virus was allowed to replicate for 24 to 48 hours before it was isolated by plaque purification on MDCK cells. The rescue of recombinant influenza A/PR/8/34 viruses was similar but instead of pPolI plasmids for each segment, the ambisense pDZ plasmids were used. Another difference was that transfected 293T cells were injected into 8 day old embryonated chicken eggs that were incubated for 48 hours at 37°C. Harvested allantoic fluid was subjected to assay for hemagglutination and virus was isolated by plaque purification on MDCK cells. The RNA of all rescued, plaque purified viruses was extracted and the NP segment sequenced. All samples were sequenced at the Mount Sinai DNA Core Sequencing facility.

Viral growth kinetics

A comparison of viral growth kinetics for the recombinant wild type (A/WSN/33 and A/PR/8/34) and the NP mutant viruses (N51G, S283P and V285I in A/WSN/33 and P283S in A/PR/8/34) was undertaken in A549 cells. A549 cells were seeded into 12-well plates at $2x10^5$ cells per well and incubated overnight at 37°C and 5% CO_2. Next, they were infected with each virus at an MOI of 0.01. Infected cells were maintained in DMEM post-infection medium. The viral titers of all recombinant viruses were determined by plaque assays for the 24, 48 and 72 hour time points; the growth curves for the A/PR/8/34 viruses contained in addition the 12, 36, 48 and 60 hours time points.

Western Blot

A549 cells were compound treated and infected as described earlier. Cell extracts were made 24 hours post infection in lysis buffer: 50mM Tris pH=8, 0.5% NP-40, 300mM NaCl, 25% glycerol, 0.007% 2-mercaptoethanol, 1xPMSF, 0.1mM Va_3NO_4 and Complete protease inhibitor cocktail (Roche). 10uL of protein lysates were loaded onto pre-casted 10% SDS-polyacrylamide gels (Biorad). Separated proteins were probed for analysis of the NP and of the M1 and M2 proteins with rabbit polyclonal antibodies (1:1000). The secondary horseradish peroxidase (HRP) labeled antibody (GE Healthcare) was used in a 1:1000 dilution.

Co-immunoprecipitation (Co-IP)

A549 cells were transfected with the influenza A/PR/8/34 mini-genome as described earlier or with pCAGGS protein expression vectors encoding for PB2 and NP of the influenza A/PR/8/34 virus. In both experiment the wild type NP and the mutated NP (P283S) were employed. A35 at different concentrations or DMSO as control was added 4 hours prior to the transfection and present throughout the transfection. Cells were harvested 24 hours later and extracts were made in lysis buffer: 50mM Tris pH=8, 0.5% NP-40, 300mM NaCl, 25% glycerol, 0.007% 2-mercaptoethanol, 1xPMSF, 0.1mM Va_3NO_4 and Complete protease inhibitor cocktail (Roche). 1% of the whole cell extract (WCE) was subjected to probe for the analysis of NP and PB2 proteins with rabbit polyclonal antibodies (1:1000). All samples were normalized to β-actin which was probed by using a mouse monoclonal antibody (1:1000). The majority of the WCE (95%) was pre-cleaned by incubating with Protein G beads (Invitrogen) overnight at 4°C. After a centrifugation step, the pre-cleaned supernatant was incubated for 8 hours at 4°C with an NP mouse monoclonal antibody (HT103) at a concentration of approximately 15ng/µL before Protein G beads were added. The samples were incubated overnight at 4°C, followed by at least 5 washes with lysis buffer before subjected to western blot analysis to probe for NP and PB2 as described earlier.

Immunofluorescence (IF)

A549 cells were seeded onto coverslips in 24-well plates at $7x10^4$ cells per well and incubated overnight at 37°C and 5% CO_2. The medium was replaced with DMEM post-infection medium supplemented with either compounds of interest at their CC_{10} or DMSO. The cells were incubated in the compound/DMSO-containing media for 4 hours prior to infection. Infection with influenza A/WSN/33 virus was performed at an MOI of 1. Compounds were absent during the 1 hour incubation with the virus but were present in the post-infection medium (same medium preparation that was used for pre-incubation) or added at 4 hours post infection. Infected cells were incubated at 37°C and 5% CO_2 for 7 hours before being fixed with 3% paraformaldehyde (PFA) diluted in water. Cells were permeabilized in 0.5% Triton-X-100 diluted in PBS for 5 min. The primary antibodies were diluted in PBS containing 5% BSA. A rabbit-polyclonal NP antibody was used at a 1:1000 dilution whereas a mouse-monoclonal M1 antibody (E10) was used at a 1:500 dilution. After 1 hour incubation, cells were washed before adding the secondary antibodies at a 1:1000 dilution. The rabbit specific antibody was labeled with a green dye (Alexa Fluor 488, Invitrogen) that emits at a wavelength of 519nm and the mouse specific antibody was labeled with a red dye (Alexa Fluor 568, Invitrogen) which emits at 619nm. The secondary antibody solution contained in addition DAPI (4',6'-diamidino-2-phenylindole) at a 1:1000 dilution. After an hour incubation, cells were washed and coverslips mounted on glass slides, to be subjected to confocal microscopy.

In vivo studies

Six-week-old female Balb/C mice (Jackson Laboratories) were anesthetized with intraperitoneal injection of 0.1mL of ketamine/xylazine (15µL ketamine and 15µL xylazine), and infectious virus was diluted in PBS and inoculated intranasally in a volume of 35µL. Antiviral compounds and oseltamivir were dissolved in vehicles of choice and administered intraperitoneally or intranasally either twice daily or three times daily. Compound treatment started 12 hours prior to infection and continued for up to 5 days post infection. To assess virus pathogenicity, groups of 3 or 5 mice were inoculated with appropriate dose and monitored daily for weight loss over

10 days. Mice that lost more than 25% of their initial body weight were killed according to institutional guidelines and scored as dead. To determine viral replication in lungs, they were collected on days 3 or 5 post infection. Lungs were homogenized in PBS and processed for virus titering. Virus titers in the supernatant of lung homogenates were determined by plaque assay in MDCK cells.

CHAPTER 1 – DEVELOPMENT OF A HIGH-THROUGHPUT SCREEN

INTRODUCTION

The goal of the project was to identify small molecular weight compounds that can negatively or positively affect influenza A virus replication. Compounds that inhibit the replication of the virus are potential anti-virals. On the other hand, compounds that increase viral replication may be potential enhancers that can be used for boosting the production of vaccines in tissue culture.

The outline to develop a high-throughput screen assay was as follows:

1. Design an influenza virus reporter and show its activation upon infection.
2. Test different cell lines and viruses in order to find the optimal conditions.
3. The reporter signal has to be robust, reproducible and specific for influenza virus.
4. Optimize assay conditions, e.g. number of cells seeded per well, amount of reporter plasmid transfected, multiplicity of infection (MOI) and time of read-out.
5. Re-optimize the assay after the miniaturization from a 96-well plate format into a 384-well plate format.
6. Run a pilot study and confirm the assay by screening known bioactive compounds.

Design of an influenza virus specific reporter plasmid and its in vitro verification

We designed an influenza mini-genome encoding firefly luciferase in the negative sense in between the 3' and 5' non-coding regions (NCR) of the influenza A/WSN/33 virus NP segment. This construct was cloned into a plasmid flanked by a human RNA polymerase I promoter and the hepatitis D virus (HDV) ribozyme (Fig. 1-1).

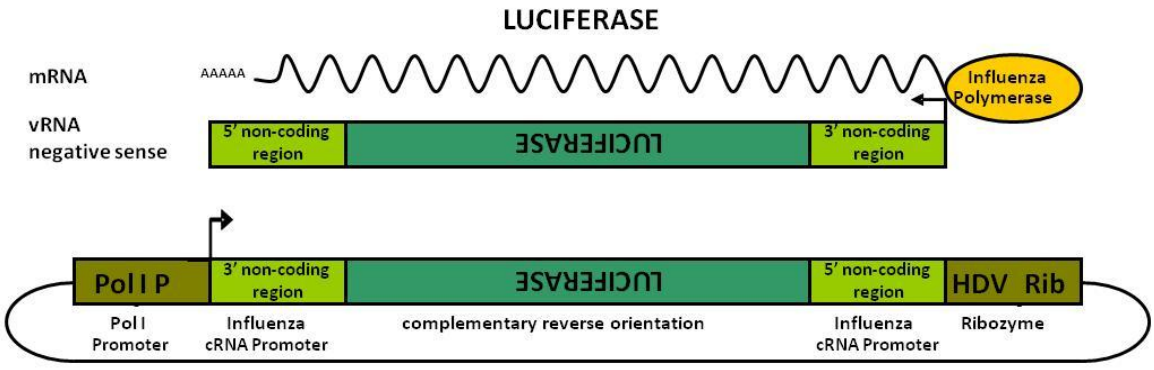

Fig. 1-1. Schematic of an influenza virus specific firefly luciferase reporter plasmid. Transcription of the reporter plasmids generates negative sense vRNA that is recognized by the viral polymerase which in turn transcribes luciferase mRNA.

Upon transfection of this reporter into a human cell line, RNA polymerase I transcription generates an RNA segment that mimics viral RNA. When these cells are subsequently infected with influenza virus, the viral polymerase recognizes this segment by its NCRs that resemble the viral promoter. It is important to note that we mutated the vRNA promoter (3'-end) of the reporter gene at position 3, 5 and 8 and converted it thus into a cRNA promoter. The cRNA promoter is reported to be more efficient compared to the vRNA promoter (Neumann and Hobom, 1995) and results in an increased mRNA production (Fig. 1-2)

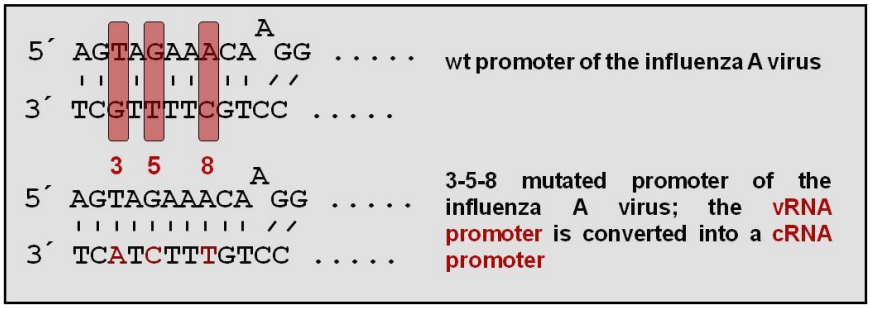

Fig. 1-2. Schematic of the influenza virus promoter region.

The infected cells translate the reporter mRNA into luciferase whose activity therefore serves as a measurement of influenza virus replication. The reporter containing the 3-5-8 mutations in its promoter region is highly advantageous compared to the reporter that contains the wt promoter, as seen in (Fig. 1-3).

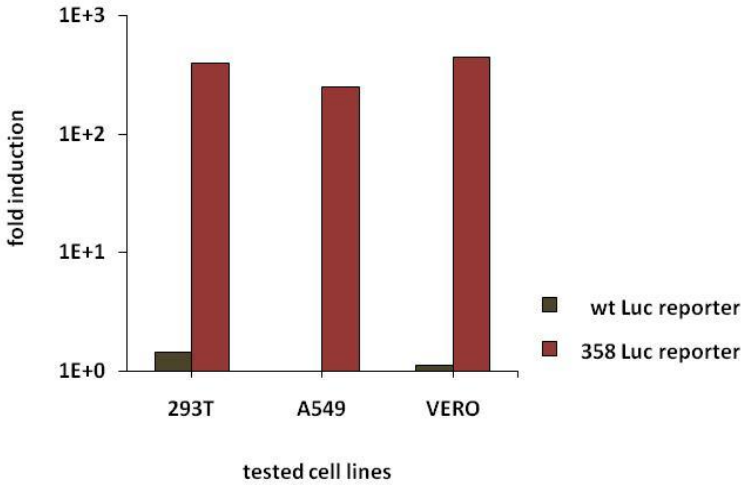

Fig. 1-3. Induction of influenza virus specific reporters upon infection with influenza virus. 293T, A549 and Vero cells were transfected with an influenza virus specific luciferase reporter plasmid that contains either the wild type or the mutated influenza virus promoter. Infection with influenza A/WSN/33 virus was performed at a MOI=3 and reporter activation was measured 24 hours post infection. Reporter activation is depicted as fold induction over mock infected cells.

Transfection of both reporter constructs into different cell lines followed by infection with an influenza A virus led to the induction of the 3-5-8 reporter but not of the wt reporter. It was

also shown that the reporter RNA alone, in the absence of the viral polymerase, is not processed hence there is no signal detectable in mock infected cells. We tested the influenza virus laboratory strains A/WSN/33 (H1N1) and A/Udorn/72 (H3N2) for their ability to induce the reporter in different cell lines. 293T cells (human kidney cells), A549 cells (human lung epithelial cells) and Vero cells (African green monkey kidney cells) were transfected with the reporter plasmid followed by infection with either WSN or Udorn at different MOIs (Fig. 1-4).

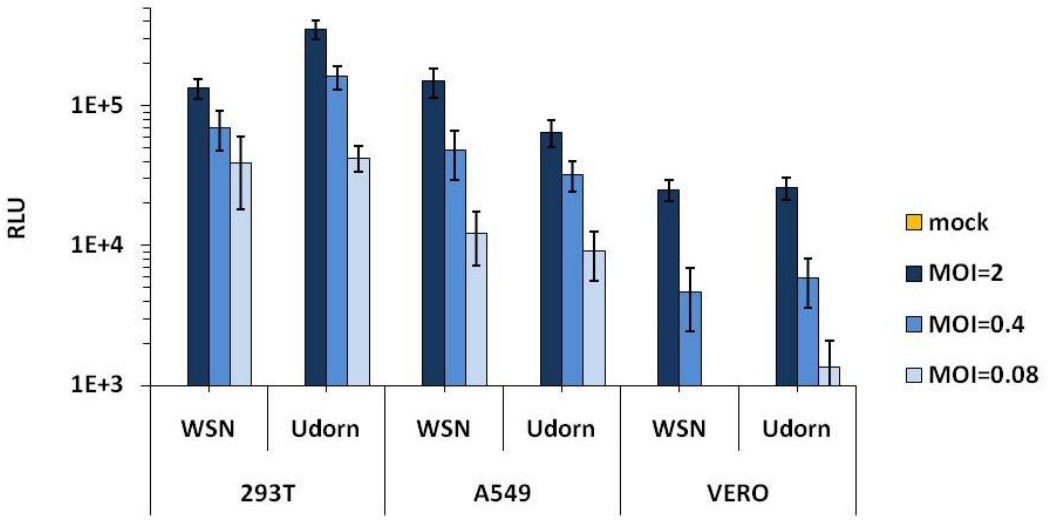

Fig. 1-4. Induction of an influenza virus specific reporter upon infection with influenza viruses. 293T, A549 and Vero cells were transfected with an influenza virus specific luciferase reporter plasmid followed by infection with influenza viruses A/WSN/33 and A/Udorn/72. Infections were performed at different MOIs and reporter activation was measured 24 hours post infection. The assay was performed in triplicate and is presented as the mean ± standard deviation.

Udorn causes a 2-3 fold higher induction of the reporter compared to WSN in 293T cells. However, in A549 cells WSN shows a higher induction compared to Udorn. Both viruses behave similarly in Vero cells but the overall reporter activation is reduced compared to the other two cell lines, perhaps due to lower transfections efficiency. Given that lung epithelial cells are a biologically relevant cell type for influenza virus infection, we decided to use A549 cells in combination with WSN for further experiments.

Optimization of the reporter assay in 96-well and 384-well plates

Next, we performed the assay in 96-well plates to determine the well-to-well signal reproducibility. Within this format, well-to-well variations in the number of seeded cells and the number of infected cells, will impact the overall standard deviation dramatically. To avoid this problem, we transfected and seeded cells in bulk and infected at a relatively high MOI of 2. For the purpose of developing a screen to identify antiviral compounds; using a high MOI that prevents multicycle replication of the virus also prevents the detection of inhibitors of late stages in the replication cycle such as assembly, budding and release. Nevertheless, all steps up to and including translation (binding, entry, uncoating, fusion, replication) are accessible. In a time course experiment it was determined at what time post infection the reporter activity peaks (Fig. 1-5)

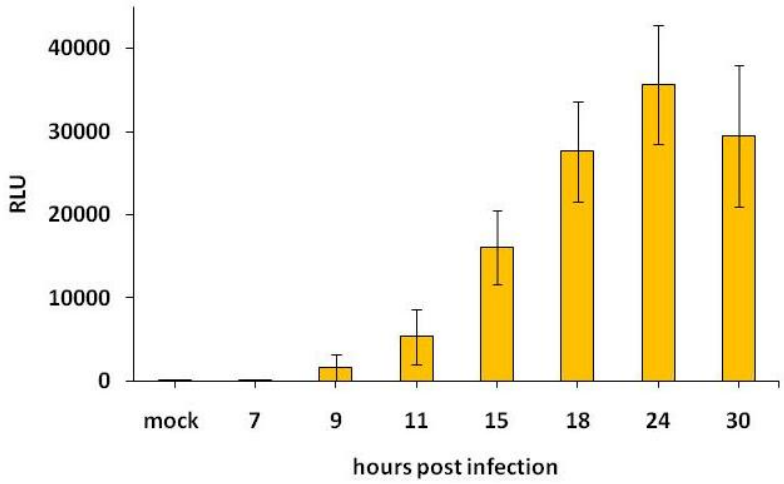

Fig. 1-5. Induction of an influenza virus specific reporter upon infection with influenza virus at different time points. A549 cells were transfected with an influenza virus specific luciferase reporter plasmid followed by infection with influenza A/WSN/33 virus. Infections were performed at a MOI of 2 and reporter activation was measured at indicated time points post infection. The assay was performed in decuplicate and is presented as the mean ± standard deviation.

Reporter activity is detected first at 9hpi, increases linearly over time and peaks at around 24hpi before the signal declines. The decrease of the reporter activity at later time points is most likely due to cell death. The standard deviation at 18hpi and 24hpi is the smallest of all time points measured but at ~20% is still too high in order to reach a Z'-factor of 0.5 that is required for high-throughput screening. The Z'-factor is a measure of reproducibility and an attempt to quantify the suitability of a particular assay for use in a full-scale, high-throughput screen. It is defined in terms of four parameters: the means and standard deviations of both the positive (p) and negative (n) controls (μ_{pos}, σ_{pos}, and μ_{neg}, σ_{neg}).

$$z'factor = 1 - \frac{3 \times (\delta_{pos} + \delta_{neg})}{\mu_{pos} - \mu_{neg}}$$

δpos – standard deviation positive control
δneg - standard deviation negative control

μpos – average positive control
μneg - average negative control

The value of the Z'-factor can never exceed 1, only assays with values of $1 > Z' \geq 0.5$ are considered to be acceptable for use in HTS and the larger the value, the higher the data quality (Zhang, 1999). After several rounds of optimization we obtained Z'-factors of 0.2 to 0.3 at best, which was still insufficient. The reporter signal was too variable from well to well and we had to find a way to increase the signal and decrease the variation. In our assay, cells are transfected in bulk to ensure that equal amounts of the reporter plasmid are transfected per cell. By using a high MOI the infection efficiency should be close to 100% and therefore we suspected that the reporter plasmid upon transfection was not being equally transcribed. Different amounts of reporter RNA would be accessible for the viral polymerase which would cause signal variation; hence having reporter RNA present in excess should overcome this problem. The cell regulates gene expression and transcriptional activity by acetylation of histones and methylation of DNA. DNA is coiled around histones and their acetylation leads to less compact and more transcriptionally active chromatin. The removal of acetyl groups from histones by histone deactetylases (HDAC) leads to the formation of a condensed and transcriptionally silenced chromatin. HDAC inhibitors (HDI) block this action and can result in hyperacetylation of

histones, therefore affecting gene expression. We tested different HDIs in our assay for their impact on reporter activity and found that Scriptaid® (N-Hydroxy-1,3-dioxo-1H-benz[de]isoquinoline-2(3H)-hexan amide) gave the desired effect (Fig. 1-6).

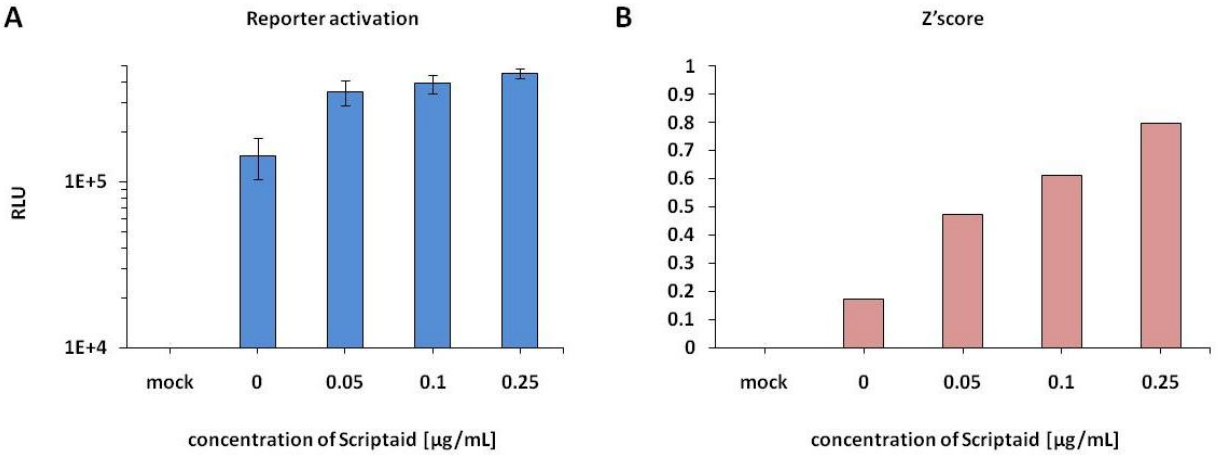

Fig. 1-6. Optimization of reporter activation by the employment of a HDAC inhibitor. A549 cells were transfected with an influenza virus specific luciferase reporter plasmid followed by infection with influenza A/WSN/33 virus (MOI=2). Transfections and infections were performed in the presence of increasing concentrations of a histone-deacetylase inhibitor (Scriptaid). (A) The reporter activation was measured 24 hours post infection. The assay was performed in decuplicate and is presented as the mean ± standard deviation. (B) The Z'scores were calculated for the tested conditions.

A concentration of 0.25 µg/mL of Scriptaid increases the reporter signal more than 3 fold and decreases the standard deviation at the same time which results in a Z'-factor of 0.8. As mentioned earlier, DNA methylation regulates gene expression and transcriptional activity. DNA methylation occurs on CpG dinucleotides and can lead to chromatin remodeling in order to silence genes. Methylation also occurs in promoter regions and prevents transcription of genes by blocking access of the polymerase. DNA methyltransferase (DNMT) inhibitors block this action and lead to hypomethylated promoter regions and enhanced transcriptional activity. We tested the effect of several DNMT inhibitors on our assay and found that addition of 1 µg/ml Decitabine® (5-aza-2'-deoxycytidine) increased the reporter signal more than 7 fold (Fig. 1-7).

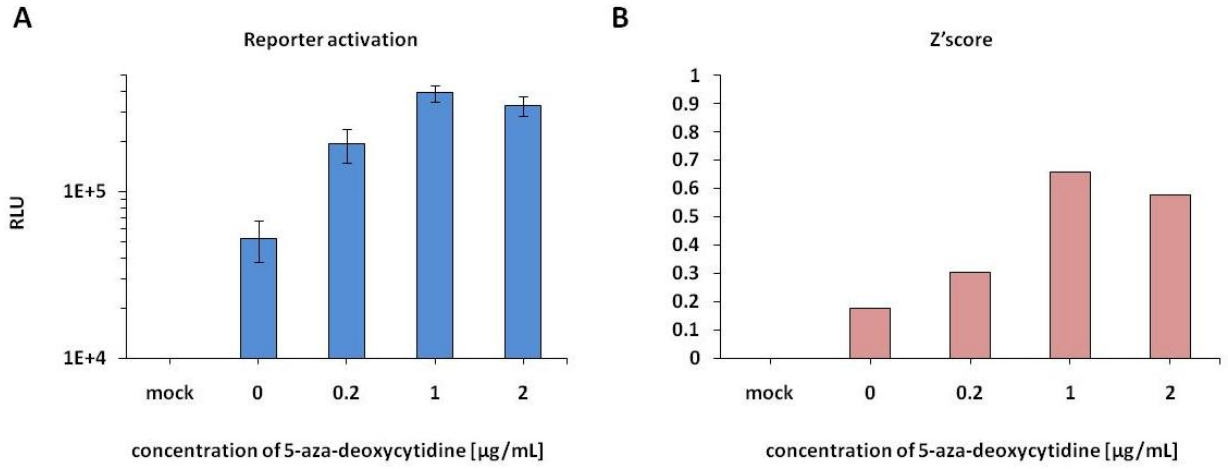

Fig. 1-7. Optimization of reporter activation by the employment of a DNMT inhibitor. A549 cells were transfected with an influenza virus specific luciferase reporter plasmid followed by infection with influenza A/WSN/33 virus (MOI=2). Transfections and infections were performed in the presence of increasing concentrations of a DNA methyltransferase inhibitor (5-aza-deoxycytidine). (A) The reporter activation was measured 24 hours post infection. The assay was performed in decuplicate and is presented as the mean ± standard deviation. (B) The Z'scores were calculated for the tested conditions.

It also decreased the standard deviation and resulted in a Z'-factor of 0.66. For all further experiments, the culture medium was supplemented with 0.25 µg/ml Scriptaid and 1 µg/ml Decitabine. The Z'-factor under these conditions for a 96-well plate was determined to be 0.79 and allowed us to miniaturize the assay into a 384-well plate format. We scaled down the assay conditions used for a 96-well plate by a factor of 4 and started to optimize from there (Fig. 1-8).

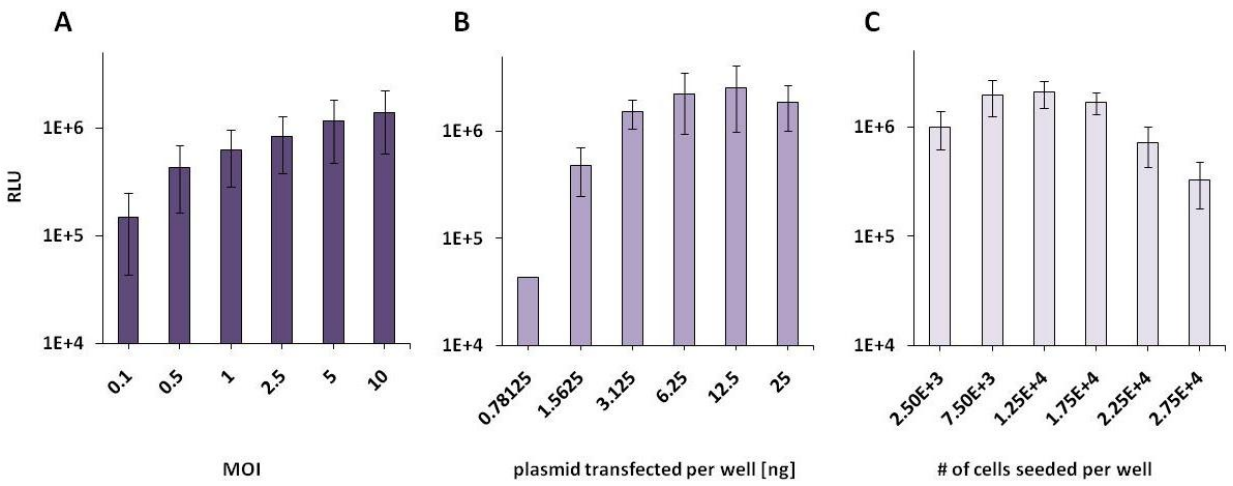

Fig. 1-8. Optimization of HTS assay performed in 384-well format. A549 cells were transfected with an influenza virus specific luciferase reporter plasmid followed by infection with influenza A/WSN/33 virus (A) at different MOIs. (B) Increasing amounts of the reporter plasmid were transfected followed by infection with influenza A/WSN/33 virus (MOI=2.5). (C) An increasing number of cells per well was transfected with 12.5ng of the reporter plasmid followed by infection with influenza A/WSN/33 virus (MOI=2.5). The assay for each condition was performed in half of a 384-well plate (192 wells) and data are presented as the mean ± standard deviation.

Different MOIs were tested and 2.5 was chosen for further experiments. It is in the linear range and allows the detection of decreases or increases in reporter activity. By titrating the number of cells seeded and amounts of plasmid transfected per well, we confirmed the conditions that were found during the optimization of the 96-well format. For further screens performed in 384-well plates, 12.5 ng of the reporter plasmid was transfected per well which contained $9x10^3$ cells. The Z'-factor for the assay performed in 384-well plates under these conditions was determined in 2 separate runs as 0.55 and 0.56. The discrepancy between the Z' factor values determined in 96-well plates and 384-well plates can be explained by the "edge effect" and higher variability in the miniaturized 384-well format. However, both formats meet the requirements for high-throughput screening with Z'-factors above 0.5. Additional parameters which verify the robustness of this assay are the coefficient of variation, CV (14.9±0.2%), the signal-to-background ratio, S/B (>10^4) and the signal-to-noise ratio, S/N (6.7±0.1).

Tab. 1-1. Summary of statistical parameters to assess the robustness of the HTS assay in 384-well format.

	Z'[a]	%CV[b]	S/B[c]	S/N[d]
Screen 1	0.56	14.7	14586	6.8
Screen 2	0.55	15.1	10734	6.6

[a] $Z' = 1 - ((3\sigma_i + 3\sigma_m)/|\mu_i - \mu_m|)$, where σ_i is the standard deviation for the negative control, σ_m is the standard deviation for the positive control, μ_i is the mean signal for the negative control (infected cells) and μ_m the mean signal for the positive control (mock-infected cells).

[b] %CV (coefficient of variation) $= \sigma_i/\mu_i \times 100$.

[c] S/B (signal-to-background ratio) $= \mu_i/\mu_m$.

[d] S/N (signal-to-noise ratio) $= (\mu_i - \mu_m)/((\sigma_i)^2 + (\sigma_m)^2)^{1/2}$.

The S/N ratio is slightly below the ratio of another reported HTS for influenza virus (S/N > 10) (Noah et al., 2007) and reflects a higher signal deviation in our assay which nonetheless is still better compared to a HTS assay for SARS coronavirus (S/N > 3) (Severson et al., 2007). Recently, a number of cell-based HTS assays were developed for screening compounds against different viruses. The S/B ratio of our assay of $>10^4$ is strongly above those of other HTS assays reported for influenza virus (S/B > 30) (Noah et al., 2007), for SARS coronavirus (S/B = ~10) (Severson et al., 2007), for human immunodeficiency virus (HIV-1) (S/B > 100) (Blair et al., 2005), for hepatitis C virus (HCV) (S/B > 13) (Zuck et al., 2004) and for dengue virus (S/B = 8) (Chu and Yang, 2007). This high S/B ratio in addition to a CV of ~15% proves the suitability of our assay for use in a high-throughput screen. The time line of the screen is demonstrated in Fig. 1-9.

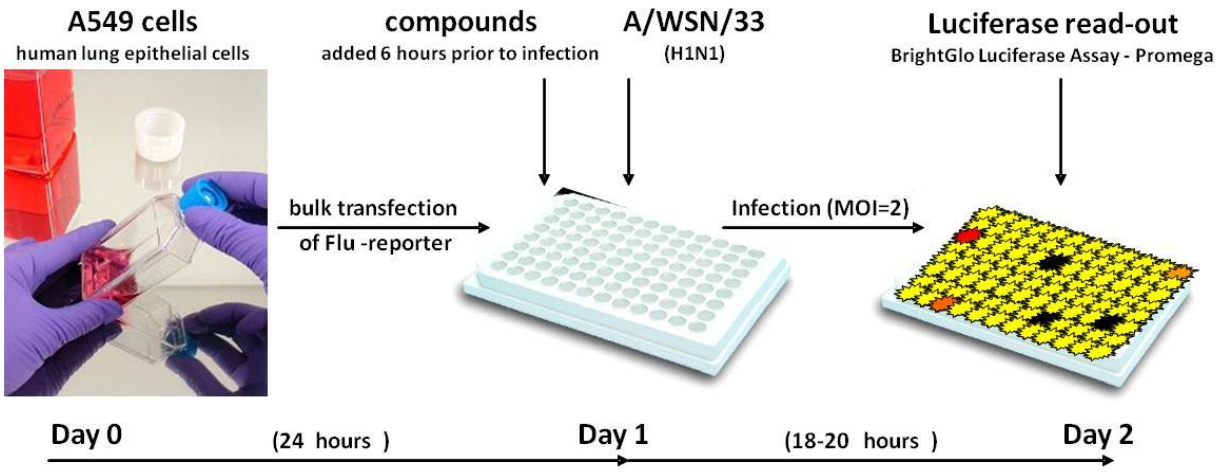

Fig. 1-9. Schematic of the high-throughput screen assay (steps and time line).

A549 cells transfected with the reporter plasmid in bulk were plated in solid white 384-well plates and incubated overnight at 37°C. Six hours prior to infection, 100 nL of the test compounds in library-defined concentrations were added automatically to each well, in duplicate. Influenza A/WSN/33 virus was added to the media at an MOI of 2.5, and infection was allowed to proceed for 18-20 hours at 37°C. After adding the luciferase substrate, luminescence was measured and compared to control wells that received no compound.

A pilot screen was conducted at the Harvard Institute for Cell and Chemical Biology (ICCB) where 2 library plates (704 compounds) were tested in duplicate. When screening a library plate containing uncharacterized compounds, we found one strong inhibitor (0.28%). The hit-rate for high-throughput screening should not significantly exceed 0.3%; if hit-rates are extremely high it is most likely unspecific and indicative of a systemic error. When screening compounds with known biological activity, 18 strong inhibitors (~5%) were detected. These compounds comprise FDA-approved drugs and compounds that target known cellular enzymes and signaling pathways. The hit-rate of 5% was relatively high but not surprising and partly due to the fact that these compounds can be quite cytotoxic. In order to eliminate these false positives we ran a counter screen in parallel for all future screens.

DISCUSSION

We developed an influenza virus specific reporter gene that is activated by the viral polymerase and reflects viral replication. The initial aim was to generate a cell line that stably expresses the reporter RNA which would be transcribed by the viral polymerase upon infection. We successfully transduced A549 cells with our reporter construct but it failed to be reproducibly induced upon virus infection. We think this may be because the reporter RNA mimics viral RNA and may therefore be activating the cellular antiviral response which prevents subsequent virus infection. Some evidence for this comes from the finding that the supernatant of the stable reporter cells exhibited elevated levels of IL-6, IL-8 and IFN-α compared to the parental cell line, as measured by multiplex ELISA. Nevertheless, we showed that our reporter can be activated by virus in a transient transfection system and therefore we optimized the high-throughput screen assay using bulk transient transfections of the reporter plasmid. In order to increase the reporter signal and improve well-to-well reproducibility, the culture medium was supplemented with an HDAC inhibitor (Scriptaid®) and a DNMT inhibitor (Decitabine®). Of course the compound libraries to be screened may contain enhancers of HDACs and DNMTs which would counteract Scriptaid and Decitabine and there may also be compounds that inhibit luciferase activity and those that are generally cytotoxic. In these cases, the reduction in reporter activity would be unrelated to viral replication. We addressed this issue by having a counter screen in which A549 cells were transfected with a luciferase expression plasmid instead of the influenza virus- induced luciferase reporter gene. The set-up of both screens was identical with the exception that luciferase expression in the counter screen started directly upon transfection, whereas luciferase expression in the virus screen started 24 hours after infection with influenza virus. In analyzing the results, we defined a compound to be a false positive if the luminescent signal from the counter screen was reduced by 30%.

Due to the fact that a high multiplicity of infection provided the greatest reproducibility, the assay is more likely to detect compounds that act on steps up to and including translation. A multicycle format would be necessary to detect inhibitors of any of the later stages such as

assembly, budding and release. In this respect our assay differs from other cell-based HTS assays for influenza virus which rely on virus-induced cytopathic effect (CPE) as a readout and which use a low multiplicity of infection (Noah et al., 2007). It should be noted that such an assay can only be performed in Madin-Darby canine kidney (MDCK) cells which display significant CPE in response to influenza virus infection. Our assay is performed in A549 cells which are a biologically relevant cell type for influenza virus infection. Another difference between our assay and a CPE-based assay is the fact that our influenza virus inducible reporter can detect enhanced viral growth by an increased reporter signal. In contrast to CPE-based assays, we are therefore able to indentify compounds that support viral replication by e.g. inhibiting host cell restriction factors. Not only can we screen for inhibitors of viral replication but also for enhancers which may be beneficial in the production of tissue culture grown vaccines.

For a high-throughput screen it would be ideal to have a virus that encodes a reporter gene as this would allow one to conduct multicycle replication assays which would capture the full virus life cycle. Due to the segmented nature of the genome, this has been challenging to do for influenza virus but through work done to define the packaging signals, an influenza virus was engineered that encodes for the green fluorescent protein (GFP) or red fluorescent protein (RFP) (Marsh et al., 2007). A *Renilla* luciferase version of this reporter virus was subsequently utilized in a genome wide siRNA screen in order to identify host cell factors required for influenza virus replication (Konig et al., 2010). The reporter gene in these viruses was flanked by the HA packaging signals and replaced the HA segment in the virus genome. HA is essential for receptor binding and viruses had to be grown in HA expressing MDCK cells. They are therefore able to infect cells and initiate a regular life cycle but they fail to produce infectious particles due to the lack of HA. Screens using these viruses are limited to a single cycle infection if there is not HA provided in trans.

CHAPTER 2 – SCREENING KNOWN BIOACTIVE COMPOUNDS

INTRODUCTION

As part of an initial study, we screened libraries consisting of compounds that have known biological activity (i.e. their cellular targets are known) which facilitates the downstream analysis.

RESULTS

Three compound libraries were screened that consist of collections from NINDS, Prestwick and BIOMOL, and totaling 2640 small molecules. Of those compounds, 59 (2.2%) were identified as strong inhibitors with the luciferase signal reduced by 90-100%. An additional 43 compounds (1.6%) were found to reduce the signal by 70-89% and 4 of the compounds (0.15%) increased luminescence by at least two-fold. Some of the same compounds were present in either two or all of the libraries and were identified as hits independently two or three times. Therefore in total, we identified 47 (1.8%) unique strong inhibitors, 37 (1.4%) unique moderate inhibitors and 4 (0.15%) enhancers. Table 2-1 shows the functional classes of the hit compounds that were identified as inhibitors in the HTS.

Tab. 2-1. Functional categories of the hit compounds with inhibitory activity.

Functional category	Number of compounds	% of total
DNA interfering compounds	20	23.8
Antibiotics/antifungals/antiparasitics	18	21.4
Kinase inhibitors	11	13.1
Cardioactive glycosides	7	8.3
Cell redox metabolism interfering compounds	4	4.8
Other compounds	24	28.5
Total number of inhibitory compounds	84	100

About 24% of the inhibitors are compounds that interfere with DNA. Another group of 21% consists of antibiotics, antifungals and antiparasitic drugs. Roughly 13% of the inhibitors target different cellular kinases like protein kinase A, protein kinase C and receptor tyrosine kinases and more than 8% of the inhibitory compounds are Na^+/K^+/ATPase pump inhibitors (ouabain, lanatoside C, digoxin, strophanthidin), known as cardioactive glycosides. The initial effect of these compounds, and of SDZ-201106 (a sodium channel opener) and lasalocid (a sodium ionophore) which were both identified as inhibitors, is to raise the intracellular Na^+ concentration. Interestingly, one of the compounds that resulted in increased luciferase signals (phenamil) is an amiloride analogue that acts as a sodium channel inhibitor. These opposing effects, by compounds that have contrasting effects on sodium channels, indicates that influenza virus is sensitive to changes in intracellular ion concentrations and that this may be a way of modulating influenza virus replication. In support of this, it has been reported that influenza virus can inhibit these amiloride-sensitive sodium channels in the respiratory epithelium (Chen et al., 2004; Kunzelmann et al., 2000). Amongst the group of inhibitory compounds we also found several protein kinase C (PKC) inhibitors, the strongest of which was rottlerin. PKC inhibitors have previously been shown to inhibit influenza virus (Kurokawa et al., 1990; Root et al., 2000; Sieczkarski et al., 2003) and furthermore, there is evidence that PKC activity is involved in the regulation of epithelial sodium channels (Booth and Stockand, 2003; Kunzelmann et al., 2000; Stockand et al., 2000; Yamagata et al., 2005). For further investigation into their effects on influenza virus growth, we therefore focused on those compounds that target either sodium ion transport or PKC.

Inhibition of influenza A and B virus replication by a sodium channel opener, a sodium ionophore and a PKC inhibitor

The high-throughput assay revealed that the sodium channel opener, SDZ-201106, the sodium ionophore, lasalocid and the PKC inhibitor, rottlerin are potential influenza virus inhibitors. In order to confirm that these findings were specific, we first determined the cytotoxicity profiles

of these compounds. A549 cells were seeded into 96-well plates and treated with increasing concentrations of SDZ-201106, lasalocid or rottlerin for 24 hours before performing an MTS assay to determine cell viability. The CC_{50} (concentration of 50% cytotoxicity) of SDZ-201106 was determined to be 29.1 µM and concentrations up to 12.5 µM were found to be non-toxic. The CC_{50} of lasalocid was determined to be 14.3 µM and concentrations up to 1 µM did not significantly decrease cell viability. The CC_{50} of rottlerin was determined to be 18.4 µM and concentrations up to 1.28 µM did not decrease cell viability. All further experiments with rottlerin were performed using a maximum concentration of 1.25 µM. To determine the IC_{50} (half maximal inhibitory concentration) for these inhibitors, A549 cells were infected for 24 hours with influenza A/WSN/33 virus at an MOI of 1 in the presence of increasing compound concentrations. Viral titers were determined by plaque assay. The IC_{50} for SDZ-201106 was determined to be 3.9 µM. This results in a selective index ($SI = CC_{50}/ IC_{50}$) of 7, which classifies this sodium channel opener as a weak inhibitor in terms of its pharmacological profile. In contrast, lasalocid, the sodium ionophore, was classified to be a strong inhibitor with an IC_{50} of 100 nM and a SI of 143. The IC_{50} of rottlerin was determined to be 380 nM. With an SI of 48, this PKC inhibitor is considered to be a moderate inhibitor (Fig. 2-1).

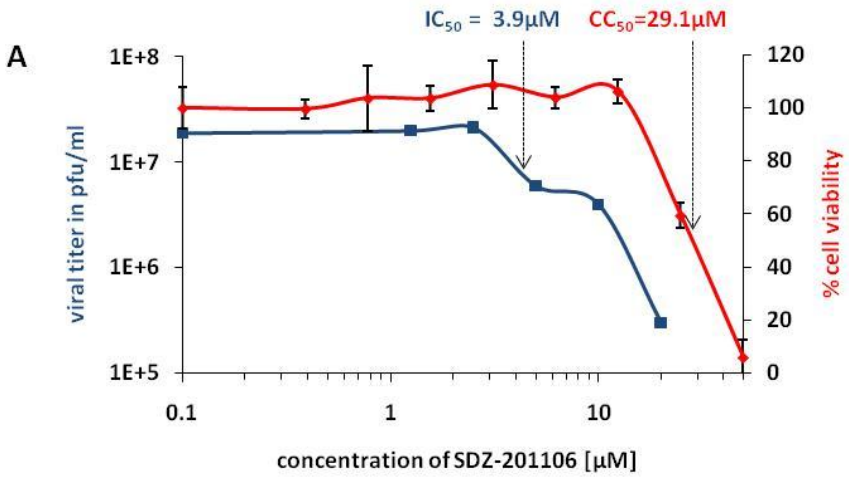

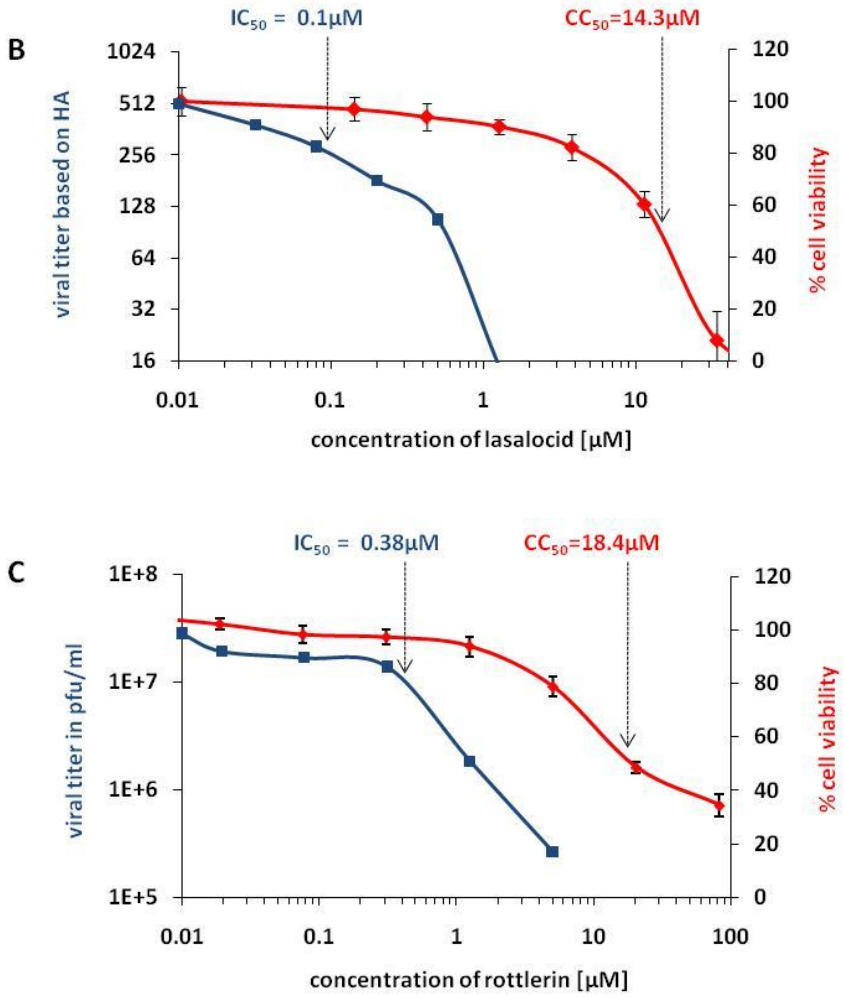

Fig. 2-1. Replication of influenza A/WSN/33 virus in the presence of inhibitors versus cytotoxicity of inhibitors. A549 cells were infected with influenza A/WSN/33 virus (MOI=1) in the presence of increasing concentrations of (A) a sodium channel opener (SDZ-201106), (B) a sodium ionophore (lasalocid) and (C) a PKC inhibitor (rottlerin). Viral titers and IC_{50s} were determined by plaque assay (A and C) or HA assay (B) at 24 hours post infection (left hand scale, blue curve). Cell viability and CC_{50}s were determined independently for a 24 hours incubation period (right hand scale, red curve).

Subsequently compounds were tested at their highest, non-toxic concentrations for their inhibitory activity against both influenza A/WSN/33 virus and influenza B/Yamagata/88 virus (Fig. 3). Titers of influenza A/WSN/33 virus are reduced by 85% in the presence of 12.5 µM SDZ-201106 compared to the untreated control and by 93% in the presence of 1.25 µM rottlerin. The growth of influenza B/Yamagata/88 virus is inhibited by 72% when SDZ-201106 is present in the culture medium and at least by 80% when rottlerin is present. The sodium

ionophore lasalocid was found to inhibit influenza A/WSN/33 virus by 92% and influenza B/Yamagata/88 virus by 65% (data not shown).

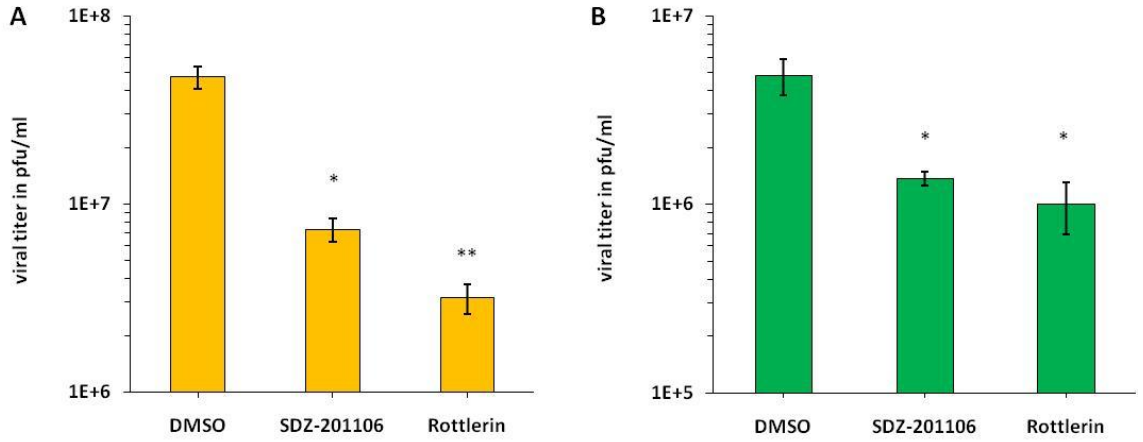

Fig. 2-2. Inhibition of influenza A and B viruses by a Na^+-channel opener and a PKC inhibitor. A549 cells were infected with either (A) A/WSN/33 (MOI=1) or (B) B/Yamagata/88 (MOI=5) in the presence of 12.5 µM SDZ-201106 (Na^+-channel opener) or 1.25 µM rottlerin (PKC inhibitor). Viral titers were determined 24 hours post infection by plaque assays in MDCK cells. The assay was performed in triplicate and is presented as the mean ± standard deviation. Student's *t* test: *, $P \leq 0.05$; **, $P \leq 0.01$.

The sodium channel opener (SDZ-201106) and the PKC inhibitor (rottlerin) target cellular proteins that are essential at certain stages in the viral life cycle. We passaged influenza A/WSN/33 virus in the presence of SDZ-201106 15 times and in the presence of rottlerin 17 times but were unable to generate escape mutants. The passaged viruses were equally sensitive to compound treatment compared to virus that was passaged in the presence of the solvent (DMSO) (Fig. 2-3).

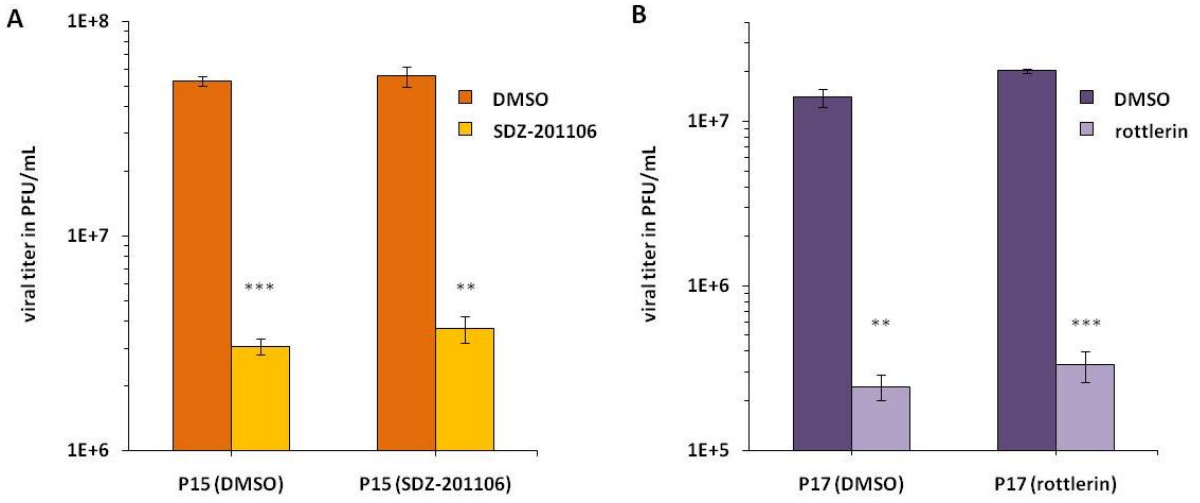

Fig. 2-3. Influenza A/WSN/33 virus passaged in the presence of a sodium channel opener and a PKC inhibitor. (A) Influenza A/WSN/33 virus that was passaged 15 times in the presence of DMSO or a sodium channel opener (SDZ-201106) was tested in A549 cells at a MOI of 1 in the presence of DMSO or 12.5µM SDZ-201106. (B) Influenza A/WSN/33 virus that was passaged 17 times in the presence of DMSO or a PKC inhibitor (rottlerin) was tested in A549 cells at a MOI of 0.1 in the presence of DMSO or 1.25µM rottlerin. (A and B) Viral titers were determined by plaque assay at 24 hours post infection. The assay was performed in triplicate and is presented as the mean ± standard deviation. Student's t test: **, $P \leq 0.01$; ***, $P \leq 0.001$.

These results underline the significance of identifying host cell factors that can be targeted with small molecules to inhibit viral replication. Viruses cannot easily overcome this obstacle through escape, as often happens with antivirals targeting viral proteins.

Enhancement of influenza A and B virus replication by sodium channel inhibitors and PKC activators

The identification of enhancers is performed best under multi-cycle replication conditions. This is a limitation of our HTS assay which is performed with a high multiplicity infection and therefore probably only allows for the detection of strong enhancers. Furthermore compounds with enhancing activity may be marked as false negatives if the concentration at which the screen is performed is cytotoxic. Although we screened the PKC activator PMA we did not

identify it as an enhancer, probably because the concentration of PMA used in the screen (~6 µM) was toxic. Nevertheless, we decided to investigate the effects of PMA and another PKC activator, mezerein, due to the link between PKC activity and sodium channel regulation and the fact that PKC inhibitors can downregulate influenza virus growth. For the sodium channel inhibitors, in addition to phenamil, which was identified in the screen as a potential enhancer, we also examined the effects of a related sodium channel inhibitor, dichlorobenzamil. A549 cells were infected with influenza A/WSN/33 virus at a low multiplicity in the presence of increasing concentrations of each compound in order to find the most effective concentration (Fig. 2-4).

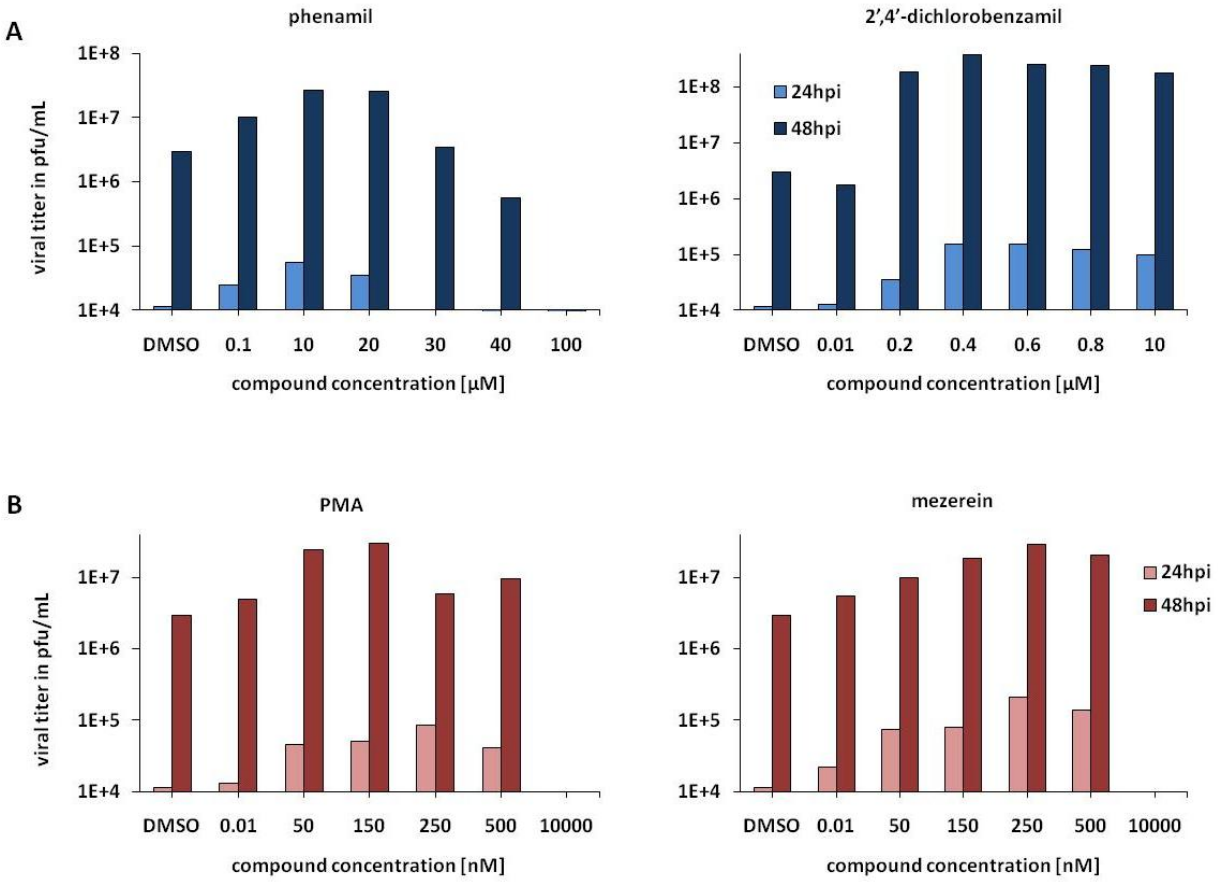

Fig. 2-4. Titration of Na^+-channel inhibitors and PKC activators that enhance influenza A virus replication. A549 cells were infected with influenza A/WSN/33 virus (MOI=0.001) in the presence of (A) increasing concentrations of Na^+-channel inhibitors (phenamil and 2',4'-dichlorobenzamil) and (B) increasing concentrations of PKC activators (PMA and mezerin). Viral titers were determined by plaque assay at 24 and 48 hours post infection.

The enhancing potential of sodium channel inhibitors is greater at 48 hours than that at 24 hours post infection and viral titers increased 9 fold in the presence of 10 µM phenamil and more than 120 fold in the presence of 400 nM 2',4'-dichlorobenzamil. PKC activators increase viral titers strongly early in the infection, the enhancement at 24 hours is greater than that at later time points most likely due to the compound cytotoxicty. In the presence of 250 nM PMA or mezerein, viral titers are enhanced 7 fold and 18 fold and 18 fold at 24hr, respectively. Multicycle growth assays for influenza A/WSN/33 virus were then performed in the presence of these compounds at their maximal enhancing concentrations (Fig. 2-5).

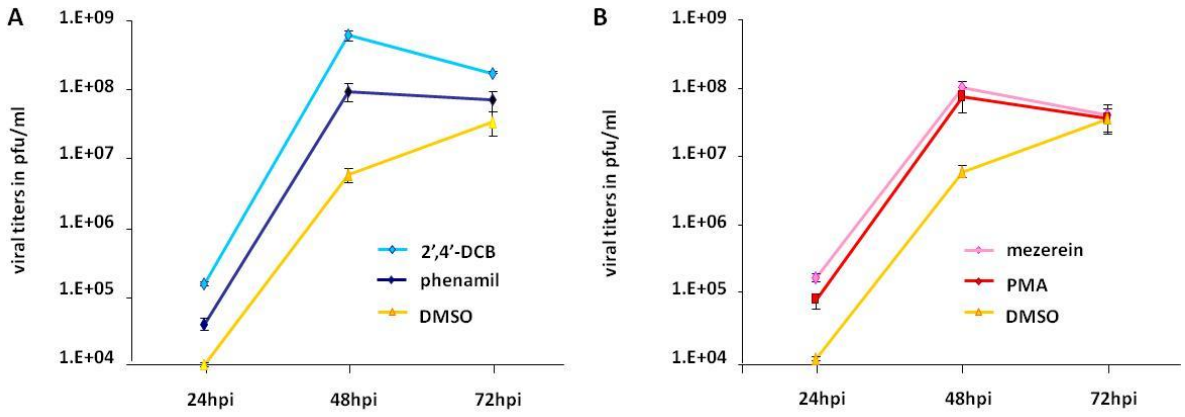

Fig. 2-5. Enhancement of influenza A virus replication by Na^+-channel inhibitors and PKC activators. A549 cells were infected with influenza A/WSN/33 virus (MOI=0.001) in the presence of (A) Na^+-channel inhibitors (400 nM 2',4'-dichlorobenzamil and 10 µM phenamil) and (B) PKC activators (250 nM mezerein and 250 nM PMA). Viral titers were measured at 24, 48 and 72 hours post infection by plaque assay in MDCK cells. The assay was performed in triplicate and is presented as the mean ± standard deviation.

These growth assays confirm the results for our enhancing compounds found earlier. The growth of influenza A/WSN/33 virus is significantly enhanced in the presence of the sodium channel inhibitors. Compared to the untreated control, the viral titer is increased 100 fold in the presence of 400 nM 2',4'-dichlorobenzamil and 13 fold in the presence of 10 µM phenamil at 48 hours post infection. In the presence of the PKC activators, the titers of influenza A/WSN/33 virus increase 20 fold with 250 nM mezerein and 9 fold with 250 nM PMA, compared to untreated cells at 24 hours post infection and is still 11 fold increased for both

compounds compared to untreated cells at 48 hours post infection. We also examined the enhancing effects of these compounds on the replication of influenza B/Yamagata/88 virus (Fig. 2-6).

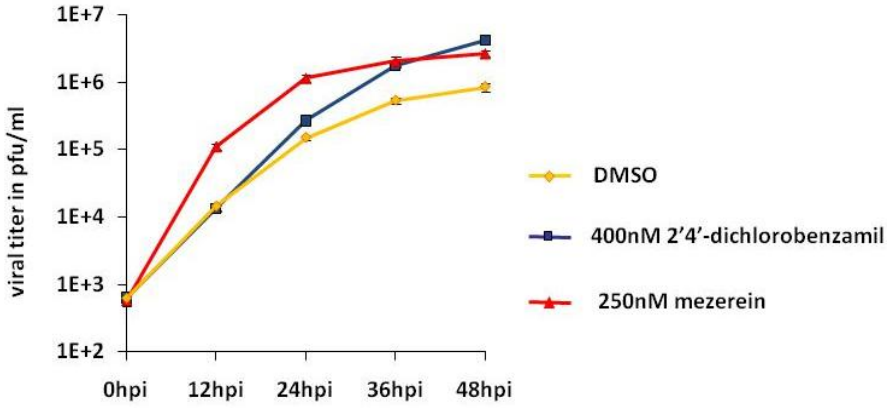

Fig. 2-6. Enhancement of influenza B virus replication by a Na^+-channel inhibitor and a PKC activator. A549 cells were infected with influenza B/Yamagata/88 virus (MOI=0.1) in the presence of 400 nM 2',4'-dichlorobenzamil (Na^+-channel inhibitor) and 250 nM mezerein (PKC activator). Viral titers were measured at 0, 12, 24, 36 and 48 hours post infection by plaque assay in MDCK cells. The assay was performed in triplicate and is presented as the mean ± standard deviation.

In the presence of 400 nM 2',4'-dichlorobenzamil, the viral titer increased 4 fold at 48 hours post infection compared to untreated cells. With mezerein, the viral growth enhancement is seen much earlier with an 8 fold increase at 12 and 24 hours post infection. Therefore the growth of both influenza A and B viruses can be enhanced by the addition of sodium channel inhibitors and PKC activators.

We also examined whether the growth-enhancing effects of these compounds could be observed with human isolates of influenza virus that have not been adapted to cell culture. For this purpose we compared the growth of influenza A/Texas/91, A/Moscow/10/99, A/Wyoming/03/2003 viruses in the absence and presence of mezerein and 2',4'-dichlorobenzamil (Fig. 2-7)

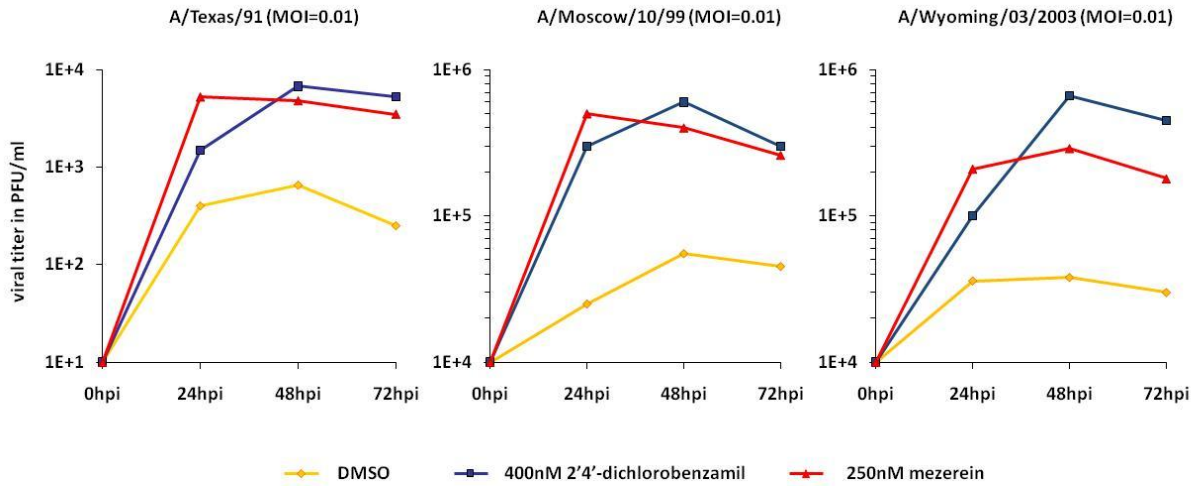

Fig. 2-7. Enhanced growth of human isolates of influenza virus in A549 cells. A549 cells were infected with influenza viruses A/Texas/91, A/Moscow/10/99 and A/Wyoming/03/2003 at a MOI of 0.01 in the presence of DMSO, 400 nM 2',4'-dichlorobenzamil or 250 nM mezerein. Viral titers were measured at 24, 48 and 72 hours post infection by plaque assay in MDCK cells.

These viruses grow poorly in A549 cells but we observed a significant increase in the maximum viral titers in the presence of mezerein and 2',4'-dichlorobenzamil compared to untreated cells. This suggests that the ability of these compounds to boost virus replication is a property that extends to many different influenza virus strains, which will be beneficial if used for production of influenza vaccines that change every year. For the current egg-grown vaccines, the seed strains for influenza A viruses are 6:2 reassortant viruses that contain the HA and NA genes of the vaccine virus in the background of influenza A/PR/8/34 virus. This is done to obtain high titers in eggs and to avoid the need to adapt each new virus strain. The same strategy is used for the H5N1 influenza vaccine that has been approved by the FDA, with the addition that the multibasic cleavage site present in the HA (which is associated with high pathogenicity in chickens) has been removed (Subbarao et al., 2003; Treanor et al., 2006). We examined the growth properties of the influenza A/Vietnam/1203/04 and the H5N1/PR8 vaccine virus in A549 cells that had been treated with 2',4'-dichlorobenzamil and found that we could significantly increase the titers by 12-20 fold compared to in untreated cells (Fig. 2-8).

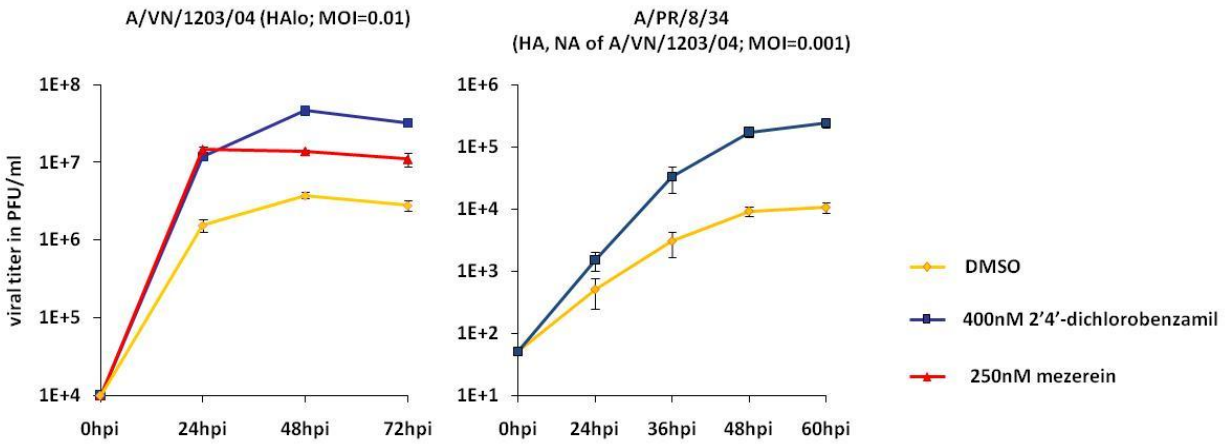

Fig. 2-8. Enhanced growth of human influenza virus H5N1 isolate and a reassortant H5N1 influenza vaccine strain. A549 cells were infected with influenza A/VN/1203/04 (HAlo) virus (MOI=0.01) and a 6:2 reassortant H5N1/PR8 (MOI=0.001) in the presence of DMSO, 400 nM 2',4'-dichlorobenzamil or 250 nM mezerein. Viral titers were measured at indicated time points post infection by plaque assay in MDCK cells.

We also observed a significant increase in viral titers in the presence of 2',4'-dichlorobenzamil and mezerein (11 fold and 15 fold, respectively) when influenza A/WSN/33 virus was grown in Vero cells which is one of the approved cell lines for vaccine production.

As these compounds are acting on cellular pathways, differences between cell types will likely be observed and optimization or compound modification may be required to achieve the best possible effects.

During the development stage, the activities of drug candidates can often be modulated by making small changes to the structure of the compound. We compared the effects of 2',4'-dichlorobenzamil versus 3',4'-dichlorobenzamil for their ability to enhance influenza virus growth (Fig. 2-9).

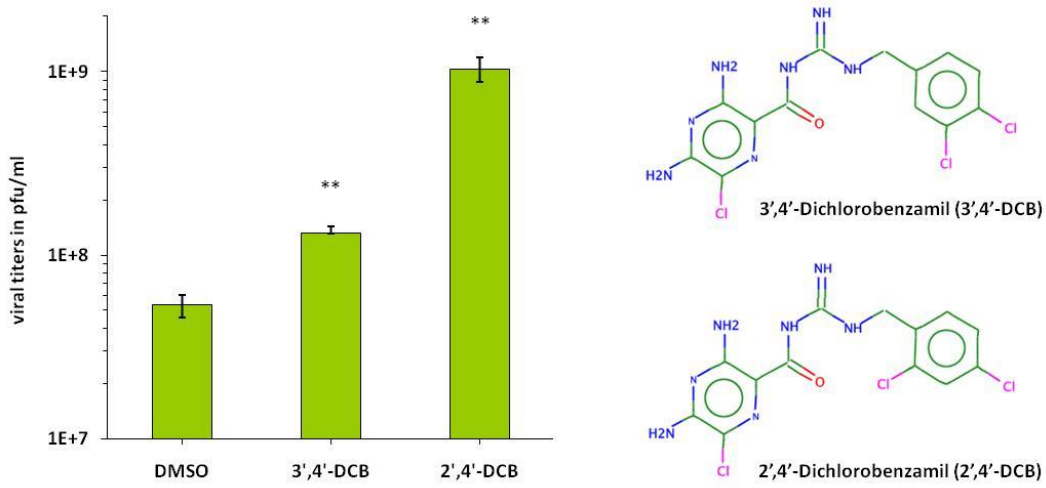

Fig. 2-9. Influenza A virus growth in response to 3',4'-dichlorobenzamil versus 2',4'-dichlorobenzamil. A549 cells were infected with influenza A/WSN/33 virus (MOI=0.001) in the presence 400 nM of 3',4'- or 2',4'-dichlorobenzamil (3',4'-DCB and 2',4'-DCB). Viral titers were determined at 48 hours post infection by plaque assay in MDCK cells. The assay was performed in triplicate and is presented as the mean ± standard deviation. Student's t test: **, $P \leq 0.01$.

Both compounds can boost influenza virus replication above that obtained with the untreated control, but the simple change of a chloride from position 2 in the benzyl group to position 3 makes it 10 times less efficient.

To address the question of whether there is a correlation between the viral inhibitory or enhancing activities of these compounds and their ability to induce or inhibit apoptosis, we monitored the activity of caspase-3, an indicator of apoptosis induction. To mimic the condition of the cells at the time of infection, A549 cells were incubated with the compounds for 6 hours and staurosporin (5 µM) was used as a positive control to induce apoptosis. Phenamil (which enhances influenza virus growth) showed a very slight induction (1.3 fold) of apoptosis during this time period, whereas all the other compounds did not display any significant increases or decreases in fluorescence compared to the untreated cells, indicating the absence of pro-apoptotic or anti-apoptotic activity (Fig. 2-10).

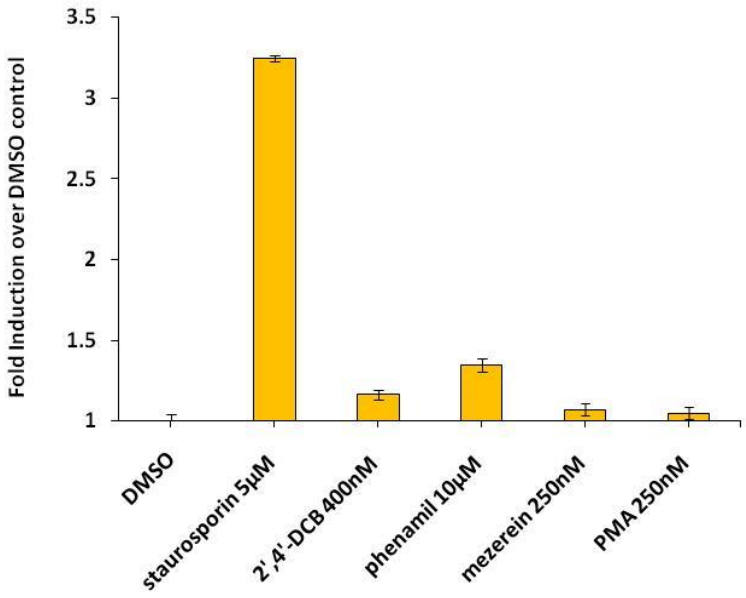

Fig. 2-10. Compound induced apoptosis monitored by caspase-3 activity. A549 cells were treated with compounds at indicated concentrations for 6 hours. Apoptosis was measured by caspase-3 activity and is depicted as fold induction over DMSO treated cells. The assay was performed in triplicate and is presented as the mean ± standard deviation.

Inhibition of RNA viruses by sodium potassium ATPase pump inhibitors

The Na^+/K^+/ATPase pump inhibitors ouabain, lanatoside C, strophanthidin, digoxin, and digitoxigenin were all identified as potential influenza virus inhibitors in the HTS. These cardioactive glycosides, which are used in the treatment of congestive heart failure and cardiac arrhythmia, have also been shown to inhibit the replication of herpes simplex virus (HSV) (Dodson et al., 2007), vaccinia virus (Deng et al., 2007), murine leukemia virus (MuLV) (Tomita and Kuwata, 1978) and Sendai virus (Nagai et al., 1972). To confirm our initial findings, we examined the ability of ouabain, lanatoside C and digitoxigenin to inhibit influenza virus replication. The CC_{50} for ouabain, lanatoside C and digitoxigenin on A549 cells was determined to be 47 nM, 210 nM and 1.5 µM, respectively. For the viral replication assays a CC_{20} (concentration of at least 80% cell viability after a 24 hours incubation period) was used for each compound. A549 cells were infected at an MOI of 1 with influenza A/WSN/33 virus in the

presence of 20 nM ouabain, 78 nM lanatoside C and 320 nM digitoxigenin. Ouabain appears to be the most potent Na^+/K^+/ATPase pump inhibitor whereas digitoxigenin is rather weak. At 24 hours post infection the viral titers were found to be decreased by 99% with ouabain treatment, by 96% with lanatoside C treatment and by 80% with digitoxigenin treatment, compared to the untreated control. Inhibition of the Na^+/K^+/ATPase pumps affects viral entry or an early step in the replication due to the fact that the inhibition is diminished if the compounds are added only 2 hours post infection (Fig. 2-11A).

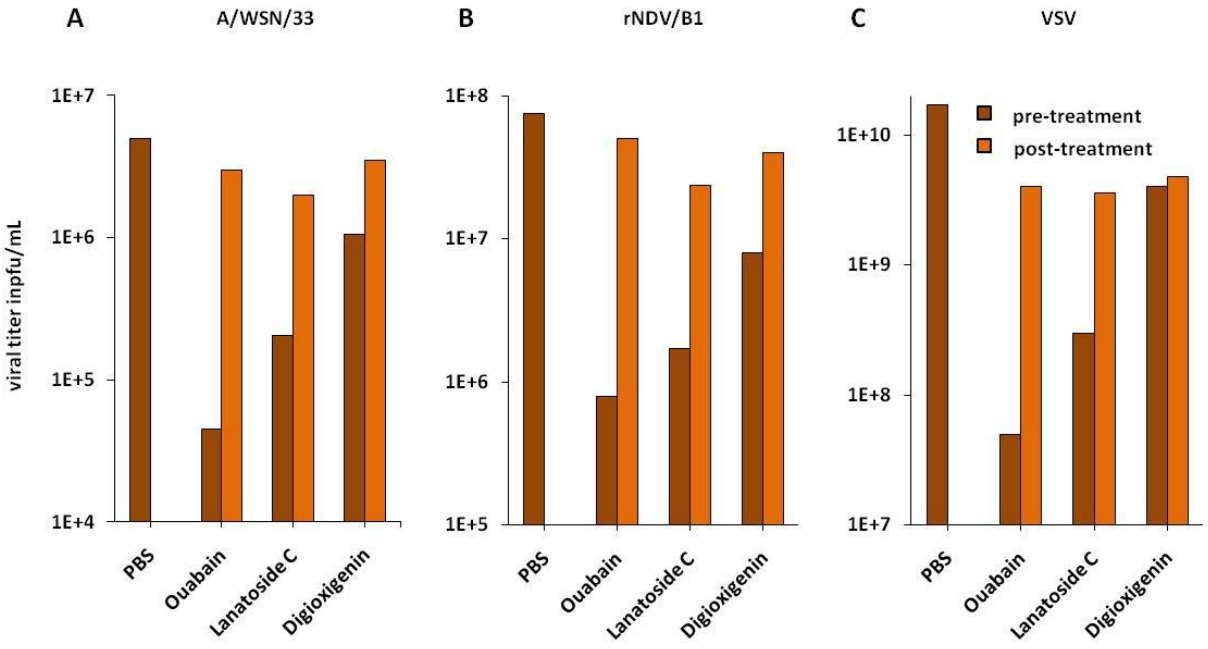

Fig. 2-11. Inhibition of negative sense RNA viruses by Na^+/K^+/ATPase pump inhibitors. A549 cells were infected with (A) A/WSN/33 (MOI=1), (B) NDV/B1 (MOI=1) or (C) VSV-GFP (MOI=1) in the presence of 20 nM ouabain, 78 nM lanatoside C or 320 nM digitoxigenin. Na^+/K^+/ATPase pump inhibitors were present prior or post infection. Viral titers were determined 24 hours post infection by plaque assays.

As these compounds have also been shown to inhibit the replication of other viruses, we investigated whether this effect on influenza viruses extends to other RNA viruses. We found that at least ouabain and lanatoside C can significantly inhibit the replication of both Newcastle disease virus (NDV) (Fig. 2-11B) and vesicular stomatitis virus (VSV) (Fig. 2-11C and Fig. 2-12).

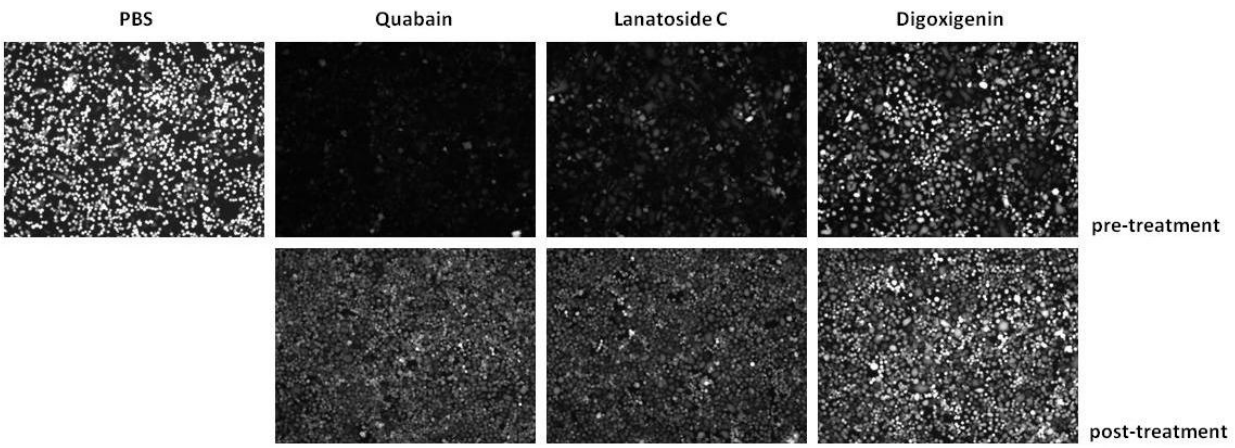

Fig. 2-12. Inhibition of VSV-GFP by Na^+/K^+/ATPase pump inhibitors. A549 cells were infected with VSV-GFP (MOI=1) in the presence of 20 nM ouabain, 78 nM lanatoside C or 320 nM digitoxigenin. Na^+/K^+/ATPase pump inhibitors were present prior or post infection. The growth of VSV-GFP was visualized by fluorescence microscopy at 24 hours post infection.

As seen for influenza A/WSN/33 virus, it also appears that an early step in the viral life cycle of NDV and VSV is targeted since the addition of compounds post infection does not decrease viral titers significantly. The results indicate that these Na^+/K^+/ATPase pump inhibitors can inhibit multiple members of RNA virus families presumably by targeting a common step in the replication cycle. To address the possibility that their broad antiviral activity may be related to the induction of interferon, we examined the effects of the compounds on influenza virus replication in Vero cells, which are deficient for interferon production. We observed a similar level of inhibition as in A549 cells, thereby excluding this possibility (Fig. 2-13).

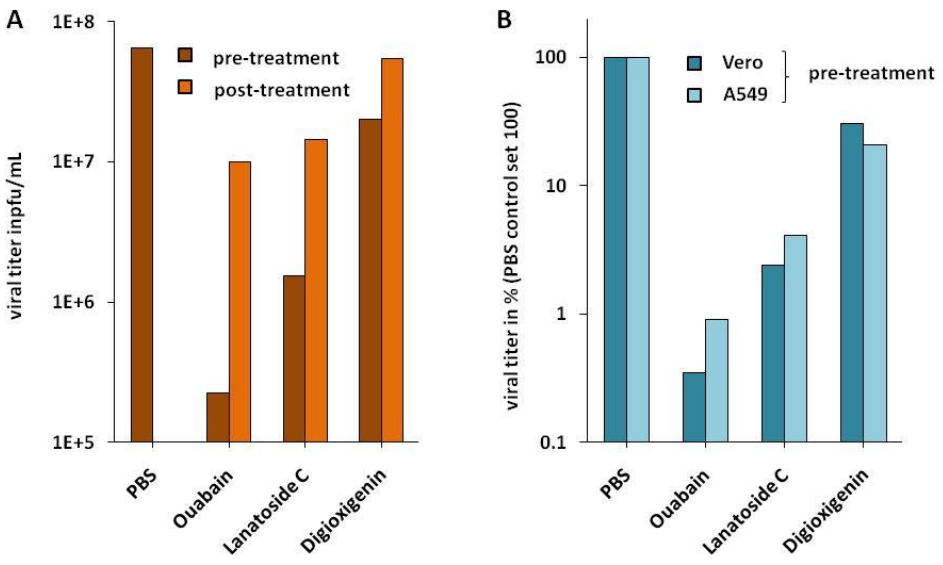

Fig. 2-13. Inhibition of influenza A/WSN/33 virus by Na^+/K^+/ATPase pump inhibitors in Vero cells. (A) Vero cells were infected with influenza A/WSN/33 virus (MOI=1) in the presence of 20 nM ouabain, 78 nM lanatoside C or 320 nM digitoxigenin. Na^+/K^+/ATPase pump inhibitors were present prior or post infection. Viral titers were determined by plaque assay. (B) Inhibition of influenza A/WSN/33 virus by Na^+/K^+/ATPase pump inhibitors in A549 cells versus Vero cells. Compounds were present prior to infection. Viral titers were determined by plaque assay and set in relation to the PBS control.

DISCUSSION

An influenza pandemic caused by a virus of avian origin could not only have the potential to cause millions of deaths worldwide but could also affect the poultry industry which is crucial for the production of egg-derived vaccines. The primary concerns that need to be addressed in preparation for the next influenza epidemic or pandemic are the abilities of the manufacturers to produce enough doses of vaccine for the susceptible population and the availability of more antiviral compounds that are effective at preventing influenza virus infection. In our luciferase-based, high-throughput screen of 2640 compounds with known biological activity, we identified 84 unique compounds with at least 70% reduction in luciferase activity and 4 compounds that increased luciferase activity at least 2 fold. We reasoned that compounds found to suppress influenza virus replication are potential anti-influenza virus drugs, whereas those that enhance influenza replication could be used as a tool to boost the growth of vaccine viruses in tissue

culture. Moreover, because the biological targets of these compounds are known, it also provides clues as to which cellular pathways and components are crucial for influenza virus replication. The use of antiviral drugs that target cellular proteins is also an advantage over the current drugs that target viral proteins and against which resistance is far more likely to develop. Of particular interest was the finding that sodium channel inhibitors and compounds that increase intracellular sodium concentration such as a sodium channel opener and a sodium ionophore had opposing effects on viral replication. By adding 2',4'-dichlorobenzamil, an amiloride-analogue that inhibits epithelial Na^+ channels (ENaC) and Na^+/Ca^{+2} exchange channels (Paltauf-Doburzynska et al., 2000), we could enhance viral replication of influenza A/WSN/33 virus 100 fold. In direct contrast, using the sodium channel opener SDZ-201106 at non-toxic concentrations we could decrease the titers of influenza A/WSN/33 virus by 85% and by 92% using the sodium ionophore lasalocid. The effects of these compounds on influenza B virus replication were more modest (4 fold increase with 2',4'-dichlorobenzamil and 72% decrease with SDZ-201106 and 65% with lasalocid respectively) but the overall trend was similar, suggesting that the cellular pathways affected by these compounds are important for both influenza A and B viruses. The fact that influenza virus has been shown to inhibit amiloride-sensitive sodium channels upon infection (Chen et al., 2004; Kunzelmann et al., 2000), suggests that this creates a cellular environment that is conducive to viral replication and one can speculate that the addition of chemical Na^+ channel inhibitors (such as phenamil or 2',4'-dichlorobenzamil) prior to infection creates pre-optimized conditions and thereby boosts virus replication.

In terms of mechanism of action, these data indicate that an increase in the intracellular Na^+ concentration caused by opening sodium channels or sodium specific pores leads to a decline in influenza virus titers, whereas a decreased intracellular Na^+ concentration caused by the inhibition of sodium channels can boost viral replication. However, because the different intracellular ion currents are tightly linked to one another, further investigation is required to evaluate the contribution of Ca^{2+} due to regulation of the Na^+/Ca^{2+} exchange channel. As many

of these compounds can target more than one type of channel, it is difficult to attribute their effects on virus replication to a specific channel. That said, several of the amiloride analogues have more potent activity against a specific channel. In our study, 2',4'-dichlorobenzamil shows slightly stronger pro-viral activity than phenamil. A comparison of their reported potencies against ENaC or the Na^+/Ca^{2+} exchange channel indicates that phenamil is more specific for ENaC while 2',4'-dichlorobenzamil is more specific for the Na^+/Ca^{2+} exchange channel (Kleyman and Cragoe, 1988). We also tested another amiloride analogue, 3',4'-dichlorobenzamil, which compared with 2',4'-dichlorobenzamil, is less effective at enhancing virus replication and has less potent activity against the Na^+/Ca^{2+} exchange channel than 2',4'-dichlorobenzamil (Kleyman and Cragoe, 1988). Therefore it appears that the ability to enhance the growth of influenza virus correlates with the strength of inhibition of the Na^+/Ca^{2+} exchange channel. It should be noted that in contrast to our findings, amiloride derivatives have been reported to inhibit the replication of several RNA viruses such as human immunodeficiency virus (HIV-1) (Ewart et al., 2004), human rhinovirus (Gazina et al., 2005), coxsackievirus (Harrison et al., 2008) and coronaviruses (Wilson et al., 2006). For HIV-1 (Ewart et al., 2002), coronaviruses, hepatitis C virus (Premkumar et al., 2004) and dengue virus (Premkumar et al., 2005), these compounds have been shown to act by inhibiting the formation of the viral ion channel. There is no evidence that the influenza virus M2 ion channel activity is adversely affected by amilorides and our results rather show that for influenza virus, these compounds have a pro-viral effect.

It is possible that the effects of these compounds on virus growth are not due to changes in ion transport directly but rather due to changes in other cellular activities that are influenced by these compounds. For example pre-treatment of the cells with the compounds prior to infection could be inducing either a pro- or anti-apoptotic state which then influences virus replication. However, as judged by caspase 3 activity, neither the inhibitory nor the enhancing compounds were found to exhibit any anti- or pro-apoptotic effects in the cells at the time of infection. Therefore this is not likely to be an explanation for the observed effects of these

compounds on influenza virus replication. Interestingly, it has been shown that influenza virus-mediated inhibition of Na^+ channels requires PKC activity (Chen et al., 2004; Kunzelmann et al., 2000) and also, that there is a stimulation or inhibition of Na^+ transport in the presence of PKC inhibitors or activators, respectively (Kunzelmann et al., 2000). These data correlate with our findings that influenza replication is inhibited in the presence of a PKC inhibitor (rottlerin) but conversely, enhanced in the presence of a PKC activator (PMA or mezerein). Influenza virus entry requires PKC activity and this is believed to be stimulated upon the binding of virus to cellular receptors (Arora and Gasse, 1998; Root et al., 2000; Rott et al., 1995; Sieczkarski et al., 2003). However, to our knowledge this is the first demonstration that a PKC activator can enhance influenza virus growth. The activation of PKC has also been found to down regulate the surface expression of the beta and gamma subunits of ENaC, resulting in a decrease in epithelial Na^+ re-absorption (Booth and Stockand, 2003; Stockand et al., 2000). Therefore it appears that there is a connection between the activation status of PKC and the transport of Na^+ and that influenza virus replication favors the presence of activated PKC and a low intracellular Na^+ concentration.

We also demonstrated that the Na^+/K^+/ATPase pump inhibitors, ouabain, lanatoside C and digitoxigenin, can inhibit the replication of influenza virus, NDV and VSV, representatives of three different RNA virus families. These data, combined with the results of previous studies that show inhibition of HSV-1, vaccinia virus, MuLV and Sendai virus (Deng et al., 2007; Dodson et al., 2007; Nagai et al., 1972; Tomita and Kuwata, 1978), indicate that these cardioactive glycosides have broad antiviral activity. Through the use of Vero cells, we determined that these compounds do not act by inducing interferon, as the same degree of virus inhibition was observed in these cells as seen in A549 cells. One other common feature shared by these viruses is that they all possess a lipid envelope, however data on ouabain-mediated inhibition of HSV-1 indicates that it acts at a post-entry stage of the viral life cycle (Dodson et al., 2007). The main function of the Na^+/K^+/ATPase pump is to pump Na^+ out of the cell and K^+ into the cell to maintain the cell potential as a driving force for several membrane transport proteins (e.g.

the Na^+-glucose symporter, the Na^+-amino acid symporter or the Na^+-hydrogen antiporter). This gradient is also important for the removal of Ca^{2+} by the Na^+/Ca^{+2} exchange channel. Thus in the presence of an inhibitor such as ouabain, there is an increase in the intracellular Na^+ concentration as well as the Ca^{2+} concentration and this is probably similar to the effects of a sodium channel opener such as SDZ-201106, which also inhibits influenza virus replication. Whether or not these compounds share the same mechanism of action for their antiviral activity will be the subject of future research, but this study has shown that influenza viruses are sensitive to changes in intracellular ion concentrations and that this may be a suitable target for novel antiviral drugs. Similarly, knowledge of these crucial factors that are required for optimal virus growth may also be used to boost virus production, as we have demonstrated through the use of PKC activators and Na^+ channel inhibitors. This technology could be used for the production of influenza virus vaccines which will most likely make the transition to in vitro culture systems in the near future. As a demonstration of this potential application, which would require activity for a wide range of influenza viruses, we used the enhancing compounds identified in the study to boost the replication of different influenza A viruses, influenza B virus and the FDA-approved H5N1 vaccine virus strain.

CONCLUSION

The identification of viral inhibitors and enhancers validates the functionality of our high-throughput screen assay and raises the possibility of finding novel antiviral or pro-viral drugs by screening libraries of uncharacterized small molecular weight molecules. In summary, through the use of a high-throughput screen of biologically active compounds, we have shown that influenza virus growth can be modulated both positively and negatively by chemical manipulation of Na^+ transport or PKC activity. These findings provide insight into the cellular pathways involved in influenza virus replication and for the first time demonstrate the feasibility of using pro-viral drugs to enhance the growth of influenza virus vaccines in tissue culture.

CHAPTER 3 – SCREENING COMPOUNDS WITH UNKNOWN BIOACTIVE PROPERTIES

INTRODUCTION

We screened in total ~73,000 compounds in duplicate. A small fraction (3.6%) consists of compounds with known bioactivity and the results were described in Chapter II. A fraction of ~12% compiled natural products by means of crude extracts derived from e.g. plants, fungi, lichens, cyano- and marine bacteria, actinomycetes and marine sponges. The hits of this screened section were difficult to follow up since they were not commercially available. Another downside was the crude composition of these extracts which makes it difficult to identify the active compound and to reproduce the results. The majority of screened compounds (~84%) were small molecules whose biological properties, if any, are unknown. They were purified and provided at a given concentrations which allowed us to easily verify found hits. For a compound to be defined as a strong inhibitor it has to decrease the luminescence signal of the reporter by at least 90% compared to untreated cells. Compounds that met this criterion and did not decrease luminescence of the counter screen by more than 30% were re-ordered and further evaluated.

Evaluation process of hit compounds identified in the primary screen

Hit compounds identified in the primary screen were subsequently tested in secondary screens where their cytotoxicity was examined at increasing concentrations. We determined the CC_{50} and CC_{10} for a 24 hour incubation period. The CC_{50} is defined as the concentration of 50% cytotoxicity or the loss of 50% cell viability whereas the CC_{10} is the concentration of 10% cytotoxicity where 90% cell viability is maintained. The $CC_{10,}$ which is different from compound to compound, was used for all further experiments (Fig. 3-1).

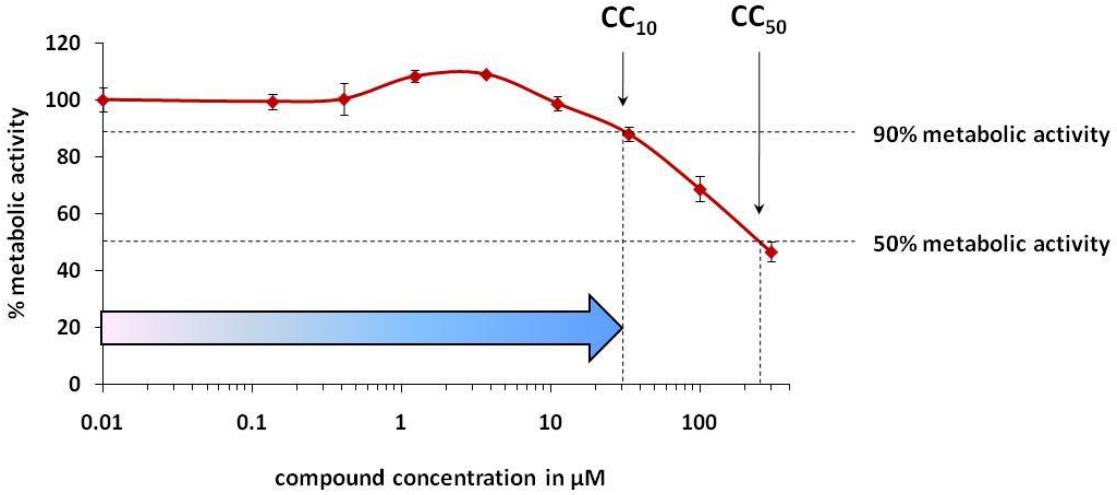

Fig. 3-1. Cell viability assay in A549 cells. A549 cells were treated with increasing compound concentrations and cell viability (metabolic activity) is measured 24 hours later. The CC_{10} is defined by a loss of 10% metabolic activity and the CC_{50} by 50%, respectively. The CC_{10} is the maximum concentration for a compound to be tested in a 24 hour experiment performed in A549 cells. The assay was performed in quintuplicate and is presented as the mean ± standard deviation.

With this we are able to eliminate the issue of compound cytotoxicity and could determine the anti-viral activity for each inhibitor. A549 cells were infected with influenza A/WSN/33 virus in the presence of increasing compound concentrations with the CC_{10} as the maximum. We used a high MOI of 1 to select for strong inhibitors and only those that were able to inhibit viral replication within a 24 hour period by 75% were pursued further. The viral titers in this replication assay were determined by hemagglutination assay (Fig. 3-2A) and a reduction of 2 HA wells corresponds with a reduction in viral titers by 75%. Those compounds that met these criteria were re-tested in replication assays under similar conditions but spanning a specific concentration range in order to determine their IC_{50} concentrations. The supernatants were titered by plaque assay, which allowed us to determine a precise IC_{50} and the maximum inhibitory activity of each compound (Fig. 3-2B).

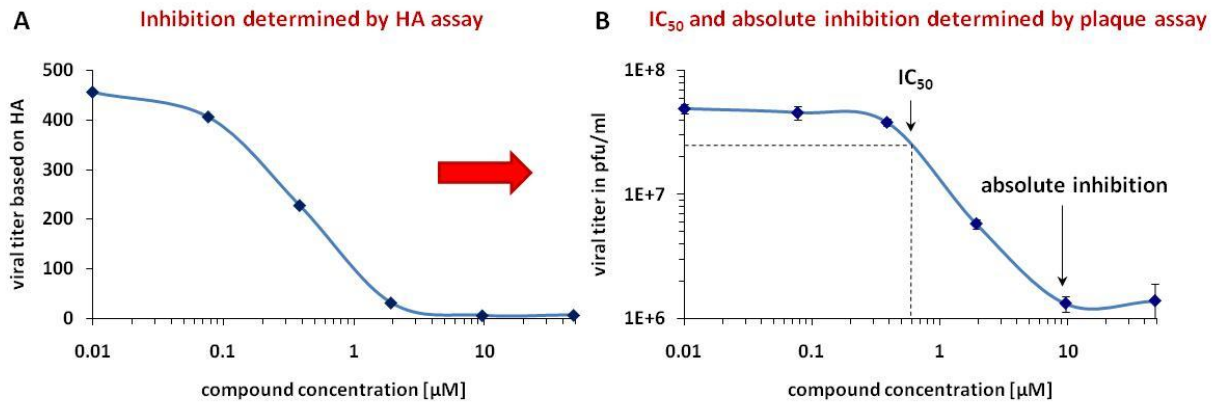

Fig. 3-2. Viral replication assay in A549 cells. A549 cells were infected with influenza A/WSN/33 virus (MOI=1) in the presence of increasing compound concentrations (c_{max}= CC_{10}). (A) Viral titers were determined 24 hours later by HA assay for various concentrations. (B) Viral titers were determined 24 hours later by plaque assay for various concentrations. The IC_{50} is defined as the concentration that reduces viral titers by 50%. The absolute inhibition is defined as the maximal inhibition determined at a non-toxic concentration under test conditions. The assay was performed in triplicate and is presented as the mean ± standard deviation.

For drug development purposes, compounds that inhibit at low concentrations (sub-micromolar) are more desirable, as are those with selective indices ($SI=CC_{50}/IC_{50}$) greater than 10. For this reason we eliminated those compounds with IC_{50} >10 µM as well as those whose with SI<10.

The remaining compounds were characterized in a variety of assays to determine their mode of action. Here we tested compounds at different time points during the replication cycle, which allowed us to identify the stage at which the compound interferes with the virus. Subsequently, we conducted entry assays using pseudotyped HIV-particles and influenza virus-like particles (VLPs) and also mini-genome assays where we tested the effect of compounds on viral polymerase activity.

Compounds that could be assigned to a specific stage of the viral life cycle and demonstrated high inhibitory activity were classified as “lead compounds”. We tested derivatives of these lead compounds hoping to increase potency and decrease toxicity. In addition, lead compounds were tested *in vivo* for their potential to conquer lethal infections in mice.

The selection process is displayed in Fig. 3-3 and includes the number of compounds at each step.

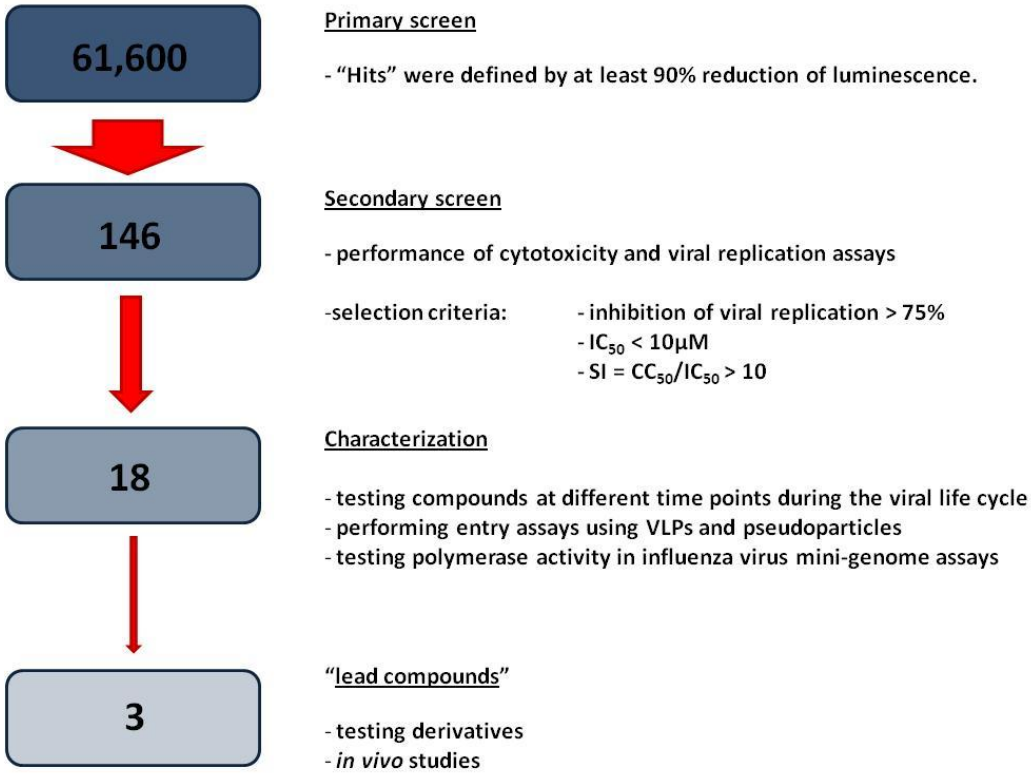

Fig. 3-3. Flow chart for selecting compounds tested in a high-throughput screen. Compound libraries were tested in a primary screen whose read-out was luminescence based. Compounds that decreased luminescence by more than 90% were tested in secondary screens. Compounds were tested for cytotoxicity and inhibitory potential and if they met the selection criteria of the secondary screen, they were further characterized in various assays. Compounds that could be assigned to a specific function or target were subjected to structure analysis and *in vivo* studies.

RESULTS

Among 61,200 screened compounds with unknown biological properties, we identified 146 (~0.24%) that decreased the luminescence signal in the primary screen by more than 90%. Compound libraries were provided to the ICCB by Asinex, ChemBridge, ChemDiv, MayBridge, LifeChemicals and TimTec. Compounds identified as hits in the primary screen were commercially available from these companies, and were re-ordered and tested in cytotoxicity

and replication assays as described above. We confirmed that 18 compounds (~0.03%) met our criteria (inhibition of viral replication >75%, IC_{50} < 10µM, SI>10) for having anti-influenza virus activity (Fig. 3-4).

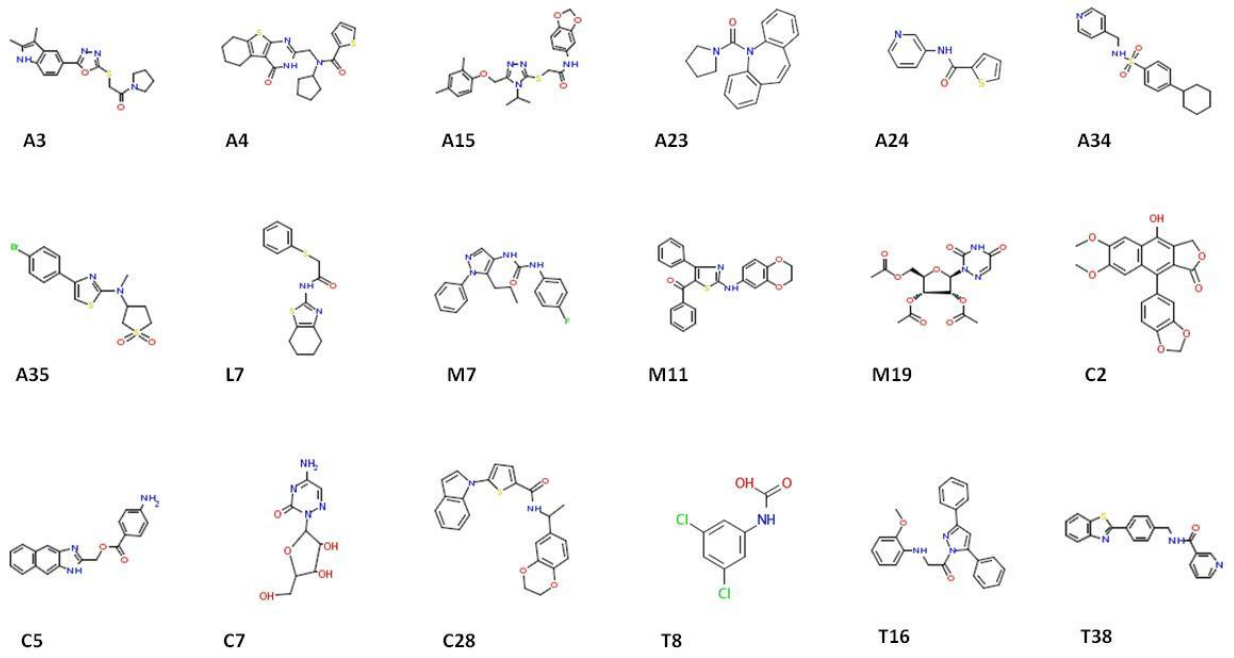

Fig. 3-4. Structures of small molecular weight compounds that exhibit anti-influenza virus activity. 18 compounds were confirmed to exhibit antiviral activity specific for influenza virus. Compounds were identified in different libraries and have an average molecular weight of 341 g/mol. A24 and T8 are the lightest compounds (204 and 206 g/mol) and A15 and M11 the heaviest (454 and 414 g/mol).

Table 3-1 contains compound characteristic data (CC_{50}, IC_{50}, SI and % inhibition) determined in A549 cells.

Tab. 3-1. *In vitro* characteristics of compounds that exhibit anti-influenza virus activity. 18 compounds were confirmed to exhibit antiviral activity specific for influenza virus. Their CC_{50} values were determined in A549 cells for a 24 hours incubation period. Their IC_{50} values for influenza A/WSN/33 virus were determined for infections in A549 cells performed at a MOI of 1. The IC_{50} and absolute inhibition of influenza A/WSN/33 virus was determined by plaque assay. The selective index (SI) is the ratio of CC_{50} over IC_{50} and gives information about the pharmacological relevance of the compound.

compound	CC_{50} [µM]	IC_{50} [µM]	SI (CC_{50}/IC_{50})	inhibition of A/WSN/33 in %
A3	268	0.54	496	99.1
A4	284	5.5	52	79.5
A15	98	1.6	61	85.8
A23	262	4.3	61	92.4
A24	278.2	2.45	114	95.8
A34	80.5	2.4	34	97.5
A35	110	2.1	53	99.988
L7	>100	2.2	>46	99.8
C2	131	0.29	452	97
C5	>300	0.97	>310	91.4
C7	>300	2.25	>130	98.9
C28	203.5	0.94	217	87.5
M7	223	2.8	80	88.1
M11	226	2.05	110	69.2
M19	301	3.95	76	94.2
T8	14.6	0.22	66	99.5
T16	38.4	2.8	14	73.4
T38	172	2.56	67	83.6

From these results, compounds A3, A35, L7, C2 and T8 looked quite interesting due to the fact that they demonstrated high inhibitory activity (A35, L7 and T8) and strong SIs (A3 and C2). Unfortunately, compound L7 was no longer commercially available and could not be pursued further. We consulted a medicinal chemist who advised us to discard compound T8 since its structure is relatively simple and its effect may be unspecific and promiscuous.

Kinetic analysis of antiviral activity

Next, we tested all remaining compounds at different time points during the viral life cycle in order to understand whether they act early or late in infection. First we compared their effect on replication when added prior or post infection. Compound C2 displayed very clearly that addition to the culture medium only one hour post infection diminishes its inhibitory potential which indicates that it may interfere with viral entry (Fig. 3-5).

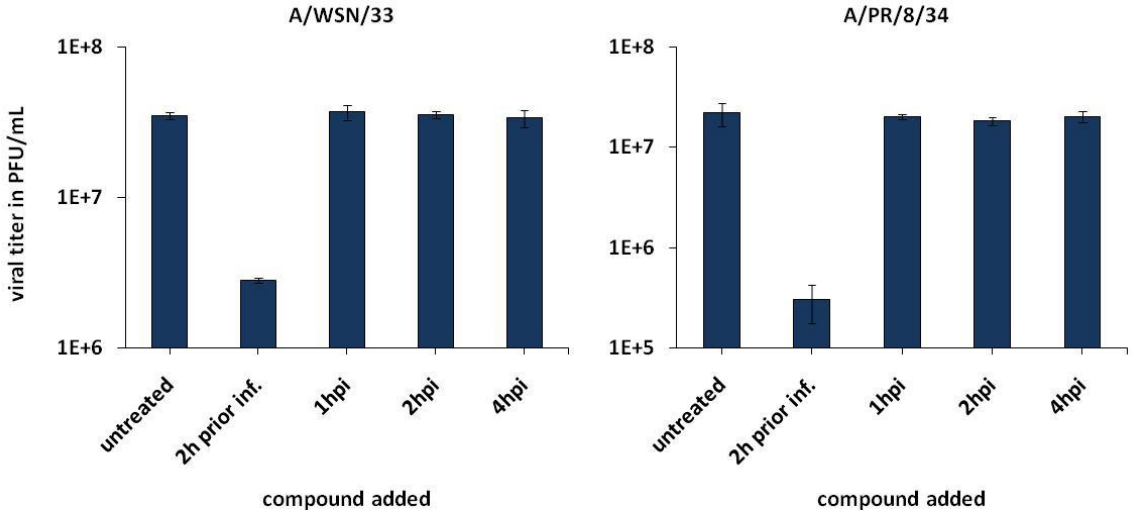

Fig. 3-5. Inhibition of influenza viruses by C2 when added at different times during the viral life cycle . A549 cells were infected with influenza viruses A/WSN/33 and A/PR/8/34 (MOI=1). Compound C2 was present in the culture medium 2 hours prior to infection or added to the medium at indicated time points post infection at a concentration of 2.1 µM (CC_{10}). Viral titers were determined 24 hours post infection by plaque assay. The assay was performed in triplicate and is presented as the mean ± standard deviation.

A549 cells were infected at a high MOI with two different influenza A viruses, A/WSN/33 and A/PR/8/34. Compound treatment started 2 hours prior to infection or at several time points post infection. If the compound is present prior to infection, viral replication is clearly inhibited by 1-2 logs. This inhibition is completely lost if the compound is added only 1 hour post infection. The steps at which the compound may inhibit the virus during this 1 hour are limited to virus attachment, virus endocytosis and fusion and uncoating (Fig. 3-6).

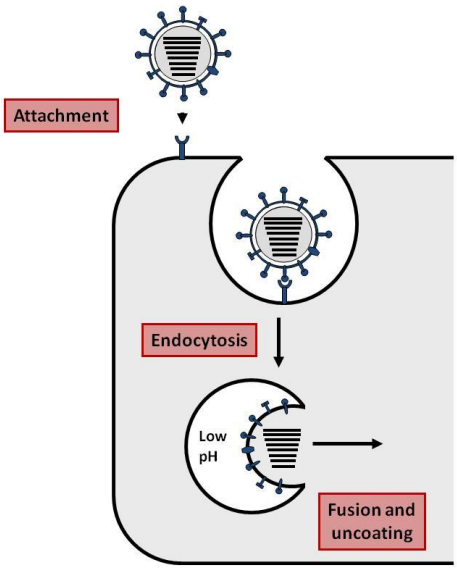

Fig. 3-6. Influenza virus entry process. The entry process of the influenza virus comprises virus attachment, receptor mediated endocytosis and fusion/uncoating triggered by a low pH step (adapted from Fields Virology 5th edition, Chapter *Orthomyxoviridae*; Palese and Shaw).

Compounds were further tested in specific entry assays to verify the results. In sharp contrast, A3 and A35 were found to inhibit even when added after virus infection (Fig. 3-7).

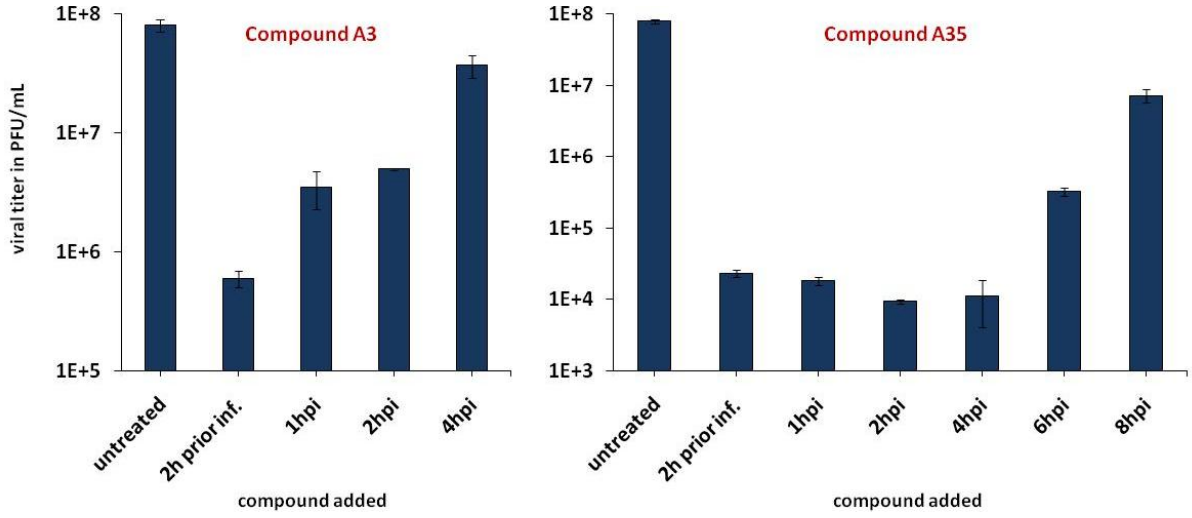

Fig. 3-7. Inhibition of influenza A/WSN/33 virus by compound A3 and A35 when added at different times during the viral life cycle. A549 cells were infected with influenza viruses A/WSN/33 (MOI=1). Compounds A3 and A35 were present in the culture medium 2 hours prior to infection or added to the medium at indicated time points post infection at a concentration of 10 µM A3 or 11.2 µM A35 (CC_{10}). Viral titers were determined 24 hours post

infection by plaque assay. The assay was performed in triplicate and is presented as the mean ± standard deviation.

A549 cells infected at a high MOI with influenza A/WSN/33 virus were treated with A3 and A35 prior and post infection. Compound A3 inhibits viral titers by ~1.5 logs if added up to 2hpi and A35 maintains strong inhibition of viral replication if added up to 4-6hpi. Both compounds seem to act at mid to late stages in the viral life cycle leading to the hypothesis that replication, transcription and/or packaging may be targeted (Fig. 3-8).

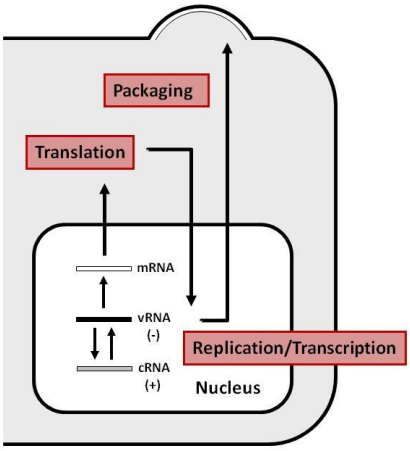

Fig. 3-8. Influenza virus post-entry processes. The viral genome is replicated and transcribed, viral proteins are translated and together with newly synthesized vRNA transported to the budding site where packaging occurs (adapted from Fields Virology 5th edition, Chapter *Orthomyxoviridae*; Palese and Shaw).

A3 and A35 were further evaluated in influenza mini-genome assays in order to determine to what degree the influenza virus polymerase activity is affected.

Entry assays

We addressed the question whether the compounds act directly on the entry step by conducting two different entry specific assays using pseudotyped lentiviral particles and virus like particles.

A pseudoparticle-based entry assay

The pseudoparticles contain a gutted HIV-1 genome expressing gaussia luciferase (GLuc). The incorporated HA and NA glycoproteins of influenza A/WSN/33 virus facilitate entry but all downstream events that drive expression of GLuc are directed by the lentiviral machinery. Entry of the pseudoparticles can be monitored by measuring GLuc in the supernatant. In addition to the influenza virus pseudotyped particles (Flu-PP) we generated pseudoparticles that incorporated the glycoprotein G of VSV (VSV-PP) as well as particles that contained the envelope protein of murine leukemia virus (MuLV-PP), to control for compound specificity (Fig. 3-9).

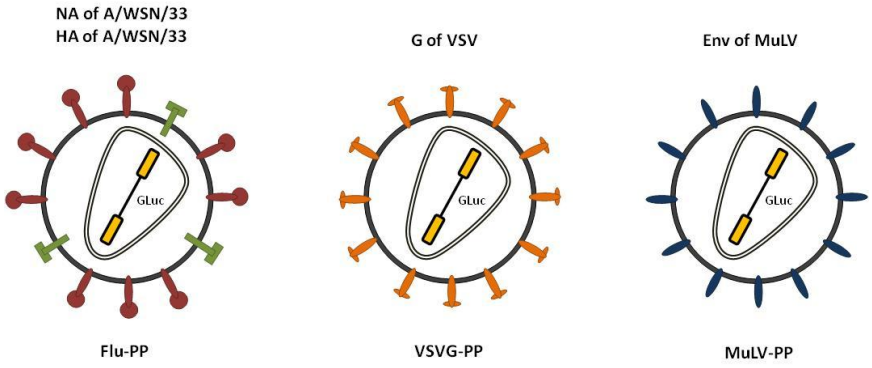

Fig. 3-9. Representation of pseudotyped lentiviaral particles. Lentiviral particles were generated that contain the HA and NA glycoproteins of influenza A/WSN/33 virus (Flu-PP), the G protein of vesicular stomatitis virus (VSVG-PP) or the env protein of murine leukemia virus (MuLV-PP). All particles encode for a secreted form of gaussia luciferase (GLuc).

A549 cells seeded in 96-well plates were infected with pseudoparticles in the presence of compound or DMSO as a control. The luciferase read-out for this assay was performed 48hpi and in the presence of C2 we observed a reduction of more than 95% for both Flu-PPs and VSV-PPs (Fig. 3-10). However, infectivity of MuLV-PPs was unaffected by the presence of C2. Compound A35 did not affect the infectivity of any of the pseudotyped particles, indicating that it does not act on the influenza virus entry step.

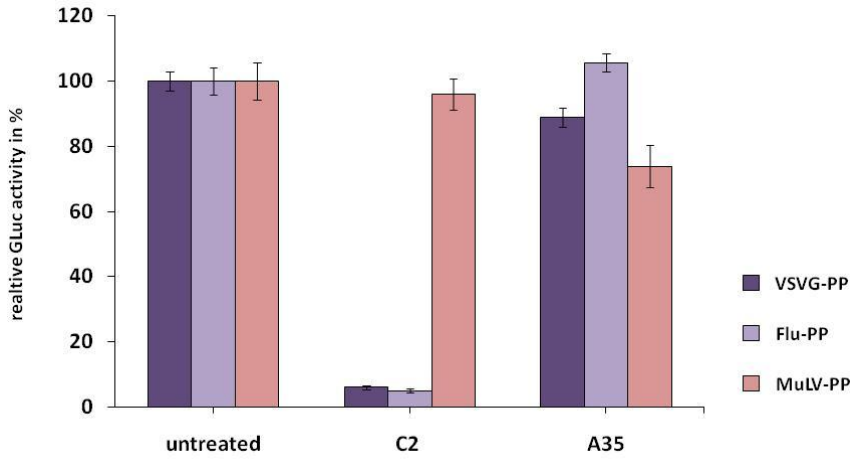

Fig. 3-10. Entry assay using pseudotyped lentiviral particles. A549 cells were infected with VSVG-PP, Flu-PP and MuLV-PP in the presence of DMSO, 2.1 µM C2 or 11.2 µM A35 (CC_{10}). Gaussia luciferase (GLuc) activity was determined 48 hours post infection. The DMSO controls were set at 100% and the luminescence signals derived from the compound treated infections were set in relation. The assay was performed in quintuplicate and is presented as the mean ± standard deviation.

This suggested that C2 generally targets entry of viruses that are endocytosed such as *orthomyxoviridae* (influenza viruses) and *rhabdoviridae* (VSV) but not of those that enter via membrane fusion such *retroviridae* (MuLV). We confirmed the inhibition of VSV by C2 in the context of a whole virus infection performed in A549 cells (Fig. 3-11B). Sindbis virus (*togaviridae*), a positive strand RNA virus that enters cells via receptor mediated endocytosis, also requires a low pH step during the entry process and was shown to be inhibited by C2 (Fig. 3-11C).

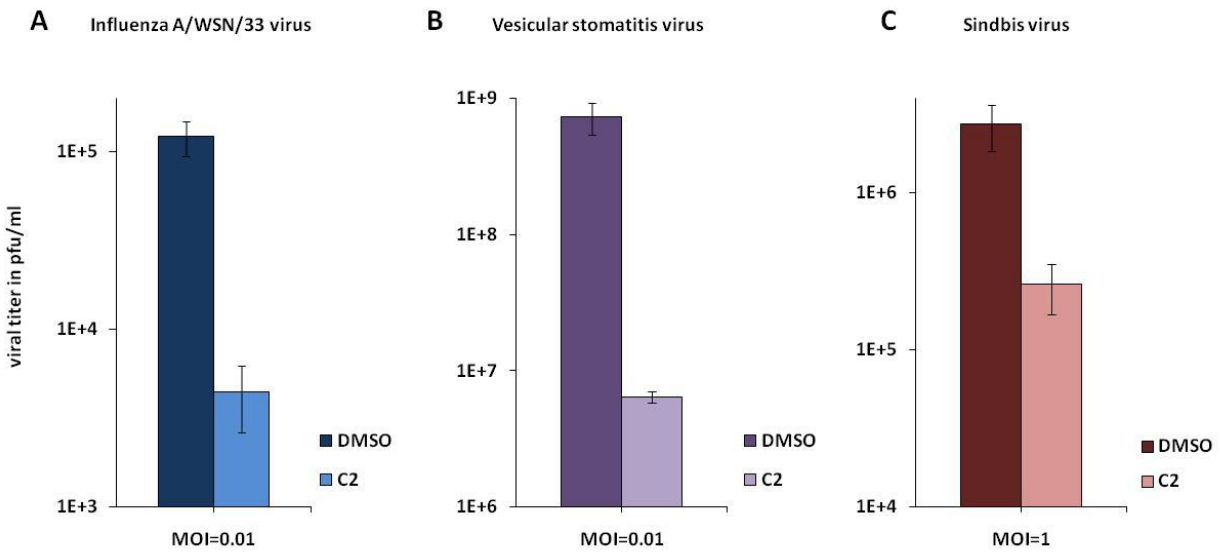

Fig. 3-11. Inhibition of different RNA viruses, dependent on a low pH entry step, by compound C2. A549 cells were infected with (A) influenza A/WSN/33 virus, (B) vesicular stomatitis virus and (C) sindbis virus. Infections were performed at a MOI of 0.01 (A and B) or 1 (C) the presence of DMSO or 2.1 µM C2 (CC_{10}). Viral titers were determined 24 hours post infection by standard plaque assay. The assay was performed in triplicate and is presented as the mean ± standard deviation.

An influenza virus like particle (VLP) based entry assay

VLPs are virus particles that do not contain a viral genome. They are comprised of the viral envelope and its embedded glycoproteins which facilitate infection. VLPs can be used as a tool to deliver proteins via infection which can be quantified. Figure 12 depicts the generation of VLPs used in the following assay (Tscherne et al.).

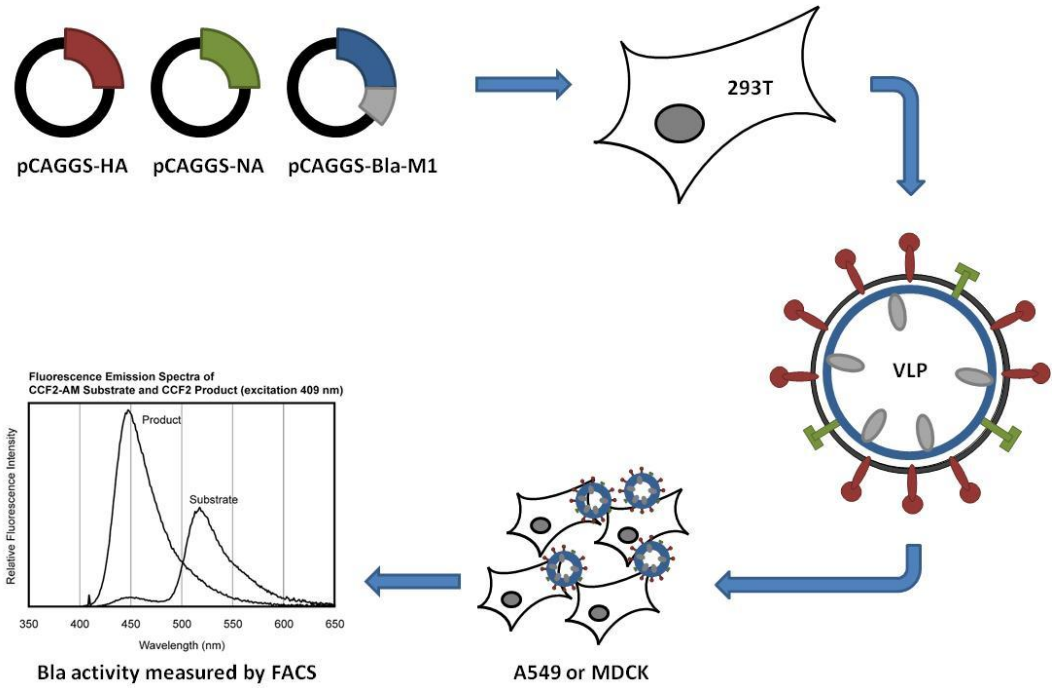

Fig. 3-12. Generation of virus like particles (VLPs) and their employment in an entry assay. Expression plasmids encoding for influenza virus proteins sufficient for generating virus like particles were transfected into 293T cells. VLPs containing beta-lactamase fused to the viral matrix protein M1 can be utilized to infect various cell lines in order to deliver the enzyme. Cells are loaded with a dye containing a beta-lactame ring which is cleaved in the present of beta-lactamase. The cleaved and uncleaved forms of the dye emit differently upon excitation which is measured by FACS.

The M1 protein is modified and fused to beta-lactamase (Bla). Expression plasmids for the HA, NA and Bla-M1 protein of influenza A/WSN/33 virus are transfected in 293T cells. Generated VLPs bear the fusion protein inside which is delivered to cells upon successful entry. Intracellular beta-lactamase activity can be measured by addition of a substrate which fluoresces differently upon cleavage. In contrast to the pseudoparticle entry assay which requires downstream events, this assay does not rely on gene expression. Shortly after infection, cells are harvested, substrate is added and the presence of intracellular beta-lactamase activity is measured by flow cytometry. Although we used A549 cells for all our previous assays we had to switch to MDCK cells due to the fact that the infectivity of A549 cells with VLPs was diminished compared to MDCK cells. This circumstance would make it difficult to measure differences caused by entry inhibitors. By switching cell lines, we had to repeat the cytotoxicity assay to determine the MDCK specific CC_{10} (concentration of 10% cytotoxicity or

90% cell viability) which can differ a lot between cell lines. Shown in figure 13, 70% of MDCK cells were infected with Bla-M1 VLPs compared to mock infected cells and infections with VLPs that lack any glycoproteins. We confirmed our previous finding of C2 of being an entry inhibitor as it inhibits entry of VLPs by ~98%. Compound A3 was included as a compound whose inhibitory effect is unrelated to entry. Compound A24 was identified as an inhibitor that lost its activity when added only 1 hour post infection (data not shown), however using this assay we could not confirm a clear role in virus entry. It's possible that it may target the uncoating step which happens shortly after endocytosis and fusion and would not be detected in the VLP assay. Rottlerin was included as an internal control to verify the assay. It is a PKC inhibitor that was identified while screening known bioactive compounds (Chapter 2). PKC is involved in viral entry and its inhibition should decrease infectivity of VLPs. Rottlerin reduces entry of VLPs by about 63% when present a concentration of 1 µM.

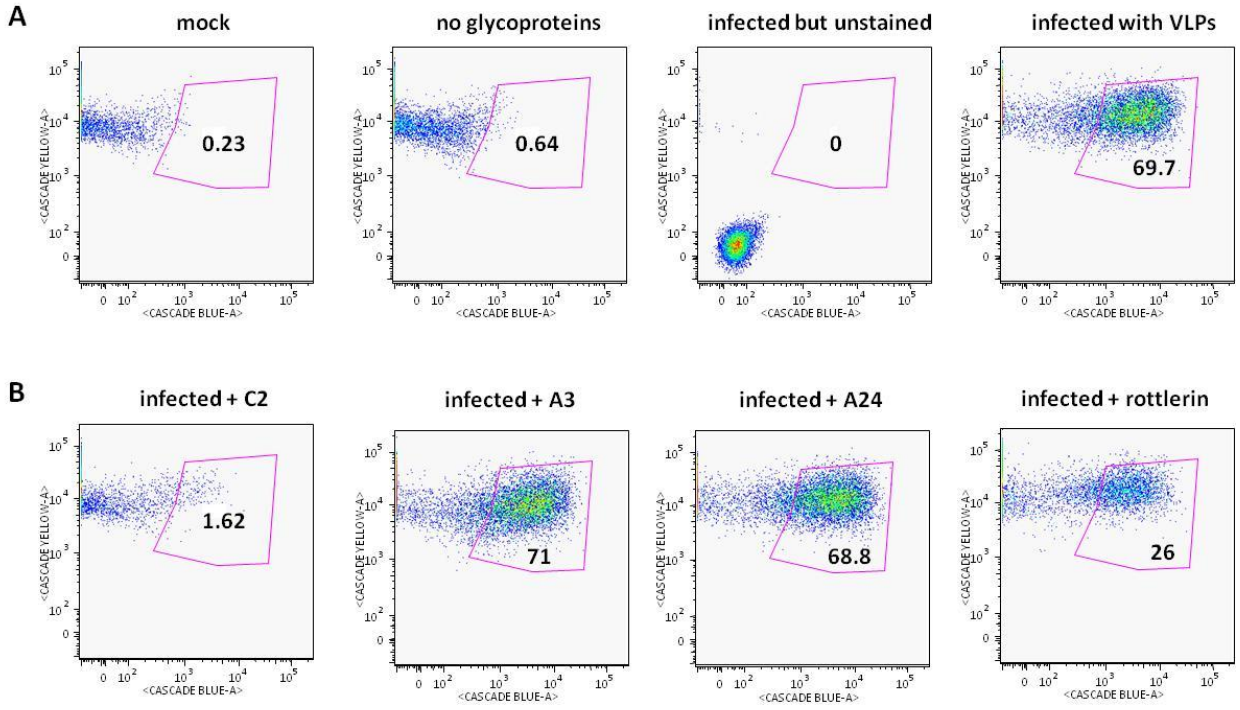

Fig. 3-13. VLP entry assay and FACS analysis. The assay controls are listed in (A) - MDCK cells were mock infected, infected with VLPs lacking glycoproteins, infected with VLPs but unstained and infected with VLPs and stained. In (B), MDCK cells were infected with VLPs and indicated compounds were present 2 hours prior to infection and

during the infection at their CC_{10}. Cells were harvested 4 hours post infection, loaded with the beta-lactame containing dye (CCF2-AM) and subjected to FACS analysis.

During the screening process we made use of a program (SciFinder Scholar) which searches the literature for published chemical structures. We found that C2 was described as a vATPase inhibitor known as dyphillin and that its ability to block vATPases is similar to that of bafilomycin A (Sorensen et al., 2007). V-ATPases acidifiy a wide array of intracellular organelles such as endosomes, lysosomes and secretory vesicles, by pumping protons across the plasma membranes of numerous cell types. V-ATPases are therefore important for viruses that are endocytosed and require a low pH during the entry phase.

Influenza A viruses in a hemolysis assay

All influenza A viruses that we tested were sensitive to C2 treatment and showed reduced viral titers by up to 3 logs underlining the importance of vATPases during the viral entry. Among those influenza virus strains we tested, influenza A/Udorn/72 virus turned out to be resistant to C2 (Fig. 3-14).

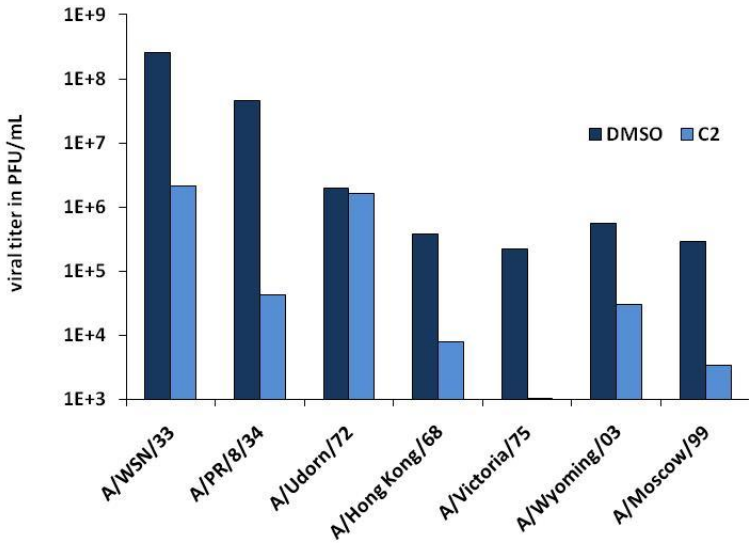

Fig. 3-14. Inhibition of different influenza A viruses by compound C2. A549 cells were infected with influenza A viruses of subtype H1N1 (A/WSN/33 and A/PR/8/34) and of subtype H3N2 (A/Udorn/72, A/HongKong/68, A/Victoria/75, A/Wyoming/03 and A/Moscow/99). Infections were performed at a MOI of 1 in the presence of DMSO or C2 at its CC_{10}. Viral titers were determined by plaque assay at 24 hours post infection.

Given the importance of endosomal acidification for the exposure of the fusion peptide that promotes fusion of the viral membrane with the endosomal membrane, we hypothesized that this virus may be able to fuse at a higher pH compared to other influenza viruses. C2 blocks vATPases but there may be residual activity left which allows for Udorn/72 to fuse where other viruses are trapped in the endosome. We addressed this hypothesis by developing a hemolysis assay. Briefly, chicken erythrocytes (red blood cells = RBC) were incubated on ice with certain amounts of virus. The pH was adjusted accordingly and samples transferred to 37 degrees for 30 min. Fusion of the virus with RBCs occurred if the pH was sufficient to provoke a conformational change in HA that exposed the fusion peptide. The fusion event results in the release of heme from the RBCs, which can be measured by absorbance at 405nm. We found that influenza viruses A/PR/8/34 and A/HK/68 which are both sensitive to C2 (Fig. 3-14) need at least a pH of 5.1 to induce hemolysis whereas influenza A/Udorn/72 virus requires a higher pH of 5.7 (Fig. 3-15). These results confirm our hypothesis that C2-sensitive viruses require a lower pH for viral entry compared to Udorn/72 which can fuse at a pH that is 0.6 units higher. Udorn/72 is therefore not as dependent on a low pH step as are the C2-sensitive viruses.

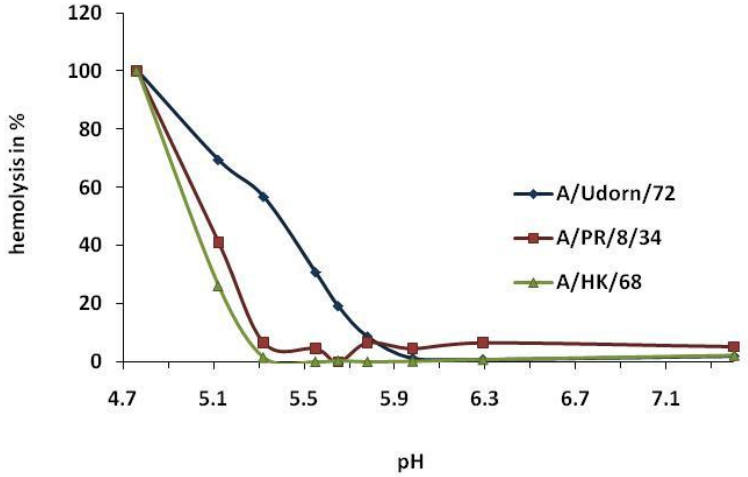

Fig. 3-15. Hemolysis of chicken red blood cells caused by influenza virus at different pH values. Influenza viruses with equal HA titers were incubated on ice with chicken red blood cells (RBCs). The pH was adjusted ranging from 4.75 to 7.3. Hemolysis was allowed to occur for 90 min at 37°C. Absorbance of released hem was measured at 405 nm. The maximum absorbance observed at the lowest pH was set at 100% and absorbencies for remaining pH values were set in relation.

Compounds in influenza virus mini-genome assays

Next, we tested the compounds in influenza virus mini-genome assays. A549 cells were transfected with expression plasmids for the influenza virus polymerase proteins (PB1, PB2 and PA), the nucleoprotein (NP) and the previously described influenza virus specific firefly luciferase reporter. To normalize for transfection efficacy, a *Renilla* luciferase plasmid was co-transfected. Compounds were added at 4 hours prior to transfection and were present for 24 hours until the cells were harvested and lysed to quantify both firefly and *Renilla* luciferase values. A decrease in firefly luciferase compared to untreated cells indicates that the polymerase function is inhibited by the compound. Among those compounds tested, only 2 (A3 and A35) strongly inhibited influenza virus polymerase function without affecting cellular gene expression (monitored by the *Renilla* luciferase plasmid) (Fig. 3-16).

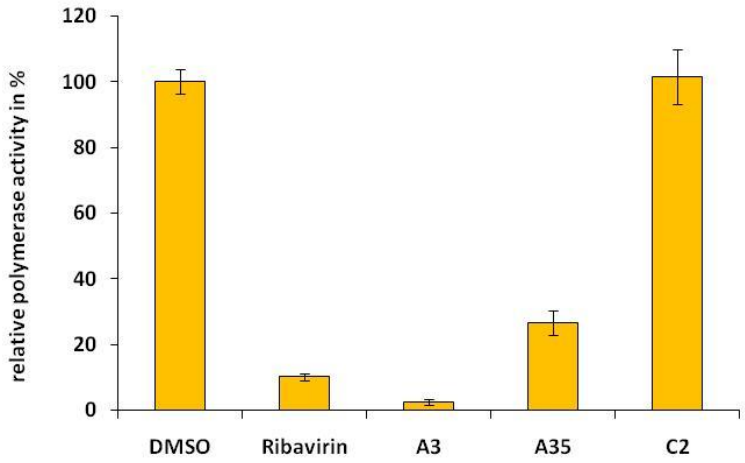

Fig. 3-16. Activity of influenza virus mini-genome in response to different influenza virus inhibitors. A549 cells were transfected with protein expression plasmids for the influenza A/WSN/33 virus polymerase subunits PB1, PB2, PA and the nucleoprotein NP. An influenza virus specific firefly luciferase reporter and a *Renilla* luciferase expression plasmid were co-transfected. Transfections were performed in the presence of DMSO or compounds to test (A3 and A35) at their CC_{10}. Ribavirin as a replication inhibitor is included as a positive control and C2 as an entry inhibitor is included as a negative control. Cells were harvested 24 hours post transfection and activation of the luciferase reporter by the viral polymerase was measured. The DMSO control is set at 100% and all other obtained values were set in relation. The assay was performed in triplicate and is presented as the mean ± standard deviation.

The DMSO control was set to 100% and all other values were calculated in relation to this control. Ribavirin, a known polymerase inhibitor of RNA viruses, was included as a positive control. Compounds A3 and A35 were found to inhibit the influenza virus polymerase function significantly by 98% and 79% respectively. Compound C2 was shown earlier to inhibit influenza virus entry and this result proves that it has no effect on viral polymerase function. It is important to note that the mini-genome activity was tested with increasing concentrations of A3. The inhibition at 2 µM A3 and 100 µM ribavirin (Fig. 3-17) were similar, thus A3 appears to be 50 times more potent than ribavirin.

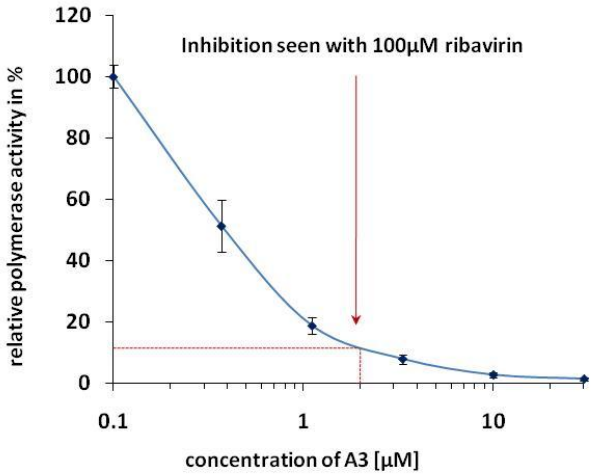

Fig. 3-17. Activity of influenza virus mini-genome in dose response to A3. A549 cells were transfected with protein expression plasmids for the influenza A/WSN/33 virus polymerase subunits PB1, PB2, PA and the nucleoprotein NP. An influenza virus specific firefly luciferase reporter and a *Renilla* luciferase expression plasmid were co-transfected. Transfections were performed in the presence of DMSO, ribavirin (100µM) or increasing concentrations of A3 (c_{max}=CC_{10}). Cells were harvested 24 hours post transfection and activation of the luciferase reporter by the viral polymerase was measured. The DMSO control is set at 100% and all other obtained values were set in relation. The assay was performed in triplicate and is presented as the mean ± standard deviation.

These data confirm that A3 and A35 act by inhibiting viral polymerase function and we can show that when used in combination (Fig. 3-18) that they show additive effects.

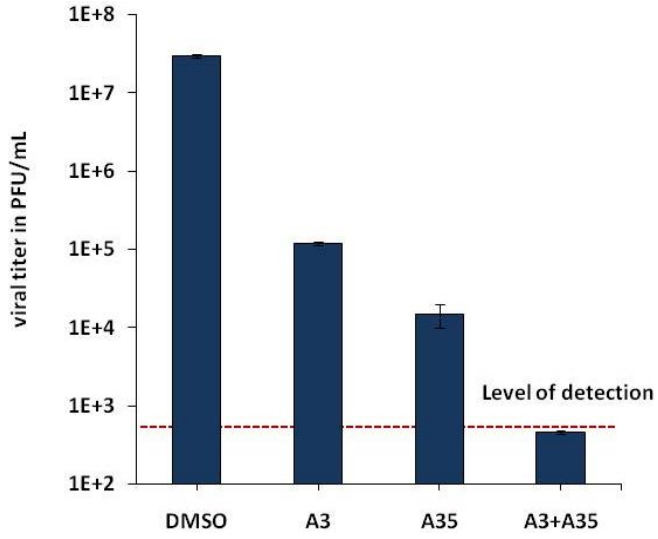

Fig. 3-18. Inhibition of influenza A/WSN/33 virus by compounds A3 and A35. A549 cells were infected with influenza A/WSN/33 virus (MOI=1) in the presence of DMSO or compounds A3, A35 and a combination of A3 and

A35 (concentration of A3 and A35 was their CC_{10}). Viral titers were determined by plaque assay at 24 hours post infection (limit of detection was 500 PFU/mL). The assay was performed in triplicate and is presented as the mean ± standard deviation.

Compound A3 inihibits viral titers by ~2.5 logs and A35 by ~ 3.5 logs. The combination of both compounds inhibits viral titers below the level of detection which was, in this case, a reduction of more then 5 logs. This result suggests that A3 and A35 act via different mechanisms and therefore probably have different targets.

To address the question whether A3 and A35 display broadband antiviral activity, we tested their effect on viral replication of RNA viruses from different families. Influenza viruses A and B virus (*orthomyxoviridae*), Newcastle disease virus (*paramyxoviridae*) and vesicular stomatitis virus (*rhabdoviridae*) are negative strand RNA viruses whereas Sindbis virus (*togaviridae*) has a positive strand RNA genome. Influenza B virus, SINV and NDV grow relatively poorly in A549 cells when infected at a low MOI and were therefore tested at an MOI of 1 together with influenza A/WSN/33 virus (Fig. 3-19A). The latter virus and VSV grow to high titers in A549 cells even when infected at a low MOI of 0.01 (Fig. 3-19B).

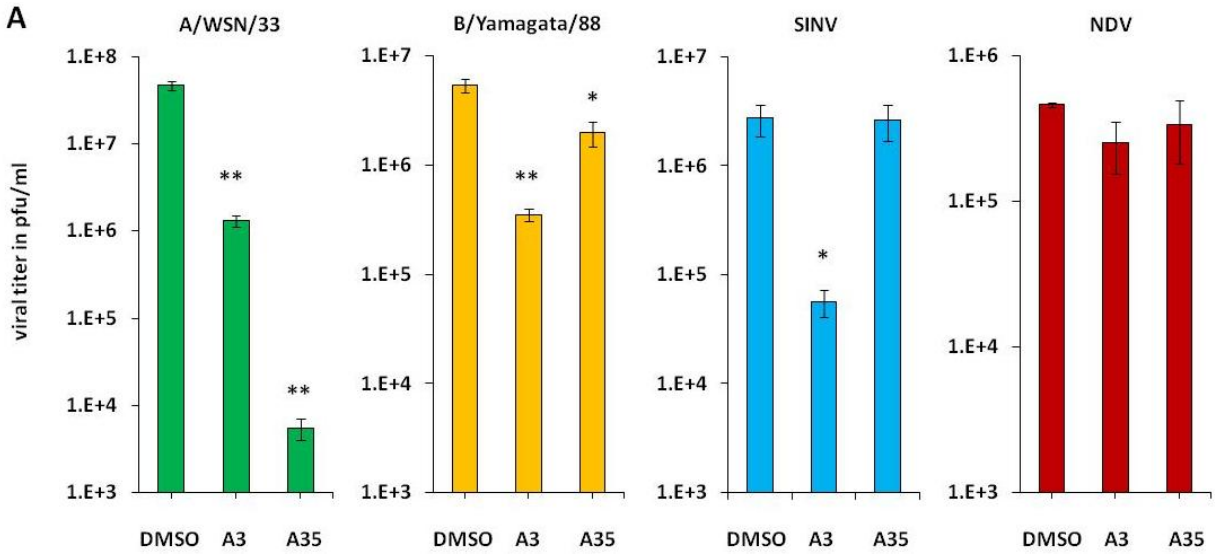

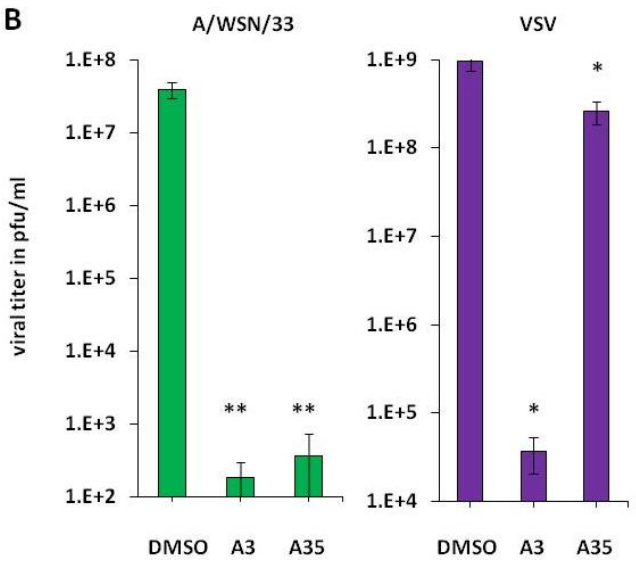

Fig. 3-19. Inhibition of different RNA viruses by compounds A3 and A35. A549 cells were infected with (A) influenza viruses A/WSN/33 and B/Yamagata/88, Sindbis Virus (SINV), Newcastle disease virus (NDV) (MOI=1) and (B) influenza A/WSN/33 virus and vesicular stomatitis virus (MOI=0.01). Infections were performed in the presence of DMSO or compounds A3 and A35 at their CC_{10}. Viral titers were determined by plaque assay at 24 hours post infection. The assay was performed in triplicate and is presented as the mean ± standard deviation. Student's *t* test: *, $P \leq 0.05$; **, $P \leq 0.01$.

Compound A3 and A35 significantly reduce viral titers of influenza A/WSN/33 virus at infections performed at a high MOI by 2 and 4 logs, respectively. In a multi cycle replication assay when infections were performed at a low MOI, both compounds reduce viral titers by 5 logs below the limit of detection. Compound A3 exhibits in addition to inhibiting influenza A virus antiviral activity against influenza B virus (-1.5 logs), SINV (-2 logs) and VSV (-4.5 logs) but only little against NDV (-0.5 logs). In contrast, compound A35 does not show broadband antiviral activity and reduces viral titers of influenza B virus, SINV, NDV and VSV only by 0.5 logs, if at all. Up to then, we had only tested compound A35 with influenza A virus strain A/WSN/33. To verify its inhibitory effect on other influenza A virus strains we performed replication assays with influenza viruses A/PR/8/34 (H1N1), A/Udorn/72 (H3N2) and A/Moscow/10/99 (H3N2) (Fig. 3-20).

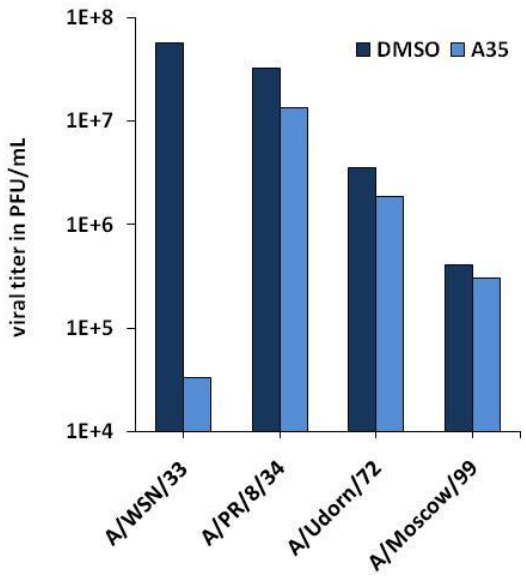

Fig. 3-20. Inhibition of different influenza A viruses by compound A35. A549 cells were infected with influenza viruses A/WSN/33, A/PR/8/34, A/Udorn/72 and A/Moscow/99 (MOI=1). Infections were performed in the presence of DMSO or compounds A35 at its CC_{10}. Viral titers were determined by plaque assay at 24 hours post infection.

We found that A35 specifically inhibits influenza A/WSN/33 virus replication but has very little effect (<50%) on the replication of other influenza A viruses. This was really surprising, especially since influenza A/PR/8/34 virus is a close relative of influenza A/WSN/33 virus. We used this circumstance to our advantage and tried to determine why one strain was sensitive to A35 and another close relative was resistant. We went back to the influenza virus mini-genome assay and tested the polymerase complexes of both influenza viruses A/WSN/33 and A/PR/8/34 for their response to A35 treatment (Fig. 3-21).

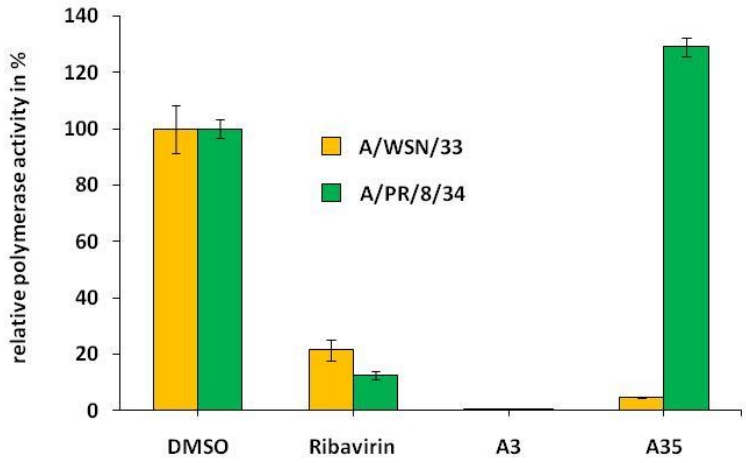

Fig. 3-21. Activity of influenza virus A/WSN/33 and A/PR/8/34 mini-genome in response to different influenza virus inhibitors. A549 cells were transfected with protein expression plasmids for influenza virus A/WSN/33 or A/PR/8/34 polymerase subunits PB1, PB2, PA and the nucleoprotein NP. An influenza virus specific firefly luciferase reporter and a *Renilla* luciferase expression plasmid were co-transfected. Transfections were performed in the presence of DMSO or compounds A3 and A35 at their CC_{10}. Ribavirin as a replication inhibitor is included as a positive control. Cells were harvested 24 hours post transfection and activation of the luciferase reporter by viral polymerases was measured. The DMSO control in both mini-genomes is set at 100% and values obtained for compound treated mini-genomes were set in relation accordingly. The assay was performed in triplicate and is presented as the mean ± standard deviation.

Again, the luciferase signal for the DMSO control for both viral polymerase complexes was set at 100% and all other values were calculated relative to this control. Ribavirin and A3 were included as positive controls and inhibited both polymerase complexes equally whereas compound A35 inhibited the complex of strain A/WSN/33 as seen earlier but there was no effect on strain A/PR/8/34. This result clearly indicated that A35 specifically targets the polymerase function of strain A/WSN/33. The polymerase complex consists of PB1, PB2 and PA and also needs NP to function. We systematically swapped each subunit of strain A/WSN/33 with those of strain A/PR/8/34 in order to determine which viral protein confers resistance to A35. We found that if the NP proteins of both strains are swapped, the sensitive polymerase complex of strain A/WSN/33 becomes resistant and vice versa, the resistant complex of strain A/PR/8/34 becomes sensitive (Fig. 3-22). Ribavirin and compound A3 were included as positive controls to show that the chimeric polymerase complexes are inhibited equally well.

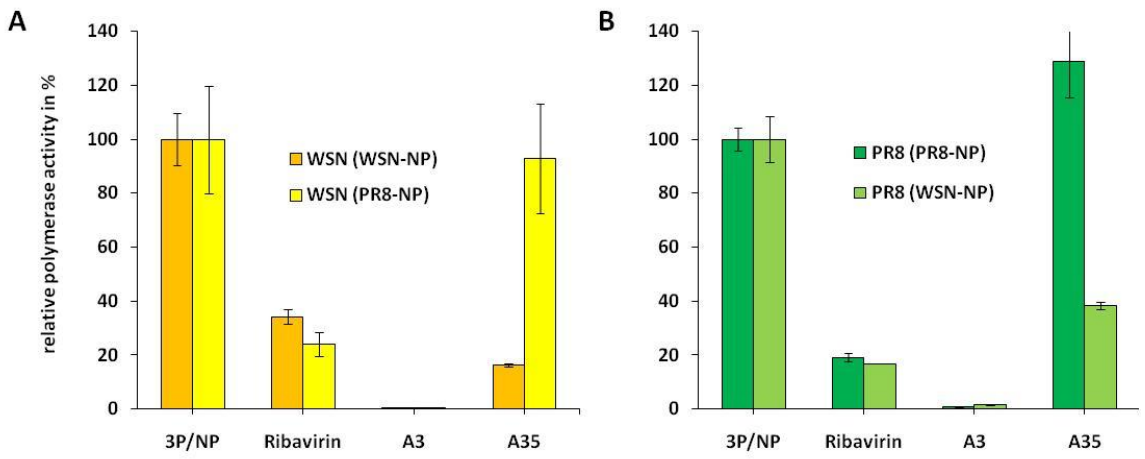

Fig. 3-22. Activity of chimeric influenza virus mini-genome in response to different influenza virus inhibitors. A549 cells were transfected with protein expression plasmids for influenza virus (A) A/WSN/33 or (B) A/PR/8/34 polymerase subunits PB1, PB2, PA and the nucleoprotein NP of both strains. An influenza virus specific firefly luciferase reporter and a *Renilla* luciferase expression plasmid were co-transfected. Transfections were performed in the presence of DMSO or compounds A3 and A35 at their CC_{10}. Ribavirin as a replication inhibitor is included as a positive control. Cells were harvested 24 hours post transfection and activation of the luciferase reporter by viral polymerases was measured. The DMSO control for the wild type and chimeric mini-genome is set at 100% and values obtained for compound treated mini-genomes were set in relation accordingly. The assay was performed in triplicate and is presented as the mean ± standard deviation.

These results evidently show that the resistance to A35 is conferred by the NP protein of PR8. The amino acid sequence of the NP protein differs by only 20 residues between these two virus strains (Fig. 3-23).

```
WSN.            MATKGTKRSYEQMETDGERQNATEIRASVGKMIDGIGRFYIQMCTELKLSDYEGRLIQNS 60
PR8.            MASQGTKRSYEQMETDGERQNATEIRASVGKMIGGIGRFYIQMCTELKLSDYEGRLIQNS 60
                **  ***************************** ************************

WSN.            LTIERMVLSAFDERRNKYLEEHPSAGKDPKKTGGPIYRRVDGKWRRELILYDKEEIRRIW 120
PR8.            LTIERMVLSAFDERRNKYLEEHPSAGKDPKKTGGPIYRRVNGKWMRELILYDKEEIRRIW 120
                ************************************ *** ***************

WSN.            RQANNGDDATAGLTHMMIWHSNLNDATYQRTRALVRTGMDPRMCSLMQGSTLPRRSGAAG 180
PR8.            RQANNGDDATAGLTHMMIWHSNLNDATYQRTRALVRTGMDPRMCSLMQGSTLPRRSGAAG 180
                ************************************************************

WSN.            AAVKGVGTMVMELIRMIKRGINDRNFWRGENGRRTRIAYERMCNILKGKFQTAAQRTMVD 240
PR8.            AAVKGVGTMVMELVRMIKRGINDRNFWRGENGRKTRIAYERMCNILKGKFQTAAQKAMMD 240
                ************ ****************** ********************  * *

WSN.            QVRESRNPGNAEFEDLIFLARSALILRGSVAHKSCLPACVYGSAVASGYDFEREGYSLVG 300
PR8.            QVRESRNPGNAEFEDLTFLARSALILRGSVAHKSCLPACVYGPAVASGYDFEREGYSLVG 300
                *************** ************************ *****************

WSN.            IDPFRLLQNSQVYSLIRPNENPAHKSQLVWMACHSAAFEDLRVSSFIRGTKVVPRGKLST 360
PR8.            IDPFRLLQNSQVYSLIRPNENPAHKSQLVWMACHSAAFEDLRVLSFIKGTKVLPRGKLST 360
                ****************************************** *** **** *******

WSN.            RGVQIASNENMETMESSTLELRSRYWAIRTRSGGNTNQQRASSGQISIQPTFSVQRNLPF 420
PR8.            RGVQIASNENMETMESSTLELRSRYWAIRTRSGGNTNQQRASAGQISIQPTFSVQRNLPF 420
                ****************************************** *****************

WSN.            DRPTIMAAFTGNTEGRTSDMRTEIIRLMESARPEDVSFQGRGVFELSDEKATSPIVPSFD 480
PR8.            DRTTIMAAFNGNTEGRTSDMRTEIIRMMESARPEDVSFQGRGVFELSDEKAASPIVPSFD 480
                ** ****** *************** ************************ ********

WSN.            MSNEGSYFFGDNAEEYDN 498
PR8.            MSNEGSYFFGDNAEEYDN 498
                ******************
```

Fig. 3-23. Sequence alignment of NP of influenza viruses A/WSN/33 and A/PR/8/34. Influenza viruses A/WSN/33 (WSN) and A/PR/8/34 (PR8) contain 498 residues; differences in the amino acid sequence are highlighted in red.

In order to identify the domain or precise residues that are responsible for the resistance to A35, we generated chimeras of both nucleoproteins and tested them for their response to A35 treatment in the mini-genome assay. We found a single residue at position 283 that is a serine in WSN and a proline in PR8 that when switched reverses the resistance pattern (Fig. 3-24).

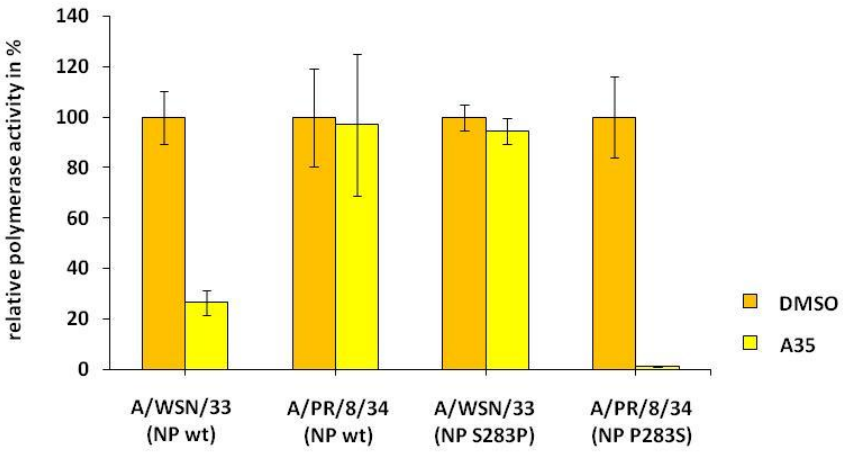

Fig. 3-24. Activity of influenza virus A/WSN/33 and A/PR/8/34 mini-genome in response to compound A35. A549 cells were transfected with protein expression plasmids for influenza virus A/WSN/33 and A/PR/8/34 polymerase subunits PB1, PB2, PA and the wild type nucleoprotein NP or a mutant NP. The NP of strain A/WSN/33 was mutated at position S283P and the NP of strain A/PR/8/34 was mutated at position P283S. An influenza virus specific firefly luciferase reporter and a *Renilla* luciferase expression plasmid were co-transfected. Transfections were performed in the presence of DMSO or A35 at its CC_{10}. Cells were harvested 24 hours post transfection and activation of the luciferase reporter by viral polymerases was measured. The DMSO control for each mini-genome is set at 100% and values obtained for A35 treated mini-genomes were set in relation. The assay was performed in triplicate and is presented as the mean ± standard deviation.

If the NP of the WSN strain is mutated at position 283 from a serine to a proline (the residue in PR8) the polymerase activity can be completely restored. In contrast, if the NP of the PR8 strain is mutated at the same position from a proline to a serine (the residue in WSN) the polymerase complex becomes highly sensitive to A35.

Interestingly, the WSN strain is the only virus in the database that contains a serine at position 283. All other viruses have a proline or a leucine in this position. We tested a variety of different viruses that have a proline at position 283 and none of them were affected by A35. In addition, we tested the NP of the influenza A/Vietnam/1203/04 virus (H5N1) which contains a leucine at position 283, in the mini-genome assay and found that a leucine also confers resistance to A35 (data not shown).

Identification of a putative binding site of A35 in NP of influenza A/WSN/33 virus

To translate the results from the mini-genome assay into the context of a whole virus infection, we generated recombinant viruses of both strains WSN and PR8 with NP segments bearing either the original residue at position 283 or the mutated version. We employed the technique of reverse genetics (Fodor et al., 1999) to rescue the recombinant viruses and tested them subsequently in tissue culture (Fig. 3-25).

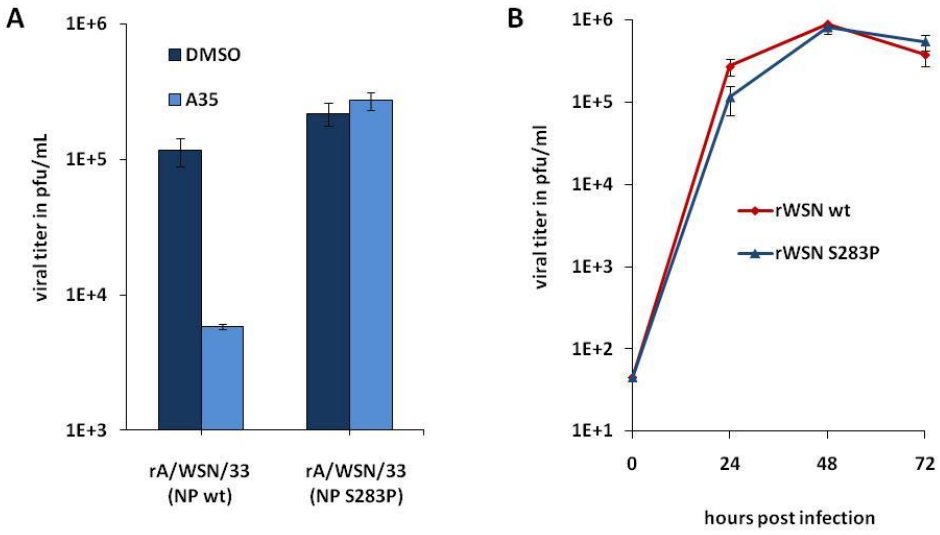

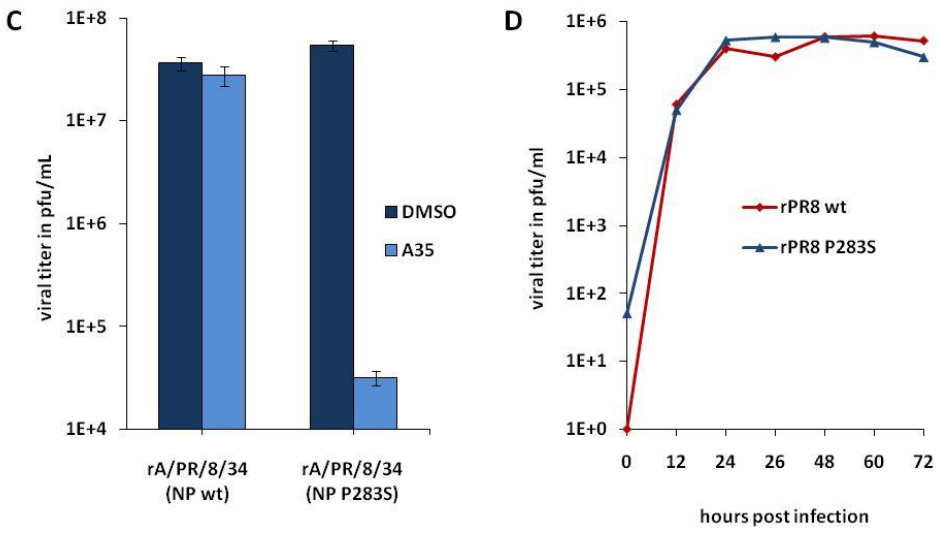

Fig. 3-25. Growth kinetics of recombinant influenza virus A/WSN/33 and A/PR/8/34 and their response to compound A35. A549 cells were infected with recombinant A35-sensitive and resistant influenza viruses (A) A/WSN/33 and (C) A/PR/8/34. Infections were performed at an MOI of 1 and in the presence of DMSO or A35 at its CC_{10}. Viral titers were determined 24 hours post infection by plaque assay. The assay was performed in triplicate and is presented as the mean ± standard deviation. A549 cells were infected with recombinant A35-sensitive and resistant influenza viruses (B) A/WSN/33 and (D) A/PR/8/34 at a MOI of 0.01. Viral titers were determined by plaque assay at indicated time points post infection.

Fig. 3-25A demonstrates the response of the recombinant WSN viruses to A35. The virus containing the NP segment with the original residue at position 283 (rWSN wt) is sensitive to A35 and inhibited compared to the DMSO control. In contrast, the virus containing the mutated NP segment (rWSN S283P) is resistant to A35 and grows to similar titers as the DMSO control. The right hand panel of Fig. 3-25A shows growth curves of both viruses in A549 cells and proves comparable fitness. The same experiment was performed for the recombinant viruses of the PR8 strain (Fig. 3-25B). The virus which contains the wt NP segment (rPR8 wt) is resistant to A35 treatment and grows to similar titers as the DMSO control, whereas the virus that contains the NP segment which was mutated at position 283 (rPR8 P283S) is highly sensitive to and strongly inhibited by A35. To test viral fitness, growth curves were performed in A549 cells. Both viruses have similar growth properties.

The recombinant PR8 viruses were utilized in primer extension assays to confirm the results of the mini-genome assay. The inhibition of viral polymerase activity should result in a decrease of

viral RNA species (v-, c- and/or mRNA). Specific primer for the v-, c- and mRNA of the NA segment bind within its non-coding regions and amplify towards the 3'end (vRNA) or the 5'end (c- and m-RNA). The different reverse transcriptase (RT) products have different sizes and can be separated on SDS-PAGE. In Fig. 3-26A, PR8 wt (A35-resistant virus) was tested in response to compounds A3, A35 and ribavirin (compounds in two different concentrations). Compound A35 does not inhibit this viral polymerase and the amounts of viral RNA species are comparable to those of the DMSO control. In contrast, A3 completely inhibits viral polymerase activity at a concentration of 2 and 10µM. There is no RNA detectable similar to the 100µM ribavirin control. In Fig. 3-26B, the A35-sensitive virus, PR8 (NP P283S) was tested in response to A35 and ribavirin and this viral polymerase is completely inhibited by A35 at a concentration of 5 and 10µM. At least a concentration of 100µM ribavirin is required to obtain a similar degree of inhibition. This assay further proved that compounds A3 and A35 target the viral polymerase function and exhibit increased potency over ribavirin.

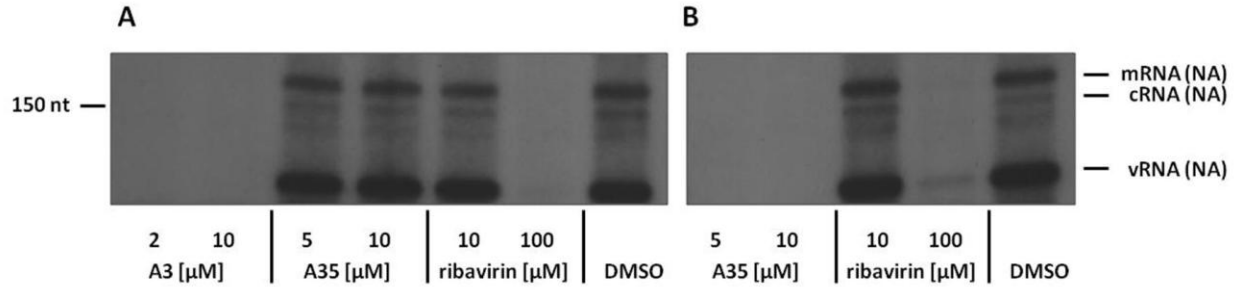

Fig. 3-26. Primer extension assay of the NA segment. A549 cells were infected with influenza viruses (A) A/PR/8/34 (NP wt) and (B) A/PR/8/34 (NP P283S) at an MOI of 7. Infections were performed in the presence of DMSO or A3, A35 and ribavirin. Viral RNA was extracted 9 hours post infection and subjected to primer extension analysis.

These data confirm that residue 283 in the WSN NP and PR8 NP is crucial and suggest that this amino acid participates in the binding of A35 to NP, but this still needs to be confirmed by compound-protein co-crystallization. Another way to confirm targets and identify potential binding sites is the generation of escape mutants. We passaged WSN in A549 cells in the presence of DMSO (solvent) or increasing concentrations of A35. The same was done for compound A3 whose target has not yet been identified. We also included compound C2, which

inhibits cellular vATPases and therefore it should be relatively difficult for a virus to escape in this case. After 5 passages with A35 we isolated a virus that was no longer sensitive to A35 (Fig. 3-27).

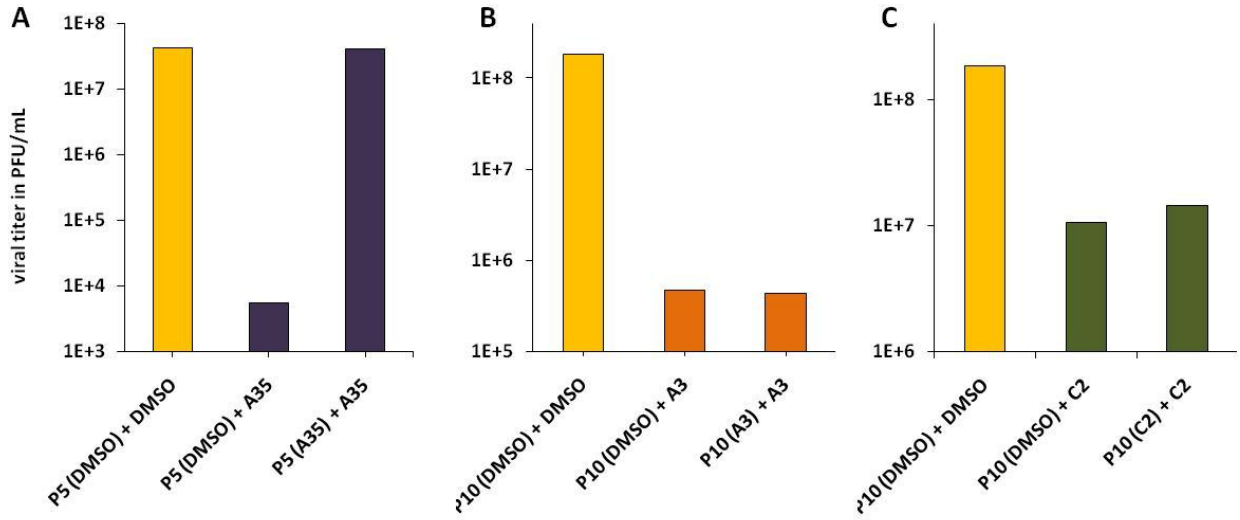

Fig. 3-27. Influenza A/WSN/33 virus passaged in the presence of compounds A3, A35 and C2. (A) Influenza A/WSN/33 virus that was passaged 5 times in the presence of DMSO or A35 was tested in A549 cells at a MOI of 1 in the presence of DMSO or A35 at its CC_{10}. (B and C) Influenza A/WSN/33 virus that was passaged 10 times in the presence of DMSO, (B) A3 or (C) C2 was tested in A549 cells at a MOI of 1 in the presence of DMSO, (B) A3 or (C) C2 at their CC_{10}. (A, B and C) Viral titers were determined by plaque assay at 24 hours post infection.

The virus passaged in the presence of DMSO is still inhibited by A35, whereas the A35-passaged is now insensitive to inhibition by A35. We passaged virus up to 10 times with increasing concentrations of A3 or C2 but we could not isolate escape mutants. In both cases, the compound-passaged virus remains sensitive to compound treatment (2.5 log decrease for A3 and 1 log decrease for C2). This result raises the hypothesis that A3 may target a host cell protein which is necessary for the viral polymerase to function.

The A35-resistant virus was plaque purified and the vRNA extracted. From previous results we speculated that we would find mutations in the NP segment, so we focused on sequencing this segment. We picked 10 individual clones for the A35-passaged virus and compared their NP sequences to the DMSO-passaged virus. 8 out of these 10 clones contained the same mutation

at position 51, which was changed from an aspartic acid to glycine. The remaining two clones had a mutation in position 285 from a valine to an isoleucine and one of the 10 clones contained both of these mutations (Fig. 3-28).

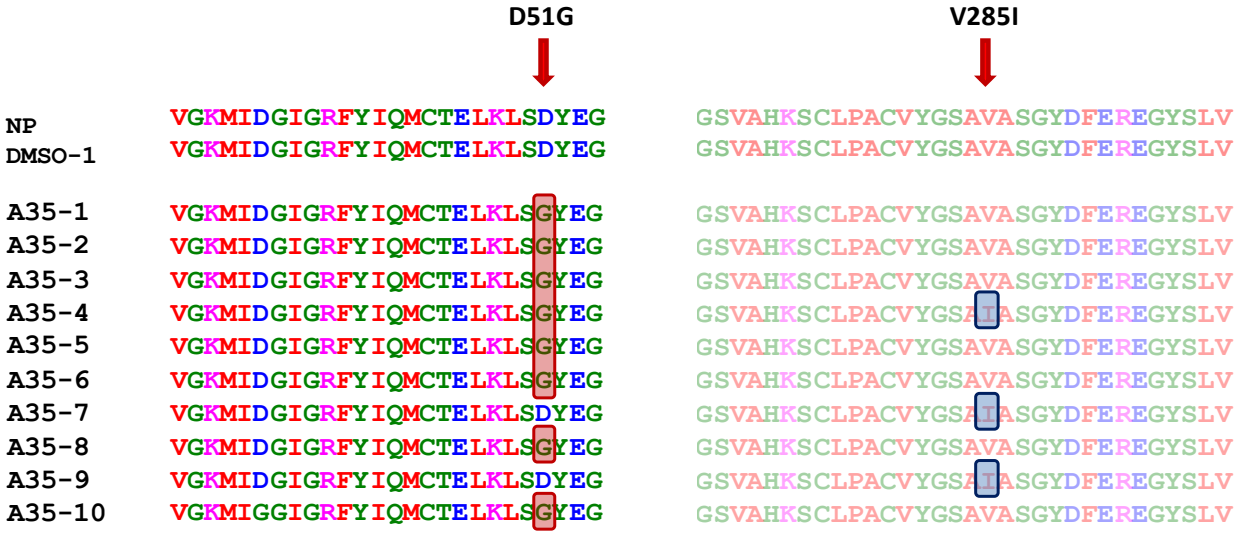

Fig. 3-28. Identification of A35 escape mutants in NP. Partial sequence alignment of a NP segment, derived from unpassaged virus, with a NP segment, derived from DMSO-passaged virus and NP segments derived from 10 individual clones of A35-passaged virus.

To confirm whether these residue changes are sufficient for conferring A35 resistance, we introduced them into the wt NP segment of WSN using site-directed mutagenesis. These mutated NP segments were co-transfected with the polymerase subunits to test their sensitivity to compound treatment. While the polymerase complex containing the wt NP is highly sensitive to A35, the polymerase complexes that harbor the mutant NPs, whether it is one of the single mutations (D51G or V285I) or the double mutation (D51G/V285I), are able to function efficiently in the presence of A35 (Fig. 3-29).

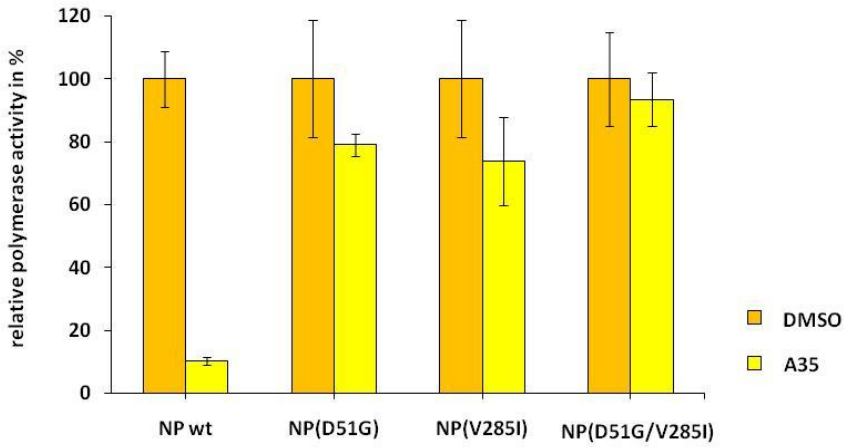

Fig. 3-29. Activity of influenza virus mini-genome containing escape mutations in NP in response to compound A35. A549 cells were transfected with protein expression plasmids for influenza A/WSN/33 virus polymerase subunits PB1, PB2, PA and different NP proteins (NP wt, NP D51G, NP V285I and NP D51G/V285I). An influenza virus specific firefly luciferase reporter and a *Renilla* luciferase expression plasmid were co-transfected. Transfections were performed in the presence of DMSO or A35 at its CC_{10}. Cells were harvested 24 hours post transfection and activation of the luciferase reporter by viral polymerases was measured. The DMSO control for each mini-genome is set at 100% and values obtained for A35 treated mini-genomes were set in relation. The assay was performed in triplicate and is presented as the mean ± standard deviation.

For both NP mutants (D51G and V285I) WSN recombinant viruses were engineered and tested for their response to A35 and found to be resistant (data not shown).

The two escape mutants (ASP 51, VAL 285) and the residue identified in the chimeric approach (SER 283) are located in the same area on the 3D structure of NP as depicted in Fig. 3-30. This region may comprise a putative binding site of A35 on NP.

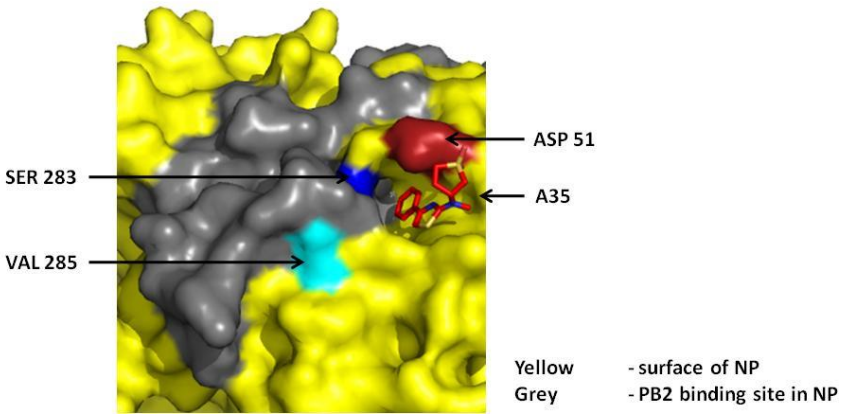

Fig. 3-30. Putative binding site of compound A35 in NP. The compound A35 was computational modeled into the crystal structure of NP of influenza A/WSN/33 virus. The protein surface of NP is stained yellow and the predicted interaction site with PB2 is stained grey. The two residues identified via the generation of escape mutants are colored in ruby (D51) and azure (V285) and the residue indentified in the chimeric approach is colored in blue.

Determination of A35's mode of action in inhibiting viral replication

Interestingly, the putative A35 binding site is in close proximity to the PB2 binding site on NP, which led to the hypothesis that A35 may inhibit binding of PB2 to NP. We addressed this by conducting co-immunoprecipitation experiments where the influenza mini-genome system was transfected into A549 cells in the presence or absence of A35. We used the PR8 system and took advantage of the resistant (wt) and sensitive (P283S) NP that was generated earlier (Fig. 3-31A). NP was precipitated with specific antibodies and the bound PB2 was quantified in western blots. Figure 3-31A shows the data obtained when the DNA of the full polymerase complex and the mini-genome plasmid are co-transfected with the NP, whereas Fig. 3-31B contains data obtained when only NP and PB2 are co-expressed.

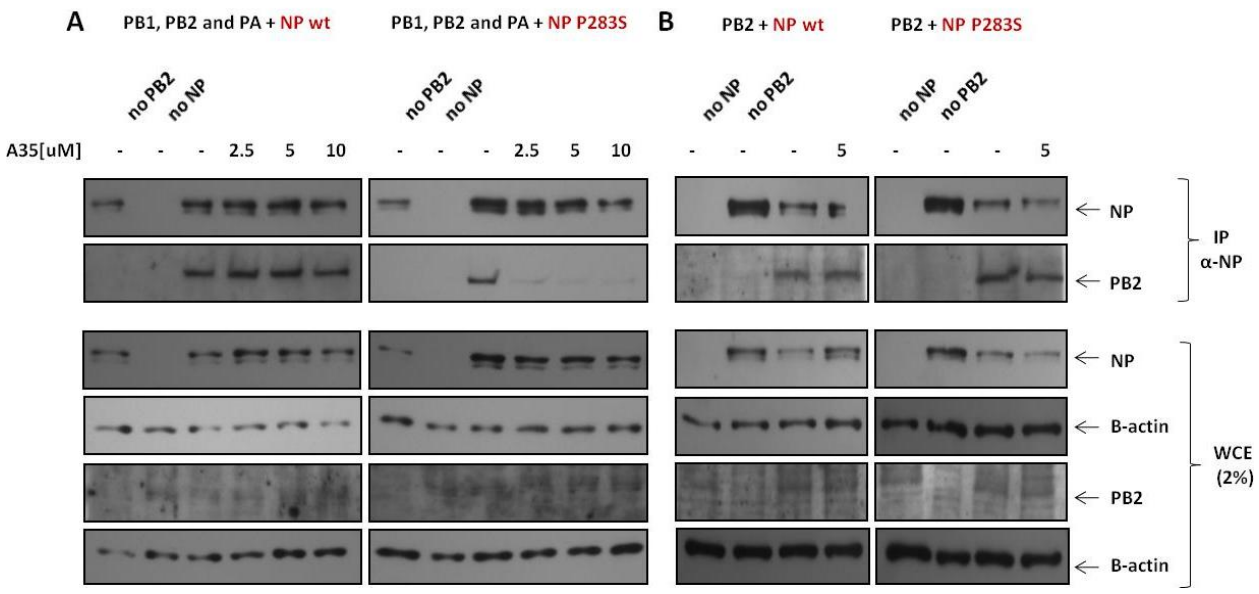

Fig. 3-31. Co-immunoprecipitation of NP and PB2. (A) A549 cells were transfected with protein expression plasmids for influenza A/PR/8/34 virus polymerase subunits PB1, PB2, PA and wild type NP or NP (P283S). In (B), A549 cells were transfected with protein expression plasmids for the influenza A/PR/8/34 virus polymerase subunit PB2 and wild type NP or NP (P283S). Transfections were performed in the presence of DMSO or A35 at indicated concentrations. Interaction of NP and PB2 and protein expression were determined 24 hours later by co-immunoprecipitation and western blot analysis.

Transfections in Fig. 3-31A were done at increasing A35 concentrations. The resistant NP (left hand panel) is not affected by A35 and equal amounts of PB2 are precipitated with NP. In contrast, in the right hand panel, the sensitive NP is clearly unable to pull down PB2 and its signal is reduced by more than 90% compared to the DMSO control (band signals were quantified; data not shown). Transfections in Fig. 3-31B were done at a concentration of A35 which was shown to be effective previously. Both NP variants, the A35-resistant (left hand panel) and the A35-sensitive (right hand panel), are able to pull down PB2 in the presence of A35 which is in contrast to the previous results. It is possible that PB2 alone can bind to NP in the presence of A35 but if the protein is complexed with PB1 and PA (or RNA), it may change its conformation, which prevents binding to NP when A35 is present.

An interesting observation was made when viral protein levels were determined in A549 cells treated with A3 and A35 prior to infection and several time points post infection. We stained

for proteins translated early in the viral life cycle such as NP, and for proteins that are produced late such as M1 and M2 (Fig. 3-32).

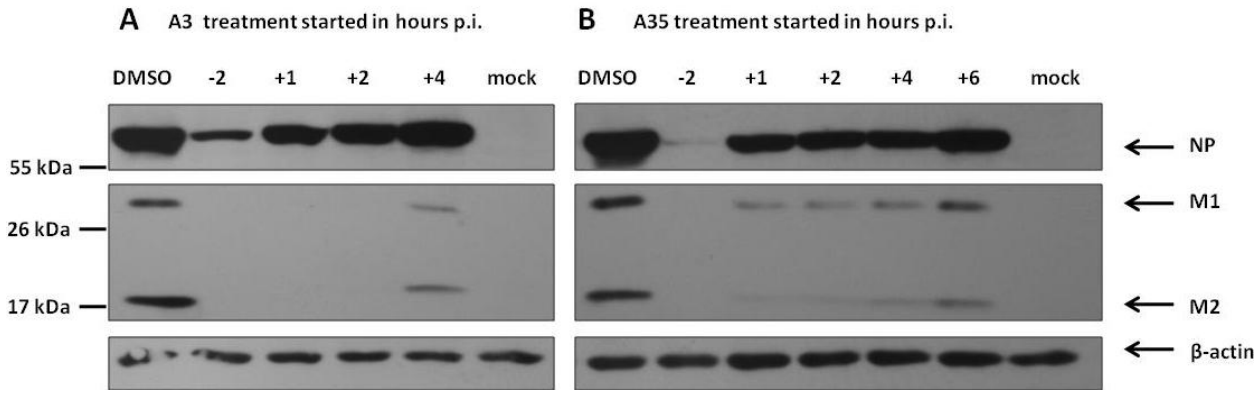

Fig. 3-32. Inhibition of viral protein expression by A3 and A35 when added at different time points during the viral life cycle. A549 cells were infected with influenza viruses A/WSN/33 (MOI=1). Compounds A3 (A) and A35 (B) were present in the culture medium 2 hours prior to infection or added to the medium at indicated time points post infection at their CC_{10}. Viral protein levels were determined 24 hours post infection by western blot analysis.

The viral protein levels for the A3 treatment correlate well with the viral titers obtained from these samples (see Fig. 3-6). For A3 the pre-treatment has the greatest impact on viral titers and on viral protein levels. The inhibition is decreased by adding A3 at later time points during the viral life cycle which is reflected by viral titers and protein levels. For A35, addition prior to infection and up to 4 hours post-infection results in a 4 log reduction in viral titers (see Fig. 3-6) but this does not correlate exactly with a reduction in viral protein expression. There is almost no NP detectable in the western blot for the pre-treatment sample but starting with 1 hour post infection viral proteins are visible, not only for NP but also for M1. The viral protein levels don't reflect the viral titers that were obtained. Similar results were found by immuno-fluorescence when looking at viral proteins for infections performed with A35 pre- or post-treatment. Viral proteins could be detected for the A35 post-treatment but not for the pre-treatment although viral titers were reduced for both samples equally by about 4 logs (Fig. 3-33).

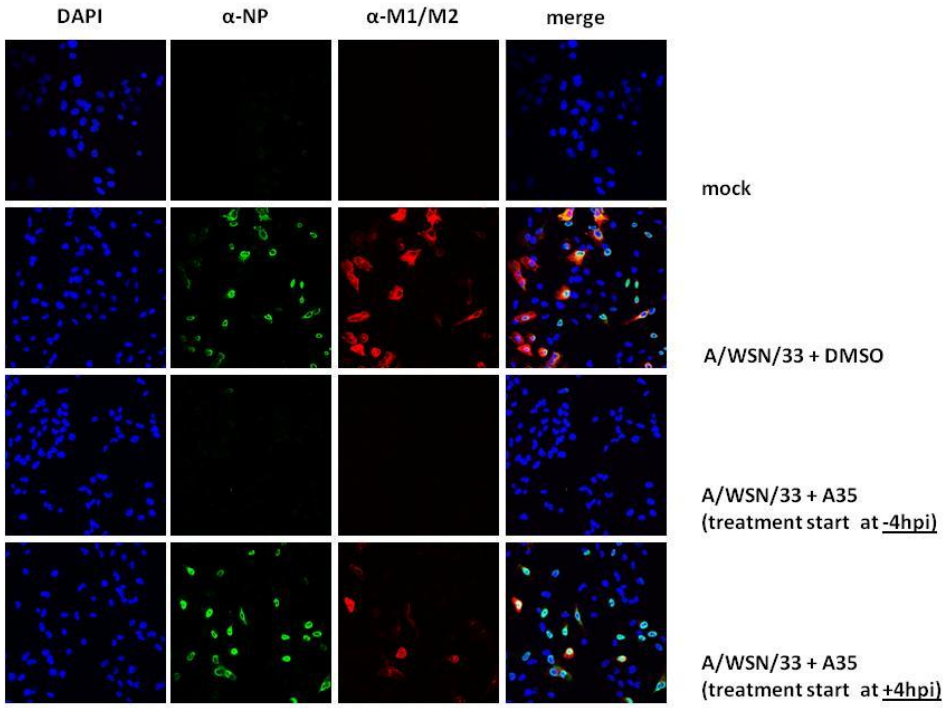

Fig. 3-33. Immunofluorescence of influenza A/WSN/33 virus infections in the presence of A35. A549 cells were infected with influenza A/WSN/33 virus at an MOI of 1. Compound A35 was present 4 hours prior to infection or added to the culture medium 4 hours post infection. Cells were fixed 7 hours post infection and stained for viral proteins expressed early (NP) and late (M1/M2) in the viral life cycle.

The influenza virus polymerase executes the production of 3 different types of RNA (vRNA into cRNA, cRNA into vRNA and vRNA into mRNA). The latter results raise the hypothesis that the viral polymerase is trapped in transcription mode by A35 treatment. This would produce viral proteins but no vRNAs that can be packaged and therefore lead to defective viral particles. This hypothesis needs to be addressed in primer extension assays in order to quantify the levels of vRNA, cRNA and mRNA. The primer extension assay performed earlier was done for infections that were pre-treated with compounds. In this case, there were no viral RNA species detectable for the A35-sensitive PR8 virus (see Fig. 3-26). This matches the observation that there is not viral protein detectable in western blots and immunofluorescence for infections that were A35 pre-treated (see Figs. 3-32 and 3-33). Primer extension assays performed for infections where A35 treatment is started post infection may reveal why viral protein expression is not inhibited.

A3 and A35 derivatives

Medicinal chemistry is often employed to improve the properties of hit compounds. This is called a structure activity relationship (SAR) study and the aim is to make modifications to the structure that changes the potency or cytotoxicity as compared to the parent compound. Under the advice of a medicinal chemist we started a small scale SAR analysis using commercial derivatives of A3 and A35. The compound A3 was modified in its pyrrole (Fig. 3-34A) and indole rings (Fig. 3-34B). The pyrrole structure is more flexible and can accommodate small changes without leading to a loss of potency (derivatives A3-2 and A3-5). If this structure becomes larger, the derivative loses about 1 log in potency (derivatives A3-4 and A3-6). On the opposite site of the molecule is an indole ring which seems to be quite important since any change leads to a total loss of antiviral potency. We did not find A3 derivatives of higher potency but we were able to characterize important substructures that are either essential or susceptible to modifications.

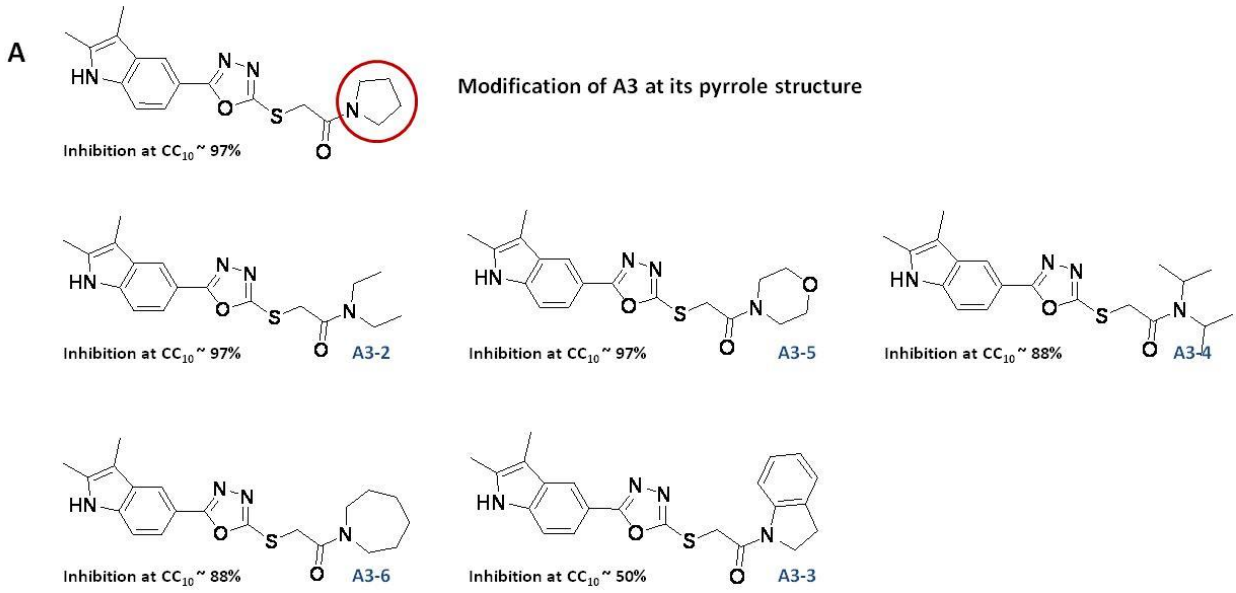

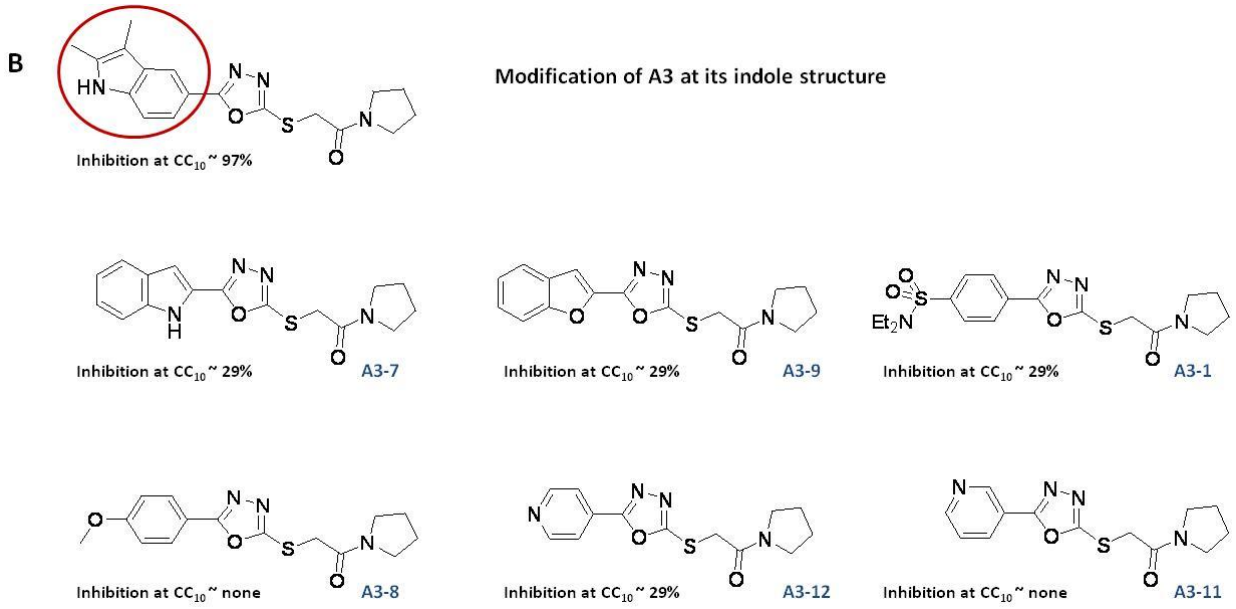

Fig. 3-34. Derivatives of compound A3. (A) A3 was modified at its pyrrol ring structure and (B) at its indole structure. Derivatives were tested at their CC_{10} for their potential to inhibit infections of influenza A/WSN/33 virus performed in A549 cells at a MOI of 1. Viral titers were determined 24 hours post infection by HA assay. Inhibition of viral replication is depicted for each derivative below its structure.

The compound A35 was modified on either one site or on several at the same time. We did not find any compounds that are as potent as the parental compound (Fig. 3-35).

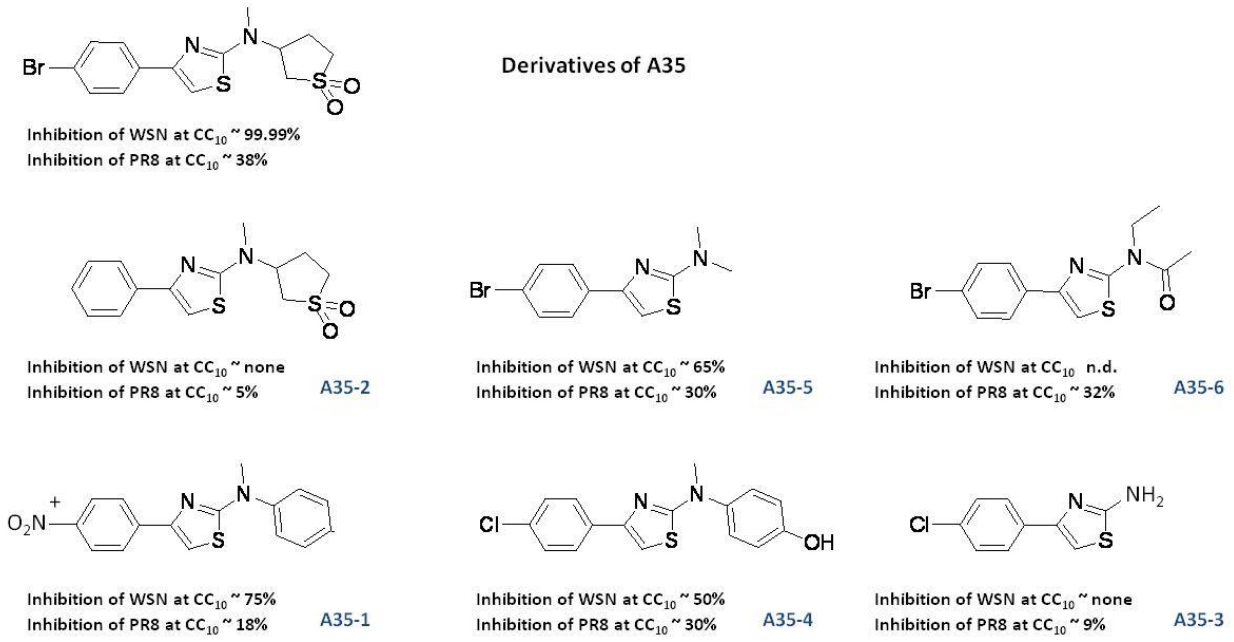

Fig. 3-35. Derivatives of compound A35. Derivatives were tested at their CC_{10} for their potential to inhibit infections of influenza viruses A/WSN/33 and A/PR/8/34 performed in A549 cells at a MOI of 1. Viral titers were determined 24 hours post infection by HA assay for influenza A/WSN/33 virus and by plaque assay for influenza A/PR/8/34 virus. Inhibition of viral replication is depicted for each derivative below its structure. The assay was performed in triplicate and is presented as the mean.

The derivative A35-2 which only lacks the bromide ion of the parental compound displays a 4 log reduced potency in inhibiting influenza virus replication. The compound appears to be highly specific for a certain structure and even the slightest modification disrupts its potency.

Compound studies in vivo

All our *in vitro* studies were performed in A549 cells. Before we tested compounds A3, A35 and C2 *in vivo*, we tested them in primary cells, specifically, in human tracheo-bronchial epithelial (HTBE) cells (Fig. 3-36).

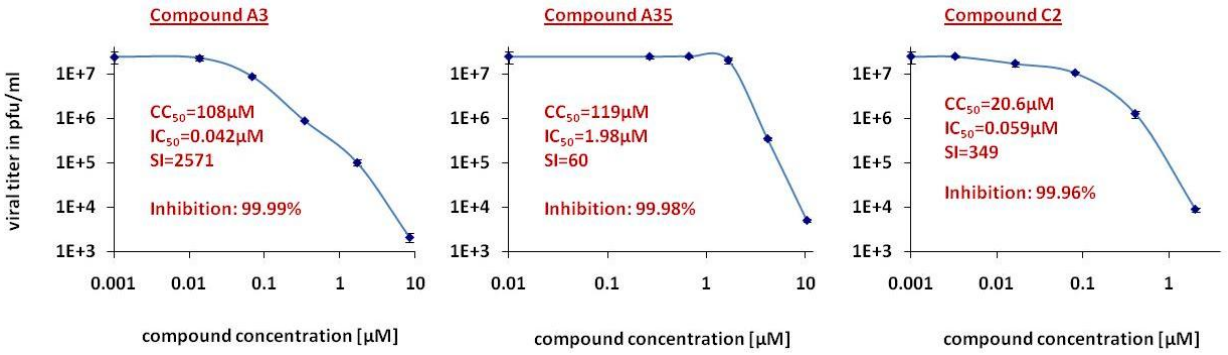

Fig. 3-36. Inhibition of influenza A/WSN/33 virus by compounds A3, A35 and C2 in human primary cells. Human tracheo-bronchial epithelial (HTBE) cells were infected with influenza A/WSN/33 virus (MOI=1) in the presence of increasing concentrations of A3, A35 and C2 (c_{max}=CC_{10}). Viral titers were determined 24 hours post infections by plaque assay. The assay was performed in triplicate and is presented as the mean ± standard deviation. Compound characteristics (CC_{50}, IC_{50}, SI and absolute inhibition) that were determined in HTBE cells are depicted.

We could show that the compounds were highly efficient at inhibiting influenza virus replication by up to 4 logs. We also confirmed their potency in mouse embryo fibroblast (MEF) cells before conducting *in vivo* studies in mice. For the in vivo infections we tested a number of parameters. We tested different amounts of viruses to infect with ($10MLD_{50}$ - $100MLD_{50}$), we tested different viruses (influenza viruses A/WSN/33, A/PR/8/34 and rA/PR/8/34 (NP P283S)), we administered the compounds via different routes (intraperitoneal and intranasally) for different periods (3 to 5 days) and in different frequencies (twice daily or tree times daily). The biggest obstacle we had to deal with was the insolubility of our compounds in aqueous solutions. We therefore had to test different solvents (DMSO, PEG400, NMP and Labrafil®) and combinations of them. The amount of compounds we were able to administer was limited by

their solubility. In Fig. 3-37A is an example shown for one experiment performed in BALB/C mice.

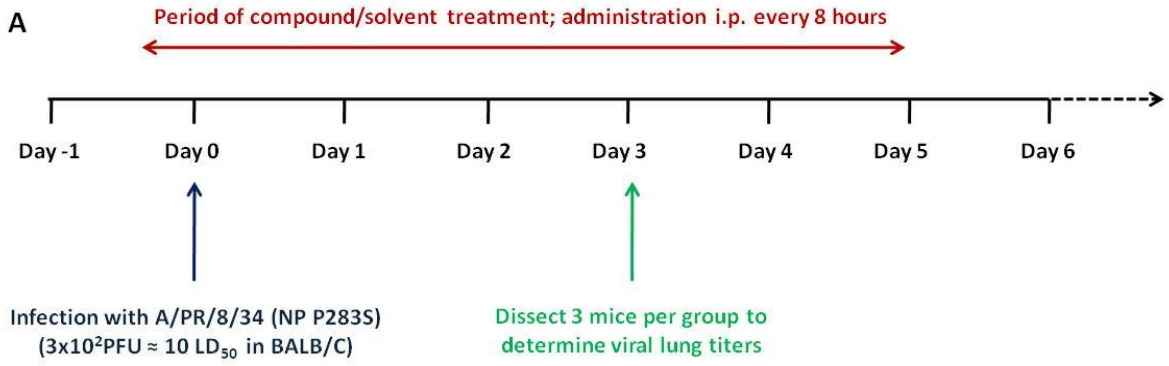

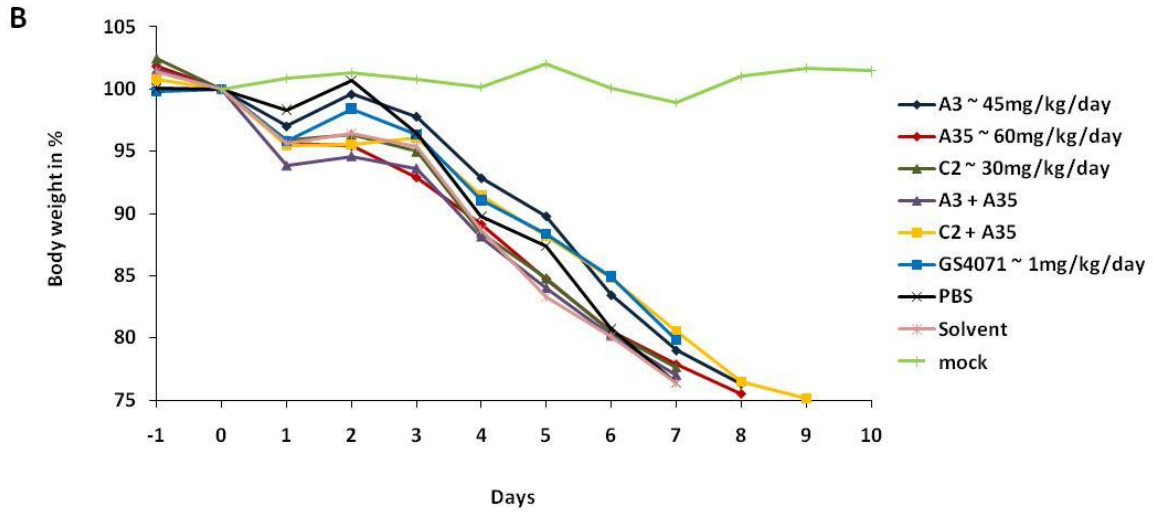

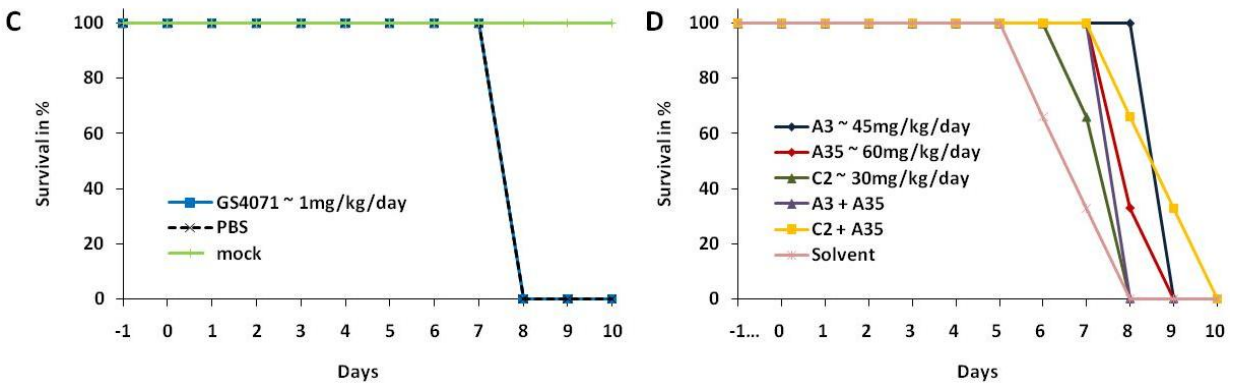

Fig. 3-37. Effects on influenza virus replication *in vivo* by compounds C2, A3 and A35. (A) Six-week old female Balb/C mice were infected intranasally with 300 PFU (10 MLD_{50}) of recombinant influenza A/PR/8/34 (NP P283S) virus. Mice in groups of six were treated 3 times daily with indicated compounds until day 5 post infection. Groups of three were sacrificed on day 3pi to determine viral lung titers. Treatment with Tamiflu (GS4071) was included as positive control and treatment with PBS and solvent as negative controls. The (B) body weight and (C and D) survival was monitored daily. Tamiflu was dissolved in PBS and compared to the PBS control group (C) whereas C2, A3 and A35 were dissolved in a vehicle and compared to the vehicle control group (D).

Balb/c mice were infected with PR8 (NP P283S) and treated via the intraperitoneal route 3 times daily with the indicated dose of compound. All mice started to lose weight by day 2 and 3 post infection including the control mice that received PBS or the compound solvent (Labrafil®/NMP) died by day 8 post infection. Surprisingly, the control group that received oseltamivir (GS4071) died on the same day suggesting that the dose administered was not protective. Mice that received A3 and a combination of C2 and A35 lost weight after treatment was stopped on day 5 post infection. The A3 group survived a day longer compared to the solvent group and the C2+A35 group survived 2 days longer. The other treatment groups of C2, A35 and A3+A35 also appeared to have a minor protective effect with a slight delay in time to death. Viral titers in lungs were determined at day 3 post infection (Fig. 3-38).

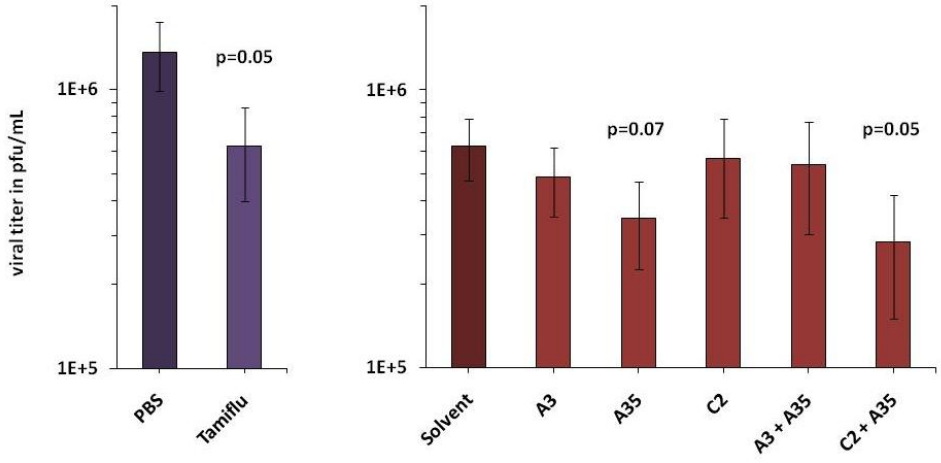

Fig. 3-38. Viral replication in mouse lungs. Six-week old female Balb/C mice were infected intranasally with 300 PFU (10 MLD_{50}) of recombinant influenza A/PR/8/34 (NP P283S) virus. Mice were treated 3 times daily with indicated compounds before they were sacrificed on day 3 post infection to determine viral lung titers by plaque assay. Mice were in groups of 3 and results are presented as the mean ± standard deviation. Tamiflu was dissolved in PBS and compared to the PBS control group whereas C2, A3 and A35 were dissolved in a vehicle and compared to the vehicle control group.

Tamiflu was dissolved in PBS and compared to the PBS control group. The viral titers of mice treated with Tamiflu are significantly reduced by 50% compared to the PBS control group which nonetheless was not protective. Compounds were dissolved in Labrafil®/NMP (9:1) and compared to the solvent control group. Compound A35 reduced viral titers by 45% and the combination of A35 and C2 reduced the titer significantly by 55% compared to the solvent control group. Compounds A3, C2 and the combination of A3 and A35 did not significantly reduce viral lung titers when compared to the solvent control group. In summary, the compounds were not protective under these conditions and pharmacokinetic studies will be needed in order to determine the bioavailability of the compounds and to define conditions which might result in protection against a lethal challenge of virus.

DISCUSSION

German scientist Paul Ehrlich, one of the fathers of modern immunology, pioneered the idea of systematically searching for drugs in 1908. Screening just over 600 synthetic compounds, he and a post-doctoral co-worker Sahachiro Hata discovered arsphenamine (Salvarsan®), a compound that changed and improved the treatment of syphilis, until penicillin was introduced in the 1940s.

Now, 100 years later, large-scale screens have become available to evaluate hundreds of thousands of compounds for activity against different pathogens. Our screening assay was designed to identify chemical inhibitors against the replication of influenza viruses. One hundered and fourty six compounds were identified in our primary screen (a luciferase-based reporter assay), and of those, 18 compounds were verified in a variety of secondary screens including assays designed to directly evaluate the compounds' effects on viral replication.

Compound concentrations used in the primary screen ranged from 40-80µM. Before testing compounds in the secondary screen, we assessed their cytotoxicity on A549 cells and found that most of them decreased cell viability by 20-50% in that concentration range. The highest compound concentration used in the secondary screen was the CC_{10}, a concentration at which less than a 10% decrease in cell viability was observed over a 24 hour incubation period. At that concentration, most of the compounds affected viral replication only little or not at all, and were thus discarded. The remaining 18 compounds did inhibit viral replication at concentrations that were not cytotoxic and were therefore considered virus-specific. Among these 18 compounds, three were identified in specific assays as targeting cellular proteins or viral functions and became our "lead compounds".

Compound C2 was identified to inhibit the viral life-cycle at an "early" stage (pre-replication). In the presence of C2, entry of pseudotyped lentiviral particles and influenza virus-like particles via endocytosis was inhibited by 95% and 98% respectively. In 2007, compound C2 was

described by another group to be an inhibitor of cellular vATPases (Sorensen et al., 2007) and its potency was found to be similar to that of bafilomycin A. vATPases are essential for viruses that require low pH for entry into the host cell as they mediate acidification of endosmes. Influenza viruses are endocytosed after attachment. The virus, contained in early endosomes, is then acidified by the action of vATPases that pump protons into the endosomal lumen. This low pH activates the M2 ion channel which in turn allows protons to enter the virus, which weakens the binding of the matrix protein M1 to the RNPs. With a further decrease in pH, the HA protein undergoes a conformational change causing fusion with the host-cell membrane, viral RNPs are released from the internal face of the viral envelope into the cytoplasm, and the entry step is completed. We showed that the inhibition of vATPases by C2 efficiently blocked entry of influenza viruses which require low pH (about 5.0) for fusion. It is not understood how the vATPase complex, comprised of different subunits, is inhibited by C2 and how much residual activity of the vATPase may remain. Influenza viruses that can be activated at slightly higher pH values such as A/Udorn/72 are not as dependent on low pH in order to complete entry and are therefore not as affected by an inhibition of vATPases. In a recent drosophila RNAi screen, vATPases were identified to be essential for viral entry (Hao et al., 2008). This result was confirmed by cell based genome wide RNAi screens that searched for host genes required for influenza viruses (Brass et al., 2009; Karlas et al., 2010; Konig et al., 2010). The latter study contained data on compound C2 inhibiting influenza virus replication and validated the concept of "druggable" host genes that may be targeted to counteract viral replication. Results from large-scale screens designed to identify host genes and proteins that are required for virus replication, have given us a better understanding of how viruses invade cells and how this step may be counteracted. Examples of such screens include those for host factors required for replication of HIV-1 (Zhou et al., 2008), of West Nile virus (Brass et al., 2009; Krishnan et al., 2008), of dengue virus (Brass et al., 2009) and of hepatitis C virus (Ng et al., 2007). In addition to the effect of C2 on influenza viruses, we believe that C2 may act as an inhibitor of replication of other viruses across different families that enter cells via receptor mediated endocytosis. We found that replication of vesicular stomatitis virus (*rhabdoviridae*) and Sindbis virus (*togaviridae*) were diminished by more than 1-2 logs in the presence of C2.

A broad-spectrum anti-viral compound for use in humans would be a very valuable therapeutic. Such a compound, LJ001, was described recently (Wolf et al., 2010) and is active against a broad range of viruses including influenza A virus, filoviruses, poxviruses, arenaviruses, bunyaviruses, paramyxoviruses, flaviviruses, and HIV-1. Intercalating into viral membranes, LJ001 irreversibly inactivates virions, without displaying overt toxicity to the host cell. Such compounds may be effective when used as prophylactic treatments and during acute infections to reduce symptoms of disease caused by viral spread.

We did conduct *in vivo* studies in mice to examine the effect of C2 on influenza virus infections. The results were not conclusive because C2 only led to a delay in time of death but was not protective. One explanation for this is that the daily dose administered was too low (30mg/kg). It is also possible that the delivery vehicle utilized was not optimal for the particular compound. C2 may also need to be delivered locally to the respiratory tract via inhalation instead of being given systemically via intra peritoneal injections.

Compounds A3 and A35 were shown in the influenza virus mini-genome assay and in the primer extension assay as potential inhibitors of the viral polymerase complex. A3 exhibited (in the mini-genome assay) a 50-fold increase in potency over ribavirin, a known replication inhibitor of RNA and DNA viruses (Gallois-Montbrun et al., 2003). This result was confirmed in primer extension assays, where a total block in viral replication and transcription was observed for A3 that was similar to ribavirin at a 50-fold higher concentration. In order to identify whether A3 targeted a viral protein or a host cell protein, we passaged WSN in the presence of A3 for the purpose of generating escape mutants. After 10 passages, the virus was still sensitive to A3 which suggested that it may target a host cell protein. C2 was passaged in parallel, but we were also unable to generate a resistant virus. Before we conducted *in vivo* studies in mice, we tested A3 in mouse embryo fibroblast (MEF) cells and found that the IC_{50} for inhibiting influenza A virus replication was 7 times higher in MEF cells as compared to A549 cells, and 86 times higher in MEF cells when compared to human tracheo-bronchial epithelial (HTBE) cells. This indicates that A3 may specifically target a human protein rather than the mouse homologue

and may explain why A3 is not protective in our mouse infection model. The impact of A3 was modest - A3 was administered until day 5 post infection and treated animals experienced approximately 7% less weight loss than controls. Withdrawal of the compound at day 5 resulted in loss of therapeutic effect and mice succumbed to infection.

Ribavirin and the novel polymerase inhibitor T-705 are pro-drugs and get activated in the cell. Ribavirin is phosphorylated on its ribose moiety and functions as a nucleoside analog. The viral polymerase incorporates it into the viral RNA and a subsequent accumulation of replicative errors may explain its antiviral effect. T-705, on the other hand, is first ribosylated and then phosphorylated to become a nucleoside analog. It disrupts viral replication although it is not clear whether it is incorporated into viral RNA or whether it inhibits the viral polymerase directly. Compound A3 contains an indole ring and A3 derivatives that lack this indole ring lose their inhibitory effect on influenza viral replication. The structure of A3 with the indole ring would appear to be similar to the structure of guanine and it raises the possibility that A3 also acts as a nucleoside analogue. This could be addressed by HPLC, looking for ribosylated and phosphorylated versions of A3 produced by host cell proteins as has been described for T-705 (Smee et al., 2009). Such a nucleoside analog may not only be specific for influenza A viruses but may actually have broad-spectrum antiviral activity. We tested different RNA viruses and found that A3 also inhibits influenza B virus, vesicular stomatitis virus (VSV) and Sindbis virus. In a multi cycle replication assay, influenza A virus and VSV where inhibited by 5 logs. Newcastle disease virus (NDV) was only moderately affected by A3 and it is questionable whether this is specific or due to the fact that NDV does not replicate well in A549 cells. We subjected A3 to both influenza VLP and pseudoparticle entry assays and found that A3, as expected, does not inhibit entry of VLPs. In contrast, *Gaussia* luciferase activity in pseudoparticle entry assays was reduced by about 40% for both influenza virus- and VSV- pseudotyped particles. Since A3 is not involved in entry, this suggests a role of A3 in inhibiting the HIV polymerase of the lentiviral machinery. Nucleoside analogs like T-705 (or potentially A3) do not target host cell proteins as they inhibit the viral polymerase.

Compound A35 inhibits viral replication when cells are treated prophylactically or therapeutically, even when added late in the viral life cycle. Infections performed at a high MOI can be blocked by more than 4 logs, and at a low MOI, infectious growth is below the limit of detection. The compound was identified to be highly specific for the influenza A/WSN/33 virus; all other tested influenza viruses were only moderately affected by A35. We compared the WSN strain with its closest relative, the PR8 strain and found by using a minigenome replication assay that the NP of WSN is responsible for the A35 sensitivity. Chimeric NP proteins (between the WSN and PR8 strain) revealed that residue 283 is crucial in conferring resistance or sensitivity to A35 in mini-genome assays and primer extension assays using recombinant viruses. Passaging WSN in the presence of A35 led to the generation of escape mutations in the NP segment. Two altered residues (D51 and V285) are in close proximity to residue 283 and comprise a putative binding site of A35 in NP. To confirm binding of the compound and the NP protein it is necessary to co-crystallize this complex. A protein-compound co-crystal structure will guide the design of logical A35 derivatives that may have activity on non-WSN influenza virus strains. The residues in NP identified in the context of A35 treatment (51, 283 and 285) are in or near the predicted binding site of the polymerase subunit PB2 (Biswas et al., 1998). We showed in co-immunopreciptiation assays using NP to pull down PB2, that A35 inhibits the interaction of NP with PB2 in the context of the polymerase complex but not by itself. This further confirms the involvement of A35 in blocking viral polymerase function. An interesting observation was made when comparing infections in A549 cells that were pre-treated with A35 or that received the compound 4 hours post infection. The viral titers for both conditions were equally diminished by about 4 logs but the viral protein levels present after infection did differ. There was no viral protein detectable by western blot analysis or by immunofluorescence analysis when cells were pre-treated with A35. In contrast, there was a substantial amount of viral protein present in the samples that were treated post-infection. This suggests that the incoming RNPs are inhibited by A35 and cannot initiate replication or transcription. Alternately, if A35 is added at some point post infection, the viral polymerase is actively replicating and may be trapped by A35 in transcription mode. This hypothesis is confirmed by the presence of viral proteins and the absence of infectious particles due to the probable lack of vRNA that is

available for packaging. This needs to be addressed in primer extension assays where both conditions of A35-pre and post-treatment are compared in infections. The primer extension assay enables the analysis of viral replication and transcriptional activity by quantification of v-, c- and mRNA.

We tested A35 *in vivo* in mice with an A35-sensitive virus and again, were limited in the compound concentration. We did not see a clear effect in body weight loss during the course of infection.

As of now, the influenza virus NP protein has not been described as a potential target for antiviral drugs. The NP is a highly conserved, multifunctional protein, it is involved in a variety of viral processes and its inhibition should affect the majority of influenza A viruses.

In summary, we conducted a high-throughput screen with the influenza A/WSN/33 virus and identified broad-spectrum antivirals that target, on one hand, a host cell protein that is involved in viral entry and, on the other hand, the polymerase function of different viruses. In addition, we identified a compound that is highly potent and specific for an influenza viral protein but only for the strain that we screened for.

BIBLIOGRAPHY

Ahmed, R., Oldstone, M.B. and Palese, P. (2007) Protective immunity and susceptibility to infectious diseases: lessons from the 1918 influenza pandemic. Nat Immunol 8(11), 1188-93.

Albertini, A.A., Wernimont, A.K., Muziol, T., Ravelli, R.B., Clapier, C.R., Schoehn, G., Weissenhorn, W. and Ruigrok, R.W. (2006) Crystal structure of the rabies virus nucleoprotein-RNA complex. Science 313(5785), 360-3.

Alonso-Caplen, F.V., Nemeroff, M.E., Qiu, Y. and Krug, R.M. (1992) Nucleocytoplasmic transport: the influenza virus NS1 protein regulates the transport of spliced NS2 mRNA and its precursor NS1 mRNA. Genes Dev 6(2), 255-67.

Arora, D.J. and Gasse, N. (1998) Influenza virus hemagglutinin stimulates the protein kinase C activity of human polymorphonuclear leucocytes. Arch Virol 143(10), 2029-37.

Baudin, F., Bach, C., Cusack, S. and Ruigrok, R.W. (1994) Structure of influenza virus RNP. I. Influenza virus nucleoprotein melts secondary structure in panhandle RNA and exposes the bases to the solvent. EMBO J 13(13), 3158-65.

Beaton, A.R. and Krug, R.M. (1986) Transcription antitermination during influenza viral template RNA synthesis requires the nucleocapsid protein and the absence of a 5' capped end. Proc Natl Acad Sci U S A 83(17), 6282-6.

Belser, J.A., Lu, X., Szretter, K.J., Jin, X., Aschenbrenner, L.M., Lee, A., Hawley, S., Kim do, H., Malakhov, M.P., Yu, M., Fang, F. and Katz, J.M. (2007) DAS181, a novel sialidase fusion protein, protects mice from lethal avian influenza H5N1 virus infection. J Infect Dis 196(10), 1493-9.

Biswas, S.K., Boutz, P.L. and Nayak, D.P. (1998) Influenza virus nucleoprotein interacts with influenza virus polymerase proteins. J Virol 72(7), 5493-501.

Biswas, S.K. and Nayak, D.P. (1994) Mutational analysis of the conserved motifs of influenza A virus polymerase basic protein 1. J Virol 68(3), 1819-26.

Blair, W.S., Isaacson, J., Li, X., Cao, J., Peng, Q., Kong, G.F. and Patick, A.K. (2005) A novel HIV-1 antiviral high throughput screening approach for the discovery of HIV-1 inhibitors. Antiviral Res 65(2), 107-16.

Booth, R.E. and Stockand, J.D. (2003) Targeted degradation of ENaC in response to PKC activation of the ERK1/2 cascade. Am J Physiol Renal Physiol 284(5), F938-47.

Boulo, S., Akarsu, H., Ruigrok, R.W. and Baudin, F. (2007) Nuclear traffic of influenza virus proteins and ribonucleoprotein complexes. Virus Res 124(1-2), 12-21.

Brass, A.L., Huang, I.C., Benita, Y., John, S.P., Krishnan, M.N., Feeley, E.M., Ryan, B.J., Weyer, J.L., van der Weyden, L., Fikrig, E., Adams, D.J., Xavier, R.J., Farzan, M. and Elledge, S.J. (2009) The IFITM proteins mediate cellular resistance to influenza A H1N1 virus, West Nile virus, and dengue virus. Cell 139(7), 1243-54.

Bright, R.A., Medina, M.J., Xu, X., Perez-Oronoz, G., Wallis, T.R., Davis, X.M., Povinelli, L., Cox, N.J. and Klimov, A.I. (2005) Incidence of adamantane resistance among influenza A (H3N2) viruses isolated worldwide from 1994 to 2005: a cause for concern. Lancet 366(9492), 1175-81.

Bright, R.A., Shay, D.K., Shu, B., Cox, N.J. and Klimov, A.I. (2006) Adamantane resistance among influenza A viruses isolated early during the 2005-2006 influenza season in the United States. JAMA 295(8), 891-4.

Bui, M., Myers, J.E. and Whittaker, G.R. (2002) Nucleo-cytoplasmic localization of influenza virus nucleoprotein depends on cell density and phosphorylation. Virus Res 84(1-2), 37-44.

Bussey, K.A., Bousse, T.L., Desmet, E.A., Kim, B. and Takimoto, T. (2010) PB2 residue 271 plays a key role in enhanced polymerase activity of influenza A viruses in mammalian host cells. J Virol.

CDC. (2010a) Flu Activity & Surveillance in the United States.

CDC. (2010b) Seasonal Influenza: The Disease.

Chase, G., Deng, T., Fodor, E., Leung, B.W., Mayer, D., Schwemmle, M. and Brownlee, G. (2008) Hsp90 inhibitors reduce influenza virus replication in cell culture. Virology 377(2), 431-9.

Chen, W., Calvo, P.A., Malide, D., Gibbs, J., Schubert, U., Bacik, I., Basta, S., O'Neill, R., Schickli, J., Palese, P., Henklein, P., Bennink, J.R. and Yewdell, J.W. (2001) A novel influenza A virus mitochondrial protein that induces cell death. Nat Med 7(12), 1306-12.

Chen, X.J., Seth, S., Yue, G., Kamat, P., Compans, R.W., Guidot, D., Brown, L.A., Eaton, D.C. and Jain, L. (2004) Influenza virus inhibits ENaC and lung fluid clearance. Am J Physiol Lung Cell Mol Physiol 287(2), L366-73.

Choppin, P.W., Murphy, J.S. and Tamm, I. (1960) Studies of two kinds of virus particles which comprise influenza A2 virus strains. III. Morphological characteristics: independence to morphological and functional traits. J Exp Med 112, 945-52.

Chu, J.J. and Yang, P.L. (2007) c-Src protein kinase inhibitors block assembly and maturation of dengue virus. Proc Natl Acad Sci U S A 104(9), 3520-5.

Claas, E.C., Osterhaus, A.D., van Beek, R., De Jong, J.C., Rimmelzwaan, G.F., Senne, D.A., Krauss, S., Shortridge, K.F. and Webster, R.G. (1998) Human influenza A H5N1 virus related to a highly pathogenic avian influenza virus. Lancet 351(9101), 472-7.

Compans, R.W., Content, J. and Duesberg, P.H. (1972) Structure of the ribonucleoprotein of influenza virus. J Virol 10(4), 795-800.

Conenello, G.M., Zamarin, D., Perrone, L.A., Tumpey, T. and Palese, P. (2007) A single mutation in the PB1-F2 of H5N1 (HK/97) and 1918 influenza A viruses contributes to increased virulence. PLoS Pathog 3(10), 1414-21.

Davies, W.L., Grunert, R.R., Haff, R.F., McGahen, J.W., Neumayer, E.M., Paulshock, M., Watts, J.C., Wood, T.R., Hermann, E.C. and Hoffmann, C.E. (1964) Antiviral Activity of 1-Adamantanamine (Amantadine). Science 144, 862-3.

Deng, L., Dai, P., Ciro, A., Smee, D.F., Djaballah, H. and Shuman, S. (2007) Identification of novel antipoxviral agents: mitoxantrone inhibits vaccinia virus replication by blocking virion assembly. J Virol 81(24), 13392-402.

Desselberger, U., Racaniello, V.R., Zazra, J.J. and Palese, P. (1980) The 3' and 5'-terminal sequences of influenza A, B and C virus RNA segments are highly conserved and show partial inverted complementarity. Gene 8(3), 315-28.

Dias, A., Bouvier, D., Crepin, T., McCarthy, A.A., Hart, D.J., Baudin, F., Cusack, S. and Ruigrok, R.W. (2009) The cap-snatching endonuclease of influenza virus polymerase resides in the PA subunit. Nature 458(7240), 914-8.

Dodson, A.W., Taylor, T.J., Knipe, D.M. and Coen, D.M. (2007) Inhibitors of the sodium potassium ATPase that impair herpes simplex virus replication identified via a chemical screening approach. Virology 366(2), 340-8.

Elton, D., Medcalf, E., Bishop, K. and Digard, P. (1999a) Oligomerization of the influenza virus nucleoprotein: identification of positive and negative sequence elements. Virology 260(1), 190-200.

Elton, D., Medcalf, L., Bishop, K., Harrison, D. and Digard, P. (1999b) Identification of amino acid residues of influenza virus nucleoprotein essential for RNA binding. J Virol 73(9), 7357-67.

Elton, D., Simpson-Holley, M., Archer, K., Medcalf, L., Hallam, R., McCauley, J. and Digard, P. (2001) Interaction of the influenza virus nucleoprotein with the cellular CRM1-mediated nuclear export pathway. J Virol 75(1), 408-19.

Ewart, G.D., Mills, K., Cox, G.B. and Gage, P.W. (2002) Amiloride derivatives block ion channel activity and enhancement of virus-like particle budding caused by HIV-1 protein Vpu. Eur Biophys J 31(1), 26-35.

Ewart, G.D., Nasr, N., Naif, H., Cox, G.B., Cunningham, A.L. and Gage, P.W. (2004) Potential new anti-human immunodeficiency virus type 1 compounds depress virus replication in cultured human macrophages. Antimicrob Agents Chemother 48(6), 2325-30.

FDA. (2000) Safe and Appropriate Use of Influenza Drugs

Fechter, P., Mingay, L., Sharps, J., Chambers, A., Fodor, E. and Brownlee, G.G. (2003) Two aromatic residues in the PB2 subunit of influenza A RNA polymerase are crucial for cap binding. J Biol Chem 278(22), 20381-8.

Ferko, B., Stasakova, J. and Romanova, J. (2004) Immunogenicity and protection efficacy of replication-deficient influenza A viruses with altered NS1 genes. J Virol 78 (23), 13037–45.

Fodor, E., Devenish, L., Engelhardt, O.G., Palese, P., Brownlee, G.G. and Garcia-Sastre, A. (1999) Rescue of influenza A virus from recombinant DNA. J Virol 73(11), 9679-82.

Fodor, E. and Smith, M. (2004) The PA subunit is required for efficient nuclear accumulation of the PB1 subunit of the influenza A virus RNA polymerase complex. J Virol 78(17), 9144-53.

Fouchier, R.A., Munster, V., Wallensten, A., Bestebroer, T.M., Herfst, S., Smith, D., Rimmelzwaan, G.F., Olsen, B. and Osterhaus, A.D. (2005) Characterization of a novel influenza A virus hemagglutinin subtype (H16) obtained from black-headed gulls. J Virol 79(5), 2814-22.

Furuta, Y., Takahashi, K., Fukuda, Y., Kuno, M., Kamiyama, T., Kozaki, K., Nomura, N., Egawa, H., Minami, S., Watanabe, Y., Narita, H. and Shiraki, K. (2002) In vitro and in vivo activities of anti-influenza virus compound T-705. Antimicrob Agents Chemother 46(4), 977-81.

Furuta, Y., Takahashi, K., Shiraki, K., Sakamoto, K., Smee, D.F., Barnard, D.L., Gowen, B.B., Julander, J.G. and Morrey, J.D. (2009) T-705 (favipiravir) and related compounds: Novel broad-spectrum inhibitors of RNA viral infections. Antiviral Res 82(3), 95-102.

Gallois-Montbrun, S., Chen, Y., Dutartre, H., Sophys, M., Morera, S., Guerreiro, C., Schneider, B., Mulard, L., Janin, J., Veron, M., Deville-Bonne, D. and Canard, B. (2003) Structural analysis of the activation of ribavirin analogs by NDP kinase: comparison with other ribavirin targets. Mol Pharmacol 63(3), 538-46.

Gao, Y., Zhang, Y., Shinya, K., Deng, G., Jiang, Y., Li, Z., Guan, Y., Tian, G., Li, Y., Shi, J., Liu, L., Zeng, X., Bu, Z., Xia, X., Kawaoka, Y. and Chen, H. (2009) Identification of amino acids in HA and PB2

critical for the transmission of H5N1 avian influenza viruses in a mammalian host. PLoS Pathog 5(12), e1000709.

Gazina, E.V., Harrison, D.N., Jefferies, M., Tan, H., Williams, D., Anderson, D.A. and Petrou, S. (2005) Ion transport blockers inhibit human rhinovirus 2 release. Antiviral Res 67(2), 98-106.

Ghosh, R.N., DeBiasio, R., Hudson, C.C., Ramer, E.R., Cowan, C.L. and Oakley, R.H. (2005) Quantitative cell-based high-content screening for vasopressin receptor agonists using transfluor technology. J Biomol Screen 10(5), 476-84.

Gibbs, J.S., Malide, D., Hornung, F., Bennink, J.R. and Yewdell, J.W. (2003) The influenza A virus PB1-F2 protein targets the inner mitochondrial membrane via a predicted basic amphipathic helix that disrupts mitochondrial function. J Virol 77(13), 7214-24.

Green, T.J., Zhang, X., Wertz, G.W. and Luo, M. (2006) Structure of the vesicular stomatitis virus nucleoprotein-RNA complex. Science 313(5785), 357-60.

Hao, L., Sakurai, A., Watanabe, T., Sorensen, E., Nidom, C.A., Newton, M.A., Ahlquist, P. and Kawaoka, Y. (2008) Drosophila RNAi screen identifies host genes important for influenza virus replication. Nature 454(7206), 890-3.

Harrison, D.N., Gazina, E.V., Purcell, D.F., Anderson, D.A. and Petrou, S. (2008) Amiloride derivatives inhibit coxsackievirus B3 RNA replication. J Virol 82(3), 1465-73.

Hatta, M., Gao, P., Halfmann, P. and Kawaoka, Y. (2001) Molecular basis for high virulence of Hong Kong H5N1 influenza A viruses. Science 293(5536), 1840-2.

Hay, A.J., Wolstenholme, A.J., Skehel, J.J. and Smith, M.H. (1985) The molecular basis of the specific anti-influenza action of amantadine. EMBO J 4(11), 3021-4.

Helenius, A. (1992) Unpacking the incoming influenza virus. Cell 69(4), 577-8.

Hellebrekers, D.M., Griffioen, A.W. and van Engeland, M. (2007) Dual targeting of epigenetic therapy in cancer. Biochim Biophys Acta 1775(1), 76-91.

Huarte, M., Falcon, A., Nakaya, Y., Ortin, J., Garcia-Sastre, A. and Nieto, A. (2003) Threonine 157 of influenza virus PA polymerase subunit modulates RNA replication in infectious viruses. J Virol 77(10), 6007-13.

Jung, T.E. and Brownlee, G.G. (2006) A new promoter-binding site in the PB1 subunit of the influenza A virus polymerase. J Gen Virol 87(Pt 3), 679-88.

Karlas, A., Machuy, N., Shin, Y., Pleissner, K.P., Artarini, A., Heuer, D., Becker, D., Khalil, H., Ogilvie, L.A., Hess, S., Maurer, A.P., Muller, E., Wolff, T., Rudel, T. and Meyer, T.F. (2010) Genome-

wide RNAi screen identifies human host factors crucial for influenza virus replication. Nature 463(7282), 818-22.

Kawaoka, Y., Krauss, S. and Webster, R.G. (1989) Avian-to-human transmission of the PB1 gene of influenza A viruses in the 1957 and 1968 pandemics. J Virol 63(11), 4603-8.

Kiso, M., Kubo, S., Ozawa, M., Le, Q.M., Nidom, C.A., Yamashita, M. and Kawaoka, Y. (2010) Efficacy of the new neuraminidase inhibitor CS-8958 against H5N1 influenza viruses. PLoS Pathog 6(2), e1000786.

Kistner, O., Muller, K. and Scholtissek, C. (1989) Differential phosphorylation of the nucleoprotein of influenza A viruses. J Gen Virol 70 (Pt 9), 2421-31.

Kleyman, T.R. and Cragoe, E.J., Jr. (1988) The mechanism of action of amiloride. Semin Nephrol 8(3), 242-8.

Klumpp, K., Ruigrok, R.W. and Baudin, F. (1997) Roles of the influenza virus polymerase and nucleoprotein in forming a functional RNP structure. EMBO J 16(6), 1248-57.

Konig, R., Stertz, S., Zhou, Y., Inoue, A., Hoffmann, H.H., Bhattacharyya, S., Alamares, J.G., Tscherne, D.M., Ortigoza, M.B., Liang, Y., Gao, Q., Andrews, S.E., Bandyopadhyay, S., De Jesus, P., Tu, B.P., Pache, L., Shih, C., Orth, A., Bonamy, G., Miraglia, L., Ideker, T., Garcia-Sastre, A., Young, J.A., Palese, P., Shaw, M.L. and Chanda, S.K. (2010) Human host factors required for influenza virus replication. Nature 463(7282), 813-7.

Kochs, G., Koerner, I. and Thiel L. (2007) Properties of H7N7 influenza A virus strain SC35M lacking interferon antagonist NS1 in mice and chickens. J Gen Virol88 (Pt 5), 1403–9.

Krishnan, M.N., Ng, A., Sukumaran, B., Gilfoy, F.D., Uchil, P.D., Sultana, H., Brass, A.L., Adametz, R., Tsui, M., Qian, F., Montgomery, R.R., Lev, S., Mason, P.W., Koski, R.A., Elledge, S.J., Xavier, R.J., Agaisse, H. and Fikrig, E. (2008) RNA interference screen for human genes associated with West Nile virus infection. Nature 455(7210), 242-5.

Kubo, S., Tomozawa, T., Kakuta, M., Tokumitsu, A. and Yamashita, M. Laninamivir prodrug CS-8958, a long-acting neuraminidase inhibitor, shows superior anti-influenza virus activity after a single administration. Antimicrob Agents Chemother 54(3), 1256-64.

Kunzelmann, K., Beesley, A.H., King, N.J., Karupiah, G., Young, J.A. and Cook, D.I. (2000) Influenza virus inhibits amiloride-sensitive Na+ channels in respiratory epithelia. Proc Natl Acad Sci U S A 97(18), 10282-7.

Kurokawa, M., Ochiai, H., Nakajima, K. and Niwayama, S. (1990) Inhibitory effect of protein kinase C inhibitor on the replication of influenza type A virus. J Gen Virol 71 (Pt 9), 2149-55.

Labadie, K., Dos Santos Afonso, E., Rameix-Welti, M.A., van der Werf, S. and Naffakh, N. (2007) Host-range determinants on the PB2 protein of influenza A viruses control the interaction between the viral polymerase and nucleoprotein in human cells. Virology 362(2), 271-82.

Lamb, R.A. and Choppin, P.W. (1983) The gene structure and replication of influenza virus. Annu Rev Biochem 52, 467-506.

Lamb, R.A., Choppin, P.W., Chanock, R.M. and Lai, C.J. (1980) Mapping of the two overlapping genes for polypeptides NS1 and NS2 on RNA segment 8 of influenza virus genome. Proc Natl Acad Sci U S A 77(4), 1857-61.

Lamb, R.A., Zebedee, S.L. and Richardson, C.D. (1985) Influenza virus M2 protein is an integral membrane protein expressed on the infected-cell surface. Cell 40(3), 627-33.

Liu, W., Zou, P. and Chen, Y.H. (2004) Monoclonal antibodies recognizing EVETPIRN epitope of influenza A virus M2 protein could protect mice from lethal influenza A virus challenge. Immunol Lett 93(2-3), 131-6.

Ma, K., Roy, A.M. and Whittaker, G.R. (2001) Nuclear export of influenza virus ribonucleoproteins: identification of an export intermediate at the nuclear periphery. Virology 282(2), 215-20.

Marsh, G.A., Hatami, R. and Palese, P. (2007) Specific residues of the influenza A virus hemagglutinin viral RNA are important for efficient packaging into budding virions. J Virol 81(18), 9727-36.

Martin-Benito, J., Area, E., Ortega, J., Llorca, O., Valpuesta, J.M., Carrascosa, J.L. and Ortin, J. (2001) Three-dimensional reconstruction of a recombinant influenza virus ribonucleoprotein particle. EMBO Rep 2(4), 313-7.

Martin, K. and Helenius, A. (1991) Nuclear transport of influenza virus ribonucleoproteins: the viral matrix protein (M1) promotes export and inhibits import. Cell 67(1), 117-30.

Matrosovich, M., Matrosovich, T., Garten, W. and Klenk, H.D. (2006) New low-viscosity overlay medium for viral plaque assays. Virol J 3, 63.

McAuley, J.L., Hornung, F., Boyd, K.L., Smith, A.M., McKeon, R., Bennink, J., Yewdell, J.W. and McCullers, J.A. (2007) Expression of the 1918 influenza A virus PB1-F2 enhances the pathogenesis of viral and secondary bacterial pneumonia. Cell Host Microbe 2(4), 240-9.

Mena, I., Jambrina, E., Albo, C., Perales, B., Ortin, J., Arrese, M., Vallejo, D. and Portela, A. (1999) Mutational analysis of influenza A virus nucleoprotein: identification of mutations that affect RNA replication. J Virol 73(2), 1186-94.

Mukaigawa, J. and Nayak, D.P. (1991) Two signals mediate nuclear localization of influenza virus (A/WSN/33) polymerase basic protein 2. J Virol 65(1), 245-53.

Nagai, Y., Maeno, K., Iinuma, M., Yoshida, T. and Matsumoto, T. (1972) Inhibition of virus growth by ouabain: effect of ouabain on the growth of HVJ in chick embryo cells. J Virol 9(2), 234-43.

Nath, S.T. and Nayak, D.P. (1990) Function of two discrete regions is required for nuclear localization of polymerase basic protein 1 of A/WSN/33 influenza virus (H1 N1). Mol Cell Biol 10(8), 4139-45.

Neumann, G., Castrucci, M.R. and Kawaoka, Y. (1997) Nuclear import and export of influenza virus nucleoprotein. J Virol 71(12), 9690-700.

Neumann, G. and Hobom, G. (1995) Mutational analysis of influenza virus promoter elements in vivo. J Gen Virol 76 (Pt 7), 1709-17.

Ng, A.K., Zhang, H., Tan, K., Li, Z., Liu, J.H., Chan, P.K., Li, S.M., Chan, W.Y., Au, S.W., Joachimiak, A., Walz, T., Wang, J.H. and Shaw, P.C. (2008) Structure of the influenza virus A H5N1 nucleoprotein: implications for RNA binding, oligomerization, and vaccine design. FASEB J 22(10), 3638-47.

Ng, T.I., Mo, H., Pilot-Matias, T., He, Y., Koev, G., Krishnan, P., Mondal, R., Pithawalla, R., He, W., Dekhtyar, T., Packer, J., Schurdak, M. and Molla, A. (2007) Identification of host genes involved in hepatitis C virus replication by small interfering RNA technology. Hepatology 45(6), 1413-21.

Nieto, A., de la Luna, S., Barcena, J., Portela, A., Valcarcel, J., Melero, J.A. and Ortin, J. (1992) Nuclear transport of influenza virus polymerase PA protein. Virus Res 24(1), 65-75.

Noah, J.W., Severson, W., Noah, D.L., Rasmussen, L., White, E.L. and Jonsson, C.B. (2007) A cell-based luminescence assay is effective for high-throughput screening of potential influenza antivirals. Antiviral Res 73(1), 50-9.

Noda, T., Sagara, H., Yen, A., Takada, A., Kida, H., Cheng, R.H. and Kawaoka, Y. (2006) Architecture of ribonucleoprotein complexes in influenza A virus particles. Nature 439(7075), 490-2.

Ortega, J., Martin-Benito, J., Zurcher, T., Valpuesta, J.M., Carrascosa, J.L. and Ortin, J. (2000) Ultrastructural and functional analyses of recombinant influenza virus ribonucleoproteins suggest dimerization of nucleoprotein during virus amplification. J Virol 74(1), 156-63.

Palese, P. and Shaw, M.L. (2007) Orthomyxoviridae: The Viruses and Their Replication. 5th ed. Fields' Virology, edited by B.N. Fields, D.M. Knipe and P.M. Howley, 2. 2 vols. Wolters Kluwer Health/Lippincott Williams & Wilkins, Philadelphia.

Palese, P. and Young, J.F. (1982) Variation of influenza A, B, and C viruses. Science 215(4539), 1468-74.

Paltauf-Doburzynska, J., Frieden, M., Spitaler, M. and Graier, W.F. (2000) Histamine-induced Ca2+ oscillations in a human endothelial cell line depend on transmembrane ion flux, ryanodine receptors and endoplasmic reticulum Ca2+-ATPase. J Physiol 524 Pt 3, 701-13.

Park, M.S., Steel, J., Garcia-Sastre, A., Swayne, D.E. and Palese. P. (2006) Engineered viral vaccine constructs with dual specificity: avian influenza and Newcastle disease. Proc Natl Acad Sci U S A 103(21), 8203-08.

Pichlmair, A., Schulz, O., Tan, C.P., Naslund, T.I., Liljestrom, P., Weber, F. and Reis e Sousa, C. (2006) RIG-I-mediated antiviral responses to single-stranded RNA bearing 5'-phosphates. Science 314(5801), 997-1001.

Pinto, L.H., Holsinger, L.J. and Lamb, R.A. (1992) Influenza virus M2 protein has ion channel activity. Cell 69(3), 517-28.

Pleschka, S., Jaskunas, R., Engelhardt, O.G., Zurcher, T., Palese, P. and Garcia-Sastre, A. (1996) A plasmid-based reverse genetics system for influenza A virus. J Virol 70(6), 4188-92.

Portela, A. and Digard, P. (2002) The influenza virus nucleoprotein: a multifunctional RNA-binding protein pivotal to virus replication. J Gen Virol 83(Pt 4), 723-34.

Premkumar, A., Horan, C.R. and Gage, P.W. (2005) Dengue virus M protein C-terminal peptide (DVM-C) forms ion channels. J Membr Biol 204(1), 33-8.

Premkumar, A., Wilson, L., Ewart, G.D. and Gage, P.W. (2004) Cation-selective ion channels formed by p7 of hepatitis C virus are blocked by hexamethylene amiloride. FEBS Lett 557(1-3), 99-103.

Quinlivan, M., Zamarin, D., Garcia-Sastre, A., Cullinane, A., Chambers, T. and Palese, P. (2005) Attenuation of equine influenza viruses through truncations of the NS1 protein. J Virol 79 (13), 8431–9.

Richardson, J.C. and Akkina, R.K. (1991) NS2 protein of influenza virus is found in purified virus and phosphorylated in infected cells. Arch Virol 116(1-4), 69-80.

Rodriguez, A., Perez-Gonzalez, A. and Nieto, A. (2007) Influenza virus infection causes specific degradation of the largest subunit of cellular RNA polymerase II. J Virol 81(10), 5315-24.

Root, C.N., Wills, E.G., McNair, L.L. and Whittaker, G.R. (2000) Entry of influenza viruses into cells is inhibited by a highly specific protein kinase C inhibitor. J Gen Virol 81(Pt 11), 2697-705.

Rott, O., Charreire, J., Semichon, M., Bismuth, G. and Cash, E. (1995) B cell superstimulatory influenza virus (H2-subtype) induces B cell proliferation by a PKC-activating, Ca(2+)-independent mechanism. J Immunol 154(5), 2092-103.

Rudolph, M.G., Kraus, I., Dickmanns, A., Eickmann, M., Garten, W. and Ficner, R. (2003) Crystal structure of the borna disease virus nucleoprotein. Structure 11(10), 1219-26.

Schnell, J.R. and Chou, J.J. (2008) Structure and mechanism of the M2 proton channel of influenza A virus. Nature 451(7178), 591-5.

Scholtissek, C. (1994) Source for influenza pandemics. Eur J Epidemiol 10(4), 455-8.

Scholtissek, C., Rohde, W., Von Hoyningen, V. and Rott, R. (1978) On the origin of the human influenza virus subtypes H2N2 and H3N2. Virology 87(1), 13-20.

Senne, D.A., Panigrahy, B., Kawaoka, Y., Pearson, J.E., Suss, J., Lipkind, M., Kida, H. and Webster, R.G. (1996) Survey of the hemagglutinin (HA) cleavage site sequence of H5 and H7 avian influenza viruses: amino acid sequence at the HA cleavage site as a marker of pathogenicity potential. Avian Dis 40(2), 425-37.

Severson, W.E., Shindo, N., Sosa, M., Fletcher, T., 3rd, White, E.L., Ananthan, S. and Jonsson, C.B. (2007) Development and validation of a high-throughput screen for inhibitors of SARS CoV and its application in screening of a 100,000-compound library. J Biomol Screen 12(1), 33-40.

Shapiro, G.I. and Krug, R.M. (1988) Influenza virus RNA replication in vitro: synthesis of viral template RNAs and virion RNAs in the absence of an added primer. J Virol 62(7), 2285-90.

Sieczkarski, S.B., Brown, H.A. and Whittaker, G.R. (2003) Role of protein kinase C betaII in influenza virus entry via late endosomes. J Virol 77(1), 460-9.

Slepushkin, V.A., Katz, J.M., Black, R.A., Gamble, W.C., Rota, P.A. and Cox, N.J. (1995) Protection of mice against influenza A virus challenge by vaccination with baculovirus-expressed M2 protein. Vaccine 13(15), 1399-402.

Smee, D.F., Hurst, B.L., Egawa, H., Takahashi, K., Kadota, T. and Furuta, Y. (2009) Intracellular metabolism of favipiravir (T-705) in uninfected and influenza A (H5N1) virus-infected cells. J Antimicrob Chemother 64(4), 741-6.

Solorzano, A., Webby, R.J., Lager, K.M., Janke, B.H., Garcia-Sastre A. and Richt, J.A. (2005) Mutations in the NS1 protein of swine influenza virus impair anti-interferon activity and confer attenuation in pigs. J Virol 79(12), 7535–43.

Sorensen, M.G., Henriksen, K., Neutzsky-Wulff, A.V., Dziegiel, M.H. and Karsdal, M.A. (2007) Diphyllin, a novel and naturally potent V-ATPase inhibitor, abrogates acidification of the osteoclastic resorption lacunae and bone resorption. J Bone Miner Res 22(10), 1640-8.

Steel, J., Burmakina, S.V., Thomas, C., Spackman, E., Garcia-Sastre, A., Swayne, D.E. and Palese, P. (2008) A combination in-ovo vaccine for avian influenza virus and Newcastle disease virus. Vaccine 26(4), 522-31.

Steel, J., Lowen, A.C., Mubareka, S. and Palese, P. (2009) Transmission of influenza virus in a mammalian host is increased by PB2 amino acids 627K or 627E/701N. PLoS Pathog 5(1), e1000252.

Stockand, J.D., Bao, H.F., Schenck, J., Malik, B., Middleton, P., Schlanger, L.E. and Eaton, D.C. (2000) Differential effects of protein kinase C on the levels of epithelial Na+ channel subunit proteins. J Biol Chem 275(33), 25760-5.

Stouffer, A.L., Acharya, R., Salom, D., Levine, A.S., Di Costanzo, L., Soto, C.S., Tereshko, V., Nanda, V., Stayrook, S. and DeGrado, W.F. (2008) Structural basis for the function and inhibition of an influenza virus proton channel. Nature 451(7178), 596-9.

Stouffer, A.L., Nanda, V., Lear, J.D. and DeGrado, W.F. (2005) Sequence determinants of a transmembrane proton channel: an inverse relationship between stability and function. J Mol Biol 347(1), 169-79.

Subbarao, E.K., London, W. and Murphy, B.R. (1993) A single amino acid in the PB2 gene of influenza A virus is a determinant of host range. J Virol 67(4), 1761-4.

Subbarao, K., Chen, H., Swayne, D., Mingay, L., Fodor, E., Brownlee, G., Xu, X., Lu, X., Katz, J., Cox, N. and Matsuoka, Y. (2003) Evaluation of a genetically modified reassortant H5N1 influenza A virus vaccine candidate generated by plasmid-based reverse genetics. Virology 305(1), 192-200.

Sugrue, R.J. and Hay, A.J. (1991) Structural characteristics of the M2 protein of influenza A viruses: evidence that it forms a tetrameric channel. Virology 180(2), 617-24.

Tang, Y., Zaitseva, F., Lamb, R.A. and Pinto, L.H. (2002) The gate of the influenza virus M2 proton channel is formed by a single tryptophan residue. J Biol Chem 277(42), 39880-6.

Taubenberger, J.K. and Morens, D.M. (2008) The pathology of influenza virus infections. Annu Rev Pathol 3, 499-522.

Taubenberger, J.K., Reid, A.H. and Fanning, T.G. (2005) Capturing a killer flu virus. Sci Am 292(1), 48-57.

Tomita, Y. and Kuwata, T. (1978) Suppression of murine leukaemia virus production by ouabain and interferon in mouse cells. J Gen Virol 38(2), 223-30.

Toriumi, H., Eriguchi, Y., Takamatsu, F. and Kawai, A. (2004) Further studies on the hyperphosphorylated form (p40) of the rabies virus nominal phosphoprotein (P). Microbiol Immunol 48(11), 865-74.

Treanor, J.J., Campbell, J.D., Zangwill, K.M., Rowe, T. and Wolff, M. (2006) Safety and immunogenicity of an inactivated subvirion influenza A (H5N1) vaccine. N Engl J Med 354(13), 1343-51.

Triana-Baltzer, G.B., Gubareva, L.V., Nicholls, J.M., Pearce, M.B., Mishin, V.P., Belser, J.A., Chen, L.M., Chan, R.W., Chan, M.C., Hedlund, M., Larson, J.L., Moss, R.B., Katz, J.M., Tumpey, T.M. and Fang, F. (2009) Novel pandemic influenza A(H1N1) viruses are potently inhibited by DAS181, a sialidase fusion protein. PLoS One 4(11), e7788.

Tscherne, D.M., Manicassamy, B. and Garcia-Sastre, A. (2009) An enzymatic virus-like particle assay for sensitive detection of virus entry. J Virol Methods 163(2), 336-43.

Vreede, F.T., Jung, T.E. and Brownlee, G.G. (2004) Model suggesting that replication of influenza virus is regulated by stabilization of replicative intermediates. J Virol 78(17), 9568-72.

Wang, C., Lamb, R.A. and Pinto, L.H. (1995) Activation of the M2 ion channel of influenza virus: a role for the transmembrane domain histidine residue. Biophys J 69(4), 1363-71.

Wang, P., Palese, P. and O'Neill, R.E. (1997) The NPI-1/NPI-3 (karyopherin alpha) binding site on the influenza a virus nucleoprotein NP is a nonconventional nuclear localization signal. J Virol 71(3), 1850-6.

Watanabe, K., Takizawa, N., Katoh, M., Hoshida, K., Kobayashi, N. and Nagata, K. (2001) Inhibition of nuclear export of ribonucleoprotein complexes of influenza virus by leptomycin B. Virus Res 77(1), 31-42.

Webster, R.G., Bean, W.J., Gorman, O.T., Chambers, T.M. and Kawaoka, Y. (1992) Evolution and ecology of influenza A viruses. Microbiol Rev 56(1), 152-79.

WHO. (2003) Influenza - Overview.

WHO. (2010a) Cumulative Number of Confirmed Human Cases of Avian Influenza A/(H5N1) Reported to WHO.

WHO. (2010b) Pandemic (H1N1) 2009 - update 93.

Wilson, L., Gage, P. and Ewart, G. (2006) Hexamethylene amiloride blocks E protein ion channels and inhibits coronavirus replication. Virology 353(2), 294-306.

Wise, H.M., Foeglein, A., Sun, J., Dalton, R.M., Patel, S., Howard, W., Anderson, E.C., Barclay, W.S. and Digard, P. (2009) A complicated message: Identification of a novel PB1-related protein translated from influenza A virus segment 2 mRNA. J Virol 83(16), 8021-31.

Wolf, M.C., Freiberg, A.N., Zhang, T., Akyol-Ataman, Z., Grock, A., Hong, P.W., Li, J., Watson, N.F., Fang, A.Q., Aguilar, H.C., Porotto, M., Honko, A.N., Damoiseaux, R., Miller, J.P., Woodson, S.E., Chantasirivisal, S., Fontanes, V., Negrete, O.A., Krogstad, P., Dasgupta, A., Moscona, A., Hensley, L.E., Whelan, S.P., Faull, K.F., Holbrook, M.R., Jung, M.E. and Lee, B. (2010) A broad-spectrum antiviral targeting entry of enveloped viruses. Proc Natl Acad Sci U S A 107(7), 3157-62.

Yamagata, T., Yamagata, Y., Masse, C., Tessier, M.C., Brochiero, E., Dagenais, A. and Berthiaume, Y. (2005) Modulation of Na+ transport and epithelial sodium channel expression by protein kinase C in rat alveolar epithelial cells. Can J Physiol Pharmacol 83(11), 977-87.

Yamanaka, K., Ishihama, A. and Nagata, K. (1990) Reconstitution of influenza virus RNA-nucleoprotein complexes structurally resembling native viral ribonucleoprotein cores. J Biol Chem 265(19), 11151-5.

Yasuda, J., Nakada, S., Kato, A., Toyoda, T. and Ishihama, A. (1993) Molecular assembly of influenza virus: association of the NS2 protein with virion matrix. Virology 196(1), 249-55.

Ye, Q., Krug, R.M. and Tao, Y.J. (2006) The mechanism by which influenza A virus nucleoprotein forms oligomers and binds RNA. Nature 444(7122), 1078-82.

Yuan, P., Bartlam, M., Lou, Z., Chen, S., Zhou, J., He, X., Lv, Z., Ge, R., Li, X., Deng, T., Fodor, E., Rao, Z. and Liu, Y. (2009) Crystal structure of an avian influenza polymerase PA(N) reveals an endonuclease active site. Nature 458(7240), 909-13.

Zamarin, D., Garcia-Sastre, A., Xiao, X., Wang, R. and Palese, P. (2005) Influenza virus PB1-F2 protein induces cell death through mitochondrial ANT3 and VDAC1. PLoS Pathog 1(1), e4.

Zamarin, D., Ortigoza, M.B. and Palese, P. (2006) Influenza A virus PB1-F2 protein contributes to viral pathogenesis in mice. J Virol 80(16), 7976-83.

Zhang, J.H., Chung, T.D. and Oldenburg, K.R. (1999) A Simple Statistical Parameter for Use in Evaluation and Validation of High Throughput Screening Assays. J Biomol Screen 4(2), 67-73.

Zhou, H., Xu, M., Huang, Q., Gates, A.T., Zhang, X.D., Castle, J.C., Stec, E., Ferrer, M., Strulovici, B., Hazuda, D.J. and Espeseth, A.S. (2008) Genome-scale RNAi screen for host factors required for HIV replication. Cell Host Microbe 4(5), 495-504.

Zuck, P., Murray, E.M., Stec, E., Grobler, J.A., Simon, A.J., Strulovici, B., Inglese, J., Flores, O.A. and Ferrer, M. (2004) A cell-based beta-lactamase reporter gene assay for the identification of inhibitors of hepatitis C virus replication. Anal Biochem 334(2), 344-55.